

NBSIR 74-388

## ELECTROMAGNETIC NOISE IN GRACE MINE

---

J. W. Adams  
W. D. Bensema  
M. Kanda

Electromagnetics Division  
Institute for Basic Standards  
National Bureau of Standards  
Boulder, Colorado 80302

June 1974

Prepared for  
U. S. Bureau of Mines  
United States Department of the Interior  
Pittsburgh, Pennsylvania 15222  
Working Fund Agreement HO 133005



NBSIR 74-388

# ELECTROMAGNETIC NOISE IN GRACE MINE

---

J. W. Adams  
W. D. Bensema  
M. Kanda

Electromagnetics Division  
Institute for Basic Standards  
National Bureau of Standards  
Boulder, Colorado 80302

The views and conclusions contained in this document should not be interpreted as necessarily representing the official policies or recommendations of the Interior Department's Bureau of Mines of the U. S. Government

June 1974

Prepared for  
U. S. Bureau of Mines  
United States Department of the Interior  
Pittsburgh, Pennsylvania 15222  
Working Fund Agreement HO 133005



---

U.S. DEPARTMENT OF COMMERCE, Frederick B. Dent, Secretary

NATIONAL BUREAU OF STANDARDS Richard W. Roberts Director

## FOREWORD

This report was prepared by the National Bureau of Standards, Boulder, Colorado, under USBM Contract No. HO 133005. The contract was initiated under the Coal Mine Health and Safety Research Program. It was administered under the technical direction of the Pittsburgh Mining and Safety Research Center with Mr. Howard Parkinson and Mr. Harry Dobroski acting as the technical project officers.

This report is a summary of the work completed as part of this contract during the period January 1973 to June 1974. This report was submitted by the authors in October 1974.

# CONTENTS

	<u>Page</u>
1. INTRODUCTION-----	1
1.1 Background-----	2
1.2 Mine Description-----	3
2. MEASUREMENT INSTRUMENTATION-----	5
3. SPECTRUM MEASUREMENT RESULTS-----	11
3.1 Introduction-----	11
3.2 Antenna Sites-----	11
3.3 Electromagnetic Noise Spectrum Results-----	12
3.3.1 Introduction-----	12
3.3.2 Uncertainties-----	13
3.3.3 Crusher Room Area-----	13
3.3.4 Production Area-----	17
3.3.5 Development Area-----	19
3.3.6 Cross Drift Substation-----	20
3.3.7 Underground Workshop-Lunchroom-----	21
3.3.8 Composite of Worst Case Steady Noise---	22
3.4 Pulse Produced with Explosion-----	22
3.5 Mine Noise Contour Maps-----	24
3.6 Miscellaneous Measurements-----	24
3.6.1 Electric Field-----	24
3.6.2 Measurement of Voltage Between "Roof Bolts"-----	25

CONTENTS (continued)

	<u>Page</u>
3.7 Intercomparison of Magnetic-Field Noise in Different Mines-----	26
3.7.1 Summary of 1 to 3 kHz Data-----	26
3.7.2 Magnetic-Field Spectra 3 kHz to 180 kHz	27
4. AMPLITUDE PROBABILITY DISTRIBUTION MEASUREMENT RESULTS-----	65
4.1 Introduction and Uncertainties-----	65
4.2 Measurement Results-----	67
4.3 RMS and Average Values-----	69
4.4 Summary Curves-----	69
5. HOIST-PHONE MEASUREMENT RESULTS-----	116
6. CONCLUSIONS-----	121
7. RECOMMENDATIONS-----	123
8. ACKNOWLEDGMENTS-----	124
9. REFERENCES-----	125
10. APPENDIX-----	126

## LIST OF FIGURES

		<u>Page</u>
Figure 2-1.	Block diagram of portable instrumentation---	8
Figure 2-2.	System for field recording data to obtain amplitude probability distributions-----	9
Figure 2-3.	Block diagram of laboratory recording system modified for field use-----	10
Figure 3-1.	Simplified map of Grace Mine where measurements were made-----	28
Figure 3-2.	Expanded map of underground development, production, and crusher-room areas-----	29
Figure 3-3.	Expanded map of underground workshop and lunchroom area-----	30
Figure 3-4.	Spectrum of area noise before explosion. Measurements at development foreman office with spectral resolution of 78.1 Hz-----	31
Figure 3-5.	Spectrum when crusher is not operating. Measurements at crusher substation with spectral resolution of 78.1 Hz-----	32
Figure 3-6.	Spectrum at higher gain when crusher is not operating. Measurements at crusher substation with spectral resolution of 78.1 Hz-	33
Figure 3-7.	Spectrum when crusher is operating. Measurements at crusher substation with spectral resolution of 78.1 Hz-----	34
Figure 3-8.	Expanded spectrum of crusher operating. Measurements at crusher substation with spectral resolution of 3.91 Hz-----	35
Figure 3-9.	Spectrum when crusher is not operating. Measurements at crusher access drift with spectral resolution of 78.1 Hz-----	36
Figure 3-10.	Spectrum when crusher is operating. Measurements at crusher access drift with spectral resolution of 78.1 Hz-----	37

LIST OF FIGURES (Continued)

	<u>Page</u>
Figure 3-11. Expanded spectrum of crusher operating. Measurements at crusher access drift with spectral resolution of 3.91 Hz-----	38
Figure 3-12. Spectrum of noise at intersection 603 production area with spectral resolution of 78.1 Hz-----	39
Figure 3-13. Spectrum comparison between steady-state background noise and LHD noise at entry and dining area 606E. Spectral resolution is 78.1 Hz-----	40
Figure 3-14. Spectrum of V-8 diesel LHD. Measurements at entry and dining area 606E with spectral resolution of 78.1 Hz-----	41
Figure 3-15. Expanded spectrum of loaded LHD. Measurements at entry and dining area 606E with spectral resolution of 3.91 Hz-----	42
Figure 3-16. Spectrum of operating pneumatic fanhole drill. Measurements at jumbo drill working face with spectral resolution of 78.1 Hz----	43
Figure 3-17. Spectrum of lowest noise level measured in Grace Mine. Measurements at Number 2 mine transfer drift with spectral resolution of 78.1 Hz-----	44
Figure 3-18. Spectrum of V-10 diesel LHD at Number 2 mine transfer drift. Spectral resolution is 78.1 Hz-----	45
Figure 3-19. Expanded spectrum of V-10 diesel LHD at Number 2 mine transfer drift. Spectral resolution is 3.91 Hz-----	46
Figure 3-20. Expanded spectrum after V-10 diesel LHD left the vicinity. Measurements at Number 2 mine transfer drift with spectrum resolution of 3.91 Hz-----	47
Figure 3-21. Spectrum of background noise measured at Number 6 crossdrift substation. Spectral resolution is 78.1 Hz-----	48



LIST OF FIGURES (Continued)

	<u>Page</u>
Figure 3-22. Spectrum of LHD's being refueled 30 meters distant. Fluorescent light area in shop office. Spectral resolution is 78.1 Hz-----	49
Figure 3-23. Expanded spectrum measured at shop office. Fluorescent light area. Spectral resolution is 3.91 Hz-----	50
Figure 3-24. Spectrum of LHD passing by the shop lunch-room area. Spectral resolution is 19.5 Hz--	51
Figure 3-25. Spectrum comparison between steady-state background noise and LHD noise which is the highest spectra measured at Grace Mine. Spectral resolution is 78.1 Hz-----	52
Figure 3-26. Spectrum of explosion impulse measured at development foreman office. Spectral resolution is 78.1 Hz-----	53
Figure 3-27. Contour map showing noise generated from a group of detonations comprising a "shot," as a function of time-----	54
Figure 3-28. Three-dimensional view of two detonations from a larger group comprising a "shot"-----	55
Figure 3-29. Grace Mine noise contour map for 2 kHz-----	56
Figure 3-30. Grace Mine noise contour map for 10 kHz-----	57
Figure 3-31. Grace Mine noise contour map for 20 kHz-----	58
Figure 3-32. Grace Mine noise contour map for 60 kHz-----	59
Figure 3-33. Unprocessed data showing electric field strength obtained with an active dipole as a function of frequency. Measurements at crusher access drift. Spectral resolution is 78.1 Hz-----	60
Figure 3-34. Voltage spectrum of roof bolt at crusher access drift-----	61

LIST OF FIGURES (Continued)

	<u>Page</u>
Figure 3-35. Comparison of magnetic field strengths of Grace and Robena Mines as a function of distance from noise source-----	62
Figure 3-36. Comparison of E-M noise levels near operating machinery (noise sources) from four different mines-----	63
Figure 3-37. Comparison of E-M noise levels along haulageways in four different operating mines. Machinery was not operating in vicinity at times of measurements-----	64
Figure 4-1. APD, 10 kHz, vertical component-----	70
Figure 4-2. APD, 30 kHz, vertical component-----	71
Figure 4-3. APD, 70 kHz, vertical component-----	72
Figure 4-4. APD, 130 kHz, vertical component-----	73
Figure 4-5. APD, 160 kHz, vertical component-----	74
Figure 4-6. APD, 250 kHz, vertical component-----	75
Figure 4-7. APD, 1 MHz, vertical component-----	76
Figure 4-8. APD, 2 MHz, vertical component-----	77
Figure 4-9. APD, 6 MHz, vertical component-----	78
Figure 4-10. APD, 14 MHz, vertical component-----	79
Figure 4-11. APD, 32 MHz, vertical component-----	80
Figure 4-12. APD, 10 kHz, vertical component-----	81
Figure 4-13. APD, 30 kHz, vertical component-----	82
Figure 4-14. APD, 70 kHz, vertical component-----	83
Figure 4-15. APD, 130 kHz, vertical component-----	84
Figure 4-16. APD, 0.5 MHz, vertical component-----	85
Figure 4-17. APD, 1 MHz, vertical component-----	86

LIST OF FIGURES (Continued)

	<u>Page</u>
Figure 4-18. APD, 2 MHz, vertical component-----	87
Figure 4-19. APD, 6 MHz, vertical component-----	88
Figure 4-20. APD, 30 kHz, vertical component-----	89
Figure 4-21. APD 70 kHz, vertical component-----	90
Figure 4-22. APD, 110 kHz, vertical component-----	91
Figure 4-23. APD, 130 kHz, vertical component-----	92
Figure 4-24. APD, 160 kHz, vertical component-----	93
Figure 4-25. APD, 205 kHz, vertical component-----	94
Figure 4-26. APD, 250 kHz, vertical component-----	95
Figure 4-27. APD, 500 kHz, vertical component-----	96
Figure 4-28. APD, 1 MHz, vertical component-----	97
Figure 4-29. APD, 2 MHz, vertical component-----	98
Figure 4-30. APD, 6 MHz, vertical component-----	99
Figure 4-31. APD, 14 MHz, vertical component-----	100
Figure 4-32. APD, 32 MHz, vertical component-----	101
Figure 4-33. APD, 10 kHz, horizontal E-W component-----	102
Figure 4-34. APD, 30 kHz, horizontal E-W component-----	103
Figure 4-35. APD, 70 kHz, horizontal E-W component-----	104
Figure 4-36. APD, 130 kHz, horizontal E-W component-----	105
Figure 4-37. APD, 160 kHz, horizontal E-W component-----	106
Figure 4-38. APD, 250 kHz, horizontal E-W component-----	107
Figure 4-39. APD, 500 kHz, horizontal E-W component-----	108
Figure 4-40. APD, 1 MHz, horizontal E-W component-----	109

LIST OF FIGURES (Continued)

	<u>Page</u>
Figure 4-41. APD, 2 MHz, horizontal E-W component-----	110
Figure 4-42. APD, 6 MHz, horizontal E-W component-----	111
Figure 4-43. Field strength excursions between 0.001 and 99% of the time as a function of frequency, vertical component, development foreman office-----	112
Figure 4-44. Field strength excursions between 0.001 and 99% of the time as a function of frequency, vertical component, crusher substation-----	113
Figure 4-45. Field strength excursions between 0.001 and 99% of the time as a function of frequency, vertical component, shop office--	114
Figure 4-46. Field strength excursions between 0.001 and 99% of the time as a function of frequency, horizontal E-W component, shop office-----	115
Figure 5-1. Top view of personnel hoist "A" skip-----	118
Figure 5-2. Magnetic field strength, dB $\mu$ A/m, or rela- tive S/N ratio as measured along the transmission line for the personnel hoist located in "A" shaft-----	119
Figure 5-3. Magnetic field strength, dB $\mu$ A/m, or rela- tive S/N ratio as measured along the hoist rope for the personnel hoist located in "A" shaft-----	120

# ELECTROMAGNETIC NOISE IN GRACE MINE

by

J.W. Adams, W.D. Bensema, and M. Kanda

Two different techniques were used to make measurements of the absolute value of electromagnetic noise in an operating hardrock mine, Grace Mine, located near Morgantown, Pennsylvania. Diesel-powered haulage equipment is used in this mine, and the electromagnetic noise environment it creates was measured to see how it differs from the environment created by electric-powered haulage equipment. One technique measures noise over the entire electromagnetic spectrum of interest for brief time periods. Data are recorded using broadband analog magnetic tape and are later transformed to give spectral plots. The other technique records noise amplitudes at several discrete frequencies for a sufficient amount of time to provide amplitude probability distributions.

The specific measured results are given in a number of spectral plots and in amplitude probability distribution plots.

Key words: Amplitude probability distribution; digital data; electromagnetic interference; electromagnetic noise; electromagnetic pulse (chemical); emergency communications; Fast Fourier Transform; Gaussian distribution; impulsive noise; magnetic field strength; measurement instrumentation; spectral density; time-dependent spectral density.

## 1. INTRODUCTION

This report gives data concerning electromagnetic noise in a hardrock mine. In this section, background information and a brief mine description are covered. In Section 2, measurement instrumentation is discussed. In Section 3, spectral plots of data are presented. In Section 4, amplitude probability distributions (APD) of magnetic-field noise are given. In Section 5, measurement results of attenuation

and electromagnetic noise on a hoist phone are reported. The last two sections (6 and 7) cover conclusions and recommendations.

Only representative samples of the total data measured are given in this report. A limited set of data-presentation formats have been used. If additional data, or data presentation in other formats, are required, contact any of the authors. With the specific permission of the Bureau of Mines, we will supply the additional data. A more complete description of the measurement systems used is given in the Robena Mine report [1].

### 1.1 Background

The need for reliable communication systems in mines is a long-standing problem. For emergency use, when all power in a mine is off, the residual electromagnetic noise is no problem. However, if a communication system were designed only for emergency use, it would have two serious drawbacks. First, it would not be ready for immediate use in an emergency; second, it would not be of any value during normal operations. Therefore, the Bureau of Mines decided to design a communication system that could be used for both emergency and normal operational conditions.

Also, two-way communication to personnel in a moving hoist is desirable for normal operating conditions, and is necessary in emergency conditions.

During operation, the machinery used in mines creates a wide range of many types of intense electromagnetic interference (EMI). This EMI is a major limiting factor in the design of a communication system.

The work reported here gives the results of comprehensive measurements of this EMI in critical communication locations where miners extract ore.

There are several EMI parameters that can be measured: magnetic field strength, H; electric field strength, E; conducted current, I; and voltage, V, between two conductors. One parameter was emphasized, magnetic field strength. There are several reasons. First, electric field sensors are very insensitive at lower frequencies, and hence probably will not be useful in any practical low frequency wireless mine communication system. Second, at any air-earth interface, only the magnetic field is essentially undisturbed, while the electric field is severely reduced. Third, any currents will induce magnetic fields, and hence measurement of the magnetic field will directly sense currents. Fourth, power line voltages are propagated as transmission line phenomena, are directly related to transmission line currents, and hence to magnetic fields generated. Thus, measuring magnetic field strength gives a representative composite picture of noise from currents and voltages from most sources, as well as measuring the magnetic fields induced by arcing equipment.

Although magnetic field strength measurements are emphasized here, even this one parameter is difficult to measure meaningfully. The IEEE definition [2] of magnetic field strength, H (magnitude of the magnetic field vector), is used in this report. Since there are a multitude of different sources that generate many types of noise, the resultant magnetic field strength noise vector is a function of frequency, time, orientation, and location. Small variations in these parameters can cause several orders of magnitude difference in measured field strength.

## 1.2 Mine Description

The results and data presented in this report are based on measurements made on April 24 and 26, 1973, in the Grace

Iron Mine located near Morgantown, south of Reading, Pennsylvania. The mine belongs to Bethlehem Steel Company and produces iron ore in the form of magnetite. The depth of level 6, where all measurements were taken, is 715 meters below the surface. The ore body is a large, flat, oval structure about a hundred meters thick, and is mined by undercutting and allowing the ore to fall into bins called entries. Air-cooled, V-8 diesel-powered, rubber-tired, Load-Haul-Dump (LHD) vehicles use front-loading scoops, typically of 5 cubic yard capacity (1 cubic yard = 0.76 m<sup>3</sup>), to pick up large chunks of ore, haul the ore to the underground crusher, and dump it into the crusher ore bin. After the ore is crushed in the ore crusher, it is transported by conveyer belt horizontally 825 meters, then lifted to the surface by a skip. Entry is made by a personnel cage in A shaft. This cage operates in one partition, while two ore skips operate in another partition of A shaft. B shaft was undergoing maintenance at the time of the measurements.

There are other types of haulage equipment used in this mine, but they, too, are diesel powered and rubber tired. Air drills are used for drilling, and nitrates are used for blasting. All haulageways are either through reliable rock or are heavily reinforced with concrete and steel. There is a mixture of incandescent, mercury-arc, and fluorescent lighting. A direct dial phone system is used for point-to-point communication. There is no portable communication system except on the personnel cages.

The temperature and humidity are high, although not excessive in most places.



## 2. MEASUREMENT INSTRUMENTATION

Two measurement techniques were used. The first technique covers a large portion of the spectrum as a "snapshot" during one relatively short period of time. In three-dimensional form, several such "snapshots" can show how drastically a signal varies, not only with frequency, but also with time. The second technique gives variations over a 20-minute time interval as measured in a very narrow band of frequencies. Usually, a set of twelve different center frequencies were used. Both techniques were used to measure two orthogonal components of magnetic field strength. This was done either by using two systems simultaneously or by varying the orientation of one system. Both techniques were used in as many different locations as possible.

With the exception of the electric dipole spectral plots, all measured noise is reported in absolute quantities (instead of relative) to allow others to make effective use of the data. For the magnetic field strength measurements, the NBS field calibration capability was used with each complete measurement system to assure correct calibration [5].

A complication in making these measurements is the mine environment, which is generally humid, dusty, and poorly lighted. In Grace Mine, a significant fraction of the dust was magnetic. We used battery-operated, dust-protected gear for all of our portable measuring equipment.

There are two types of noise recorded in the spectral plots, and hence two different magnetic field strength parameters are required,  $H$  and  $H_d$ . Results are given as the rms value of one component of magnetic field strength,  $H$ , versus frequency for discrete frequencies, or as one component of magnetic-field-strength spectrum density level [2],  $H_d$ , versus frequency for broadband noise in the spectral plots. In the amplitude

probability distributions, results are given as the rms value of one component of magnetic field strength versus percent of time this value is exceeded. The APD gives the distribution of the actual instantaneous values only as far as the measurement-system detector bandwidth will allow the detector to follow the time variations of the actual magnetic field. (In this context, noise envelope is sometimes used.) Thus, the results are applicable for a communication receiver whose bandwidth is similar to the measurement-system detector bandwidth.

Three measurement systems were used to make measurements underground. The three block diagrams are shown in figures 2-1, 2-2, and 2-3. Figures appear at the end of each section in this report. For a detailed description of these systems, see a previous report, Electromagnetic Noise in Robena #4 Coal Mine [1]. The changes in the measurement systems as used in Grace Mine from the way they were in Robena Mine are as follows:

First, the portable spectral measurement system had 10 kHz, high-pass filters added on two channels while a third channel remained unchanged. The purpose of these two filters was to reduce the effect of power line harmonics so that receiving system noise could be reduced by increasing pre-amplifier gain. In some locations where there were fluorescent lights (broadband noise sources), this strategy gave only moderate improvement, but in some cases the improvement was significant.

Second, the portable APD measuring system was unchanged in design except for the addition of a dust-proof enclosure. A procedural change is that about twelve frequencies were covered rather than eight, at the expense of eliminating measurement of one component of horizontal field strength. Thus, the same amount of time was required underground to make these measurements as before.

Third, the system that had been used on the surface was changed significantly and was used underground to increase the amount of data recorded underground. It is not a mine-permissible system. The recorder was equipped to operate at 30 ips speed in addition to 15 ips speed. Two channels of FM card sets were replaced by two sets of direct record cards. This gave an upper spectral limit of 180 kHz rather than 20 kHz. These two direct channels also had 10 kHz, high-pass filters added for the same reason as mentioned in the first system. One FM channel was retained to measure the vertical component of magnetic field strength below a frequency of 20 kHz. It did not have a 10 kHz, high-pass filter. The recorder was operated mostly at 30 ips. Two direct channels on this third system were used to record data for APD's. This gave APD measurements at two underground locations instead of one. At 30 ips, this system recorded 24 minutes of time instead of 48 minutes at 15 ips, but 24 minutes had been determined to be an adequate time for statistical validity in the Robena work [1] reported earlier. The data processing equipment was unchanged.

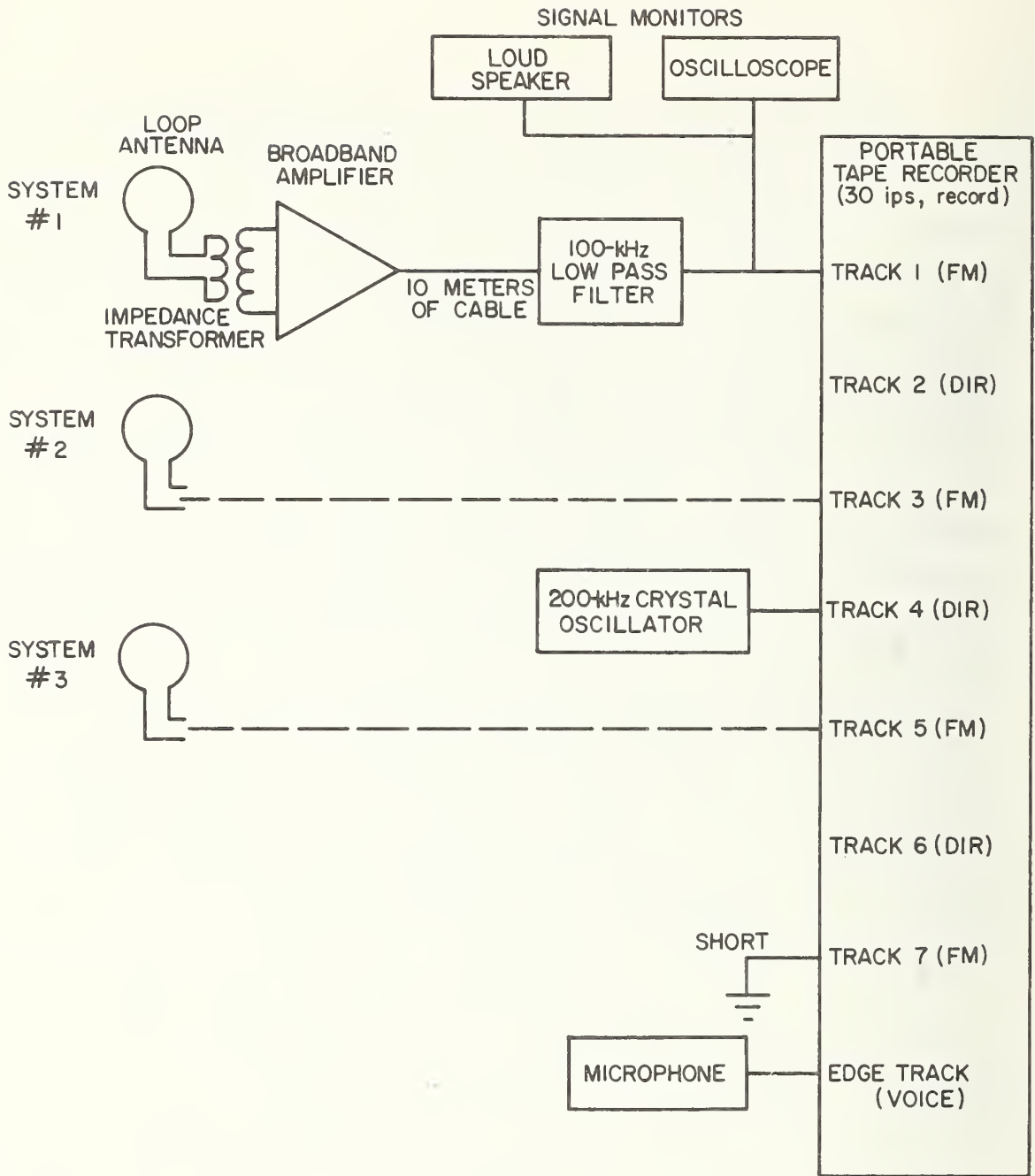


Figure 2-1 Block diagram of portable instrumentation. The tape recorder's FM tracks are used to record from 40 Hz to 100 kHz; direct tracks are used from 3 kHz to 320 kHz. Systems 2 and 3 are identical to system 1. When the direct tracks are used, the 100-kHz low pass filters are eliminated, and the amplifier bandwidth is increased from 100 kHz to 300 kHz. The microphone is used for occasional vocal comments by the operator.

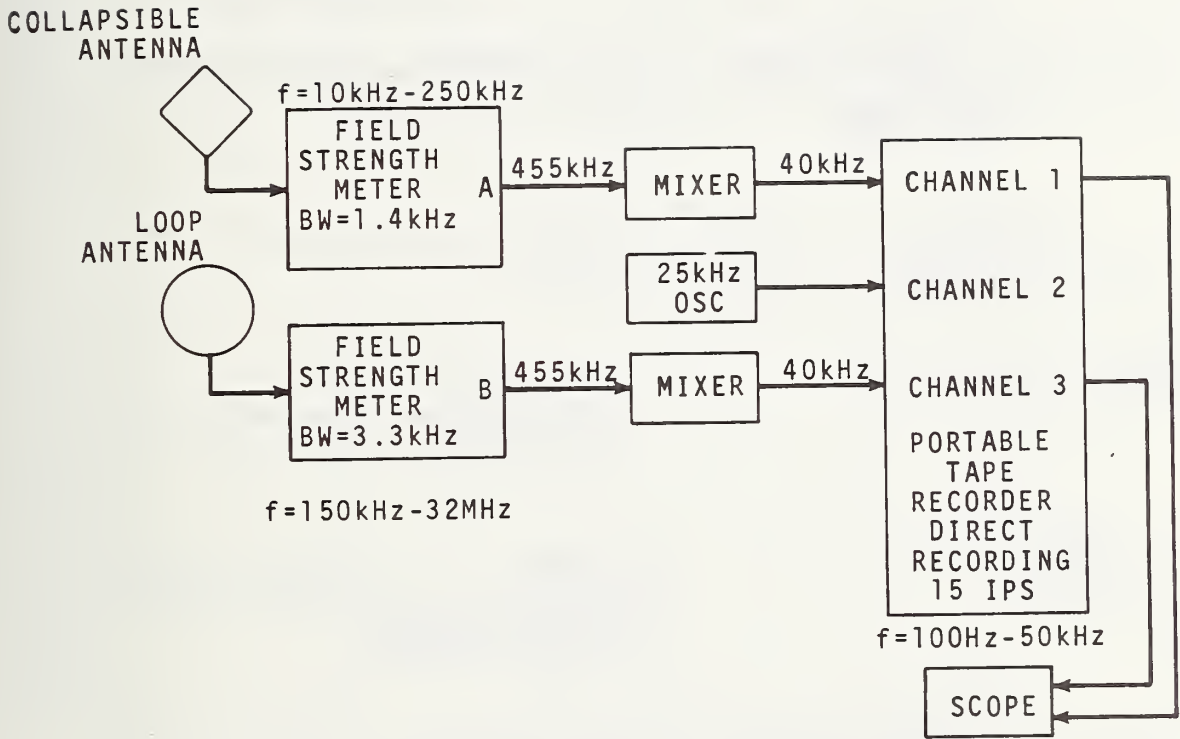


Figure 2-2 System for field recording data to obtain amplitude probability distributions.

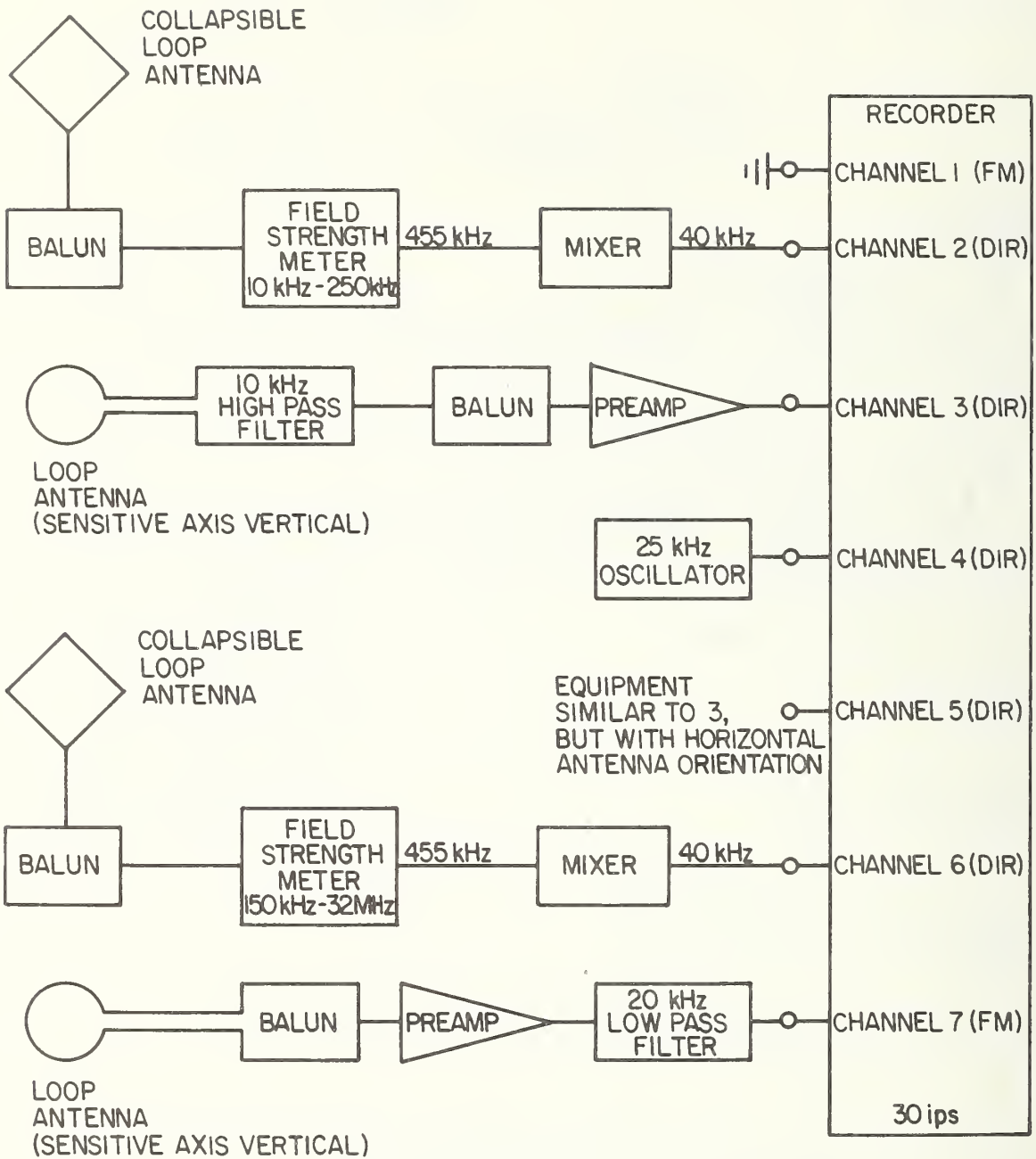


Figure 2-3 Block diagram of laboratory recording system modified for field use.

### 3. SPECTRUM MEASUREMENT RESULTS

#### 3.1 Introduction

In this section of the report, spectrum plots are presented and discussed. Most of these plots are of magnetic field strength up to 100 kHz. Measurements were made at many different locations, and results can be used to characterize electromagnetic noise levels generated by most fixed and mobile equipment used in this mine.

#### 3.2 Antenna Sites

Figure 3-1 is a map of most of level 6 where measurements were made. The map has been simplified by the removal of overlying (and a few underlying) workings, and is intended to show the scale relationship of the entire mine. There is an 825-meter separation between mining operations near the crusher and the vertical shafts where all the ore and personnel are transported to the surface. This separation is to prevent mining operations and resulting subsidence in and over the ore body from interfering with the integrity of the shafts.

Figure 3-2 is an expanded map of the underground development, production, and crusher-room areas. Figure 3-3 is an expanded map of the underground workshop and lunchroom area located near the main shafts. Noise spectrum measurements were taken in eleven locations, designated by letters A through K on figures 3-2 and 3-3. These locations were chosen (after consulting with mine personnel) as being locations where men are normally found working, and therefore, where communications would potentially be used.

### 3.3 Electromagnetic Noise Spectrum Results

#### 3.3.1 Introduction

When reading values from the spectral plots in this report, keep the following points in mind:

1. Field strength values above the upper roll-off frequency and below the lower roll-off frequency are not calibrated and are therefore not shown on the spectral plots.
2. The correct units for the spectral peaks are microamperes per meter ( $\mu\text{A}/\text{m}$ ).
3. The broadband noise between spectral peaks is as seen by a receiver having the same bandwidth as the Fast Fourier Transform (FFT) spectral resolution bandwidth used to compute the spectrum. The correct units for the background noise between peaks are microamperes per meter per square root x hertz [ $(\mu\text{A}/\text{m})/\sqrt{x \text{ Hz}}$ ], where x is the spectral resolution of the FFT (x equals 78.1 Hz for the 1-to-100-kHz plots).

An easy way to obtain the spectral density per (one) root hertz for broadband noise is to subtract the required number of dB, remembering that the units have now changed to  $(\mu\text{A}/\text{m})/\sqrt{\text{Hz}}$ . For spectra with a resolution bandwidth of 78.1 Hz, subtract  $10 \log_{10} (78.1)$  or 18.93 dB.

The Appendix gives the code key used in determining the meaning of the numbers in the header block at the top of each spectrum. The resolution bandwidth is also given on the ordinate of the plots.

The underground mine workings are divided into three parts for discussion purposes, and are called the crusher-room area, the production area, and the development area.



The crusher room area is defined arbitrarily to be the crusher room and adjoining areas within 30 meters. The production areas are those areas producing ore, while the development areas are those areas that do not yet produce ore.

### 3.3.2 Uncertainties

The spectra to 100 kHz, to 4 kHz, and to 20 kHz have uncertainties of  $\pm 1$  dB over the following portions of the spectra. The 100 kHz spectra are valid either from 1 to 100 kHz or 10 kHz to 100 kHz as stated or shown. The 40 Hz to 4 kHz spectra shown in this report have the usual uncertainty limits ( $\pm 1$  dB) between 100 Hz and 3 kHz. From 40 Hz to 100 Hz, the uncertainty limits are  $\pm 6$  dB. From 3 kHz to 4 kHz the uncertainty is  $\pm 1$  dB but the aliased signals are less than the specified 60 dB down. The 20 kHz spectra have an uncertainty of  $\pm 1$  dB from 750 Hz to 20 kHz.

The spectra shown to 180 kHz have an uncertainty of  $\pm 2$  dB from 3 kHz to 180 kHz.

### 3.3.3 Crusher Room Area

Figure 3-4, upper curve, shows the magnetic field noise spectrum received at the antenna location identified as A (in figure 3-2). Location A is the development foreman's office and is about 6 meters from the corner of the crusher room. The lowest curve in this, and in following figures, is the receiving system noise. It is included to indicate frequency ranges in which system noise may predominate. The lower curve is obtained by replacing the antenna with a dummy antenna. In figure 3-4, mine noise is higher than system noise at all frequencies. The antenna loop was

placed flat on the ground (the sensitive axis was therefore pointed up-down, i.e., vertically). The noise spectrum at location B (known as "601 intersection") is similar to location A above and is not shown.

The electrical substation at the ore-crusher is identified by letter C on figure 3-2. The ore-crusher substation contains two 500 KVA transformers for stepping down three-phase 4160 volts, to three-phase 480 volts. The stepped down voltage is used by crusher feeders, small conveyers, fans, and other similar equipment in the area of the crusher. The ore-crusher (a jaw crusher type) is run by a 150-horsepower, three-phase, 4160 volt, 20.3 ampere, wound-rotor motor. The main contactors for this motor are activated by dc current. The dc current is supplied by a single-phase, 230 volt, bridge rectifier. The spectrum of the noise measured in the crusher substation is shown in figure 3-5. From 20 kHz up, the spectrum is similar in amplitude and slope to the noise spectrum at the development foreman's office (location A). Below 20 kHz several differences appear. At about 13 kHz, there is a relative maximum, 10 dB higher than at A. Also, the noise at 60 Hz is about 30 dB stronger at C (crusher substation) than at A. Figure 3-6 was taken at location C, but with higher gain to reduce receiver-system noise. To be able to use higher receiver gain, the high-amplitude, low-frequency noise was attenuated below 10 kHz, and therefore the spectrum shows data only from 10 kHz to 100 kHz. Figure 3-6 was taken with the crusher not operating. Figure 3-7 was taken with the crusher operating. The only noise apparently caused by the crusher occurs between 60 kHz and 90 kHz as an increase varying from 0 to 8 dB. Interference lines are present and are separated by approximately 360 Hz.

The three locations A, B, and C are all within 30 meters (directly through rock) of the crusher room. The three locations show about the same noise amplitude, and the same rate of noise reduction (slope) with increasing frequency above 20 kHz. The slope is measured to be 4.5 dB decrease in noise per 10 kHz, i.e., the noise decreases with increasing frequency (-4.5 dB per 10 kHz). These spectra show background noise that is present at all times. Superimposed on this background are short duration spikes, presumably switching transients. This pattern of steady background with superimposed spikes was found at every location. At all other locations (other than A, B, and C) however, the amplitude was less and the rate of noise decrease with frequency was greater. In the immediate vicinity of the crusher room, the noise was greatest. The steady-state noise background consisted of a train of powerline related spikes averaging 2.78 ms apart. This time separation indicates rectification or other full-wave use of three-phase power. A three-phase mercury rectifier for trolley haulage purposes is present elsewhere in the mine (more than 250 meters away horizontally and about 90 meters vertically). As will be shown later, measurements made near the 4160 volt lines powering the crusher showed much lower noise than the crusher room area. The conclusion is that something, as yet unidentified, in the crusher room area generated the harmonics of 360 Hz. Noise contour maps that confirm this conclusion will be presented later.

Figure 3-8 shows the spectrum (measured in location C with the crusher running) from 40 Hz to 4 kHz. This shows the largest amplitude 60 Hz measured in the mine. Features of this spectrum are (1) the presence of strong odd numbered harmonics, and (2) the absence of strong 360 Hz and its

harmonics. Strong 360 Hz and harmonics have been associated with three-phase full wave rectifiers in other mines measured. To cover the amplitude range of the measured signal, the abscissa of figure 3-8 shows 130 dB of amplitude range. All other spectra use an abscissa with 100 dB of amplitude range.

Two other areas that were also within 30 meters of the crusher room are the crusher access drift (labeled D on figure 3-2) and the 603 intersection (labeled E). Figure 3-9 shows the spectrum measured at location D. The noise amplitude is lower at D than at A by 10 to 20 dB below 1000 Hz, and by about 3 dB between 1500 Hz and 10 kHz. Above 10 kHz the noise changes with a slope of -6.75 dB per 10 kHz of increasing frequency (as opposed to -4.5 dB per 10 kHz at location A). Location D was the only area where measurements were made on two different days. Figure 3-10 shows the spectrum obtained two days later at location D. Although the spectrum slope is similar, the amplitude is 3 to 8 dB lower on the later day. An exception is a minor "bump" between 12 and 15 kHz where the amplitude is only about 1 to 2 dB less. The spectrum obtained for a horizontal antenna, oriented for maximum pickup, was about 6 dB lower, and is not shown. In general, noise fluctuations were less in this mine than in other mines where EM noise has been measured. Figure 3-11 shows the 40 Hz to 4 kHz spectrum measured at location D.

The one remaining measurement taken within 30 meters of the crusher room was taken at intersection 603 (location E) and is shown in figure 3-12. Immediately apparent is the much faster rate of noise decrease with increasing frequency (steeper slope). The slope measures -14.75 dB per 10 kHz. The amplitude in the region of 5 to 6 kHz is 1 or 2 dB lower than at A (the highest noise location). The noise amplitude below 1 kHz is 10 to 20 dB lower. No explanation is offered for the variation in slope.

### 3.3.4 Production Area

The production areas are defined as areas that are currently producing ore. The production area measured was the 606E entry labeled F on figure 3-2. This entry was one of a series of similar entries lined up 15 meters under the ore body where LHD's would load with ore. No power lines were in the area. The particular entry where noise was measured was in use as a dinner area. The middle curve in figure 3-13 shows the background noise measured at location F. The background noise at 10 kHz is about 9 dB lower than that found at location A. The rate of change of the noise with frequency (slope) is -6.0 dB per 10 kHz, slightly steeper than at A. At location A, pickup by the antenna with the sensitive axis horizontal and oriented for maximum pickup (45° to tunnel) varied from 11 dB less at 10 kHz to 14 dB less at 35 kHz (not shown) than for vertical pickup. In figure 3-13, the upper curve shows a type of "high frequency" noise produced by a LHD that has passed by. The LHD was out of sight around a corner and was about 10 to 15 meters away. The fundamental is near 11,900 Hz, and harmonics (up through the 8th near 96 kHz) are visible. This "high frequency" noise is higher than the background by at least 10 dB at 60 kHz. The loop antenna with horizontal sensitive axis picked up about 12 dB less "high frequency" LHD noise than the loop with the sensitive axis vertical (not shown). The source of this "high frequency" LHD noise is unknown.

Figure 3-14 shows a much more severe type of noise emitted by the LHD at location F. The LHD was passing directly by the antenna set in the entry (sensitive axis vertical) and was therefore about 2 meters away. The frequency of the fundamental component of this noise is about 425 Hz. This "low frequency" LHD noise is some 6 dB stronger

than the "high frequency" LHD noise at 96 kHz. The "low frequency" LHD noise at 850 Hz at location F, is some 40 dB higher than the background noise at 850 Hz at location A. At 2550 Hz (the 6th harmonic) the LHD noise is some 20 dB higher than the background noise at location A. Figure 3-15 shows the 40 Hz to 4 kHz spectrum of the LHD going by location F. In this spectrum, the comparatively weak fundamental can be seen. This spectrum covers a real time period of 1.34 seconds. During this time, the diesel engine changed its speed so that the alternator interfering fundamental frequency swept over the range from 330 Hz to 410 Hz. The second harmonic swept over twice the range or 660 Hz to 820 Hz. The third harmonic is not visible. The fourth harmonic swept over the range from about 1320 Hz to 1640 Hz, and so on. While not considered necessary, a 3-D plot could resolve whether the engine speed was increasing or decreasing, and whether the LHD was approaching or receding. The frequency of this noise was noted in the mine to vary over wide limits in proportion with engine speed, certainly over a frequency range greater than two to one. This noise can therefore be expected to cover all the spectrum above the lowest fundamental (i.e., it will leave no permanent holes). The noise is presumed to be generated by the alternator on the diesel engine. The power is used for headlights, battery charging, and other vehicle accessories. The LHD's utilize a mechanical torque converter, so a possible noise field from a diesel-electric type drive system can be ruled out. The LHD's are highly mobile. Level 6 is designed to be 100 percent accessible by LHD. Therefore, any place in the mine will be subject to the type of noise shown in figures 3-13, 3-14, and 3-15, whenever a LHD is present.

### 3.3.5 Development Area

The development portions of the mine are defined as areas not yet producing ore. Measurements were made at three locations, lettered G, H and I. Locations G and H were near pneumatic rock drills and location I was near the excavation of a new underground crusher room. These three locations were 100 meters, 140 meters, and 200 meters distant from the crusher room, respectively. The background noise measured at these three areas decreased monotonically as distance from the crusher room increased. The noise measured at location G, the jumbo-drilling face, is shown in figure 3-16. The noise spectrum at location G is 20 dB lower than at location A. The slope is the same as at A (-4.5 dB/10 kHz).

Location H was located near an operating fanhole drill. The pneumatic, fanhole drill was very noisy acoustically (the operator wore ear protectors). However, since the drill used no electrical power, it produced no measurable magnetic noise. The spectrum measured at location H is not shown. It is similar to that shown in figure 3-16, but is about 10 dB lower.

The lowest noise level measured in the mine was at location I. Here, excavation was taking place for a future underground crusher room (more exactly, the No. 2 mine transfer drift). This location was 200 meters away horizontally and 85 meters lower than the crusher room operating on level 6. Location I contained a 40-horsepower, three-phase, 480-volt ventilating fan. Figure 3-17 shows the noise measured at I, the lowest noise level measured in the Grace mine. The noise shown is essentially system noise, and as such establishes an upper limit to mine noise in quiet conditions.

The excavation at location I was being performed by a huge V-10 diesel LHD with an eight cubic-yard (6.17 m<sup>3</sup>) scoop capacity. This LHD would load at I, travel 750 meters to the operating crusher, dump, and return. Figure 3-18 shows the spectrum measured with the LHD about 5 meters from the antenna. The fundamental frequency here is 535 Hz, with the sixth harmonic predominating. The sixth harmonic (at about 3210 Hz) is some 42 dB stronger than the background noise. Again, frequency varied widely with the engine RPM. Figure 3-19 shows the low frequency portion of the spectrum with the V-10 LHD present. Figure 3-20 was taken with the LHD absent, with higher gain, (lower system noise) and shows the background power-line noise.

### 3.3.6 Cross Drift Substation

A second substation where measurements were made is located in the #6 cross drift, identified as J in figure 3-2. This substation contains a 300 KVA step-down transformer (4160 volts to 480 volts) for supplying power to ventilating fans. Both circuits feeding power to the crusher room area pass through this substation. Figure 3-21 shows the spectrum measured at the substation. The spectrum slope is the same as the slope measured at location A; however the amplitude at J is 10 dB less. Since the amplitude is less at J than at A near the crusher, and all the power for the crusher room equipment passes through J, it is concluded the primary steady-state mine background noise is generated in or near the crusher room. The low frequency expanded spectrum is similar to that shown for location D; with the exception that the 60 Hz fields at location J were about 13 dB more than those at D.



### 3.3.7 Underground Workshop-Lunchroom

Figure 3-3 shows an expanded view of the underground servicing and fueling facilities for the LHD's. Figure 3-1 shows the relationship between the rest of the mine and the shop area. This area also contains offices, a LHD parking area, a lunchroom (with fluorescent lights), ore storage silos, and the motor for the main conveyer belt from the crusher room. The conveyer-belt motor has a 200 horsepower rating and uses 4160 volts. The only rectifier identified in this area was a small 110 volt single-phase unit used for lighting indicator lamps on the conveyer control panel.

Measurements were taken in the lunchroom, labeled by letter K on figure 3-3. Figure 3-22 shows the spectrum measured in the lunchroom. The antenna sensitive axis was vertical. With the antenna axis horizontal and oriented for maximum pickup, the measured spectrum is essentially the same as shown in figure 3-22, with the exception that the horizontal spectrum is 2 to 4 dB lower between 2 kHz and 5 kHz (not shown). In comparing the spectra measured at location K and location A, the spectrum at K: (1) is about 15 dB lower, (2) has about the same slope between 5 and 40 kHz (except for a bump at 10 to 15 kHz), and (3) exhibits aperiodic noise below 5 kHz and between about 40 and 90 kHz. We speculate that the aperiodic noise comes from the fluorescent lights in the lunchroom. The powerline-related train of pulses, averaging 2.78 ms spacing, was observed with the portable oscilloscope at the lunchroom as well as at the opposite end of the mine near the crusher room.

Figure 3-23 shows the low-frequency, expanded spectrum measured in the lunchroom. Strong odd harmonics of 60 Hz are evident.

Figure 3-24 shows a LHD passing by area K. It was measured with different instrumentation. This spectrum extends out to 20 kHz. Spectra taken out to 180 kHz indicate LHD noise continues at a constant or slightly rising level from 100 to 180 kHz (not shown).

### 3.3.8 Composite of Worst Case Steady Noise

Figure 3-25 is a composite of the highest steady-state background noise (area A) overlain by the highest LHD spectra measured (area F). A line (or envelope) drawn over the peaks of the LHD and background noise may reasonably be used for highest expected noise levels in Grace Mine. Figure 3-17 shows the lowest noise level measured (area I), some 65 dB lower at 1000 Hz to 35 dB lower at 40 kHz.

### 3.4 Pulse Produced with Explosion

Several impulses associated with blasting in the mine were recorded. The closest explosion produced the strongest impulse; the compression wave in the rock and the sound followed the impulse by a fraction of a second. Figure 3-26 shows the spectrum of the impulse, which was recorded at location A a few seconds after the noise background spectrum was recorded. Compared to the worst case composite (figure 3-25), the impulse spectrum amplitude is 13 dB lower at 1 kHz, equal at 5 kHz, and up to 7 dB higher from 10 kHz to 90 kHz.

Figure 3-27 shows a 1.02 second segment of data taken during the explosion. The figure is a contour map (produced from 157 individual spectra) showing magnetic field strength from 1 to 100 kHz as a function of time. The contour interval is 3.33 dB. The figure coordinate axis format is intentionally chosen to be unconventional so that the axes will

be consistent with the 3-D figure presented later. Figure 3-27 shows three groups of 5 to 7 individual detonations with a single detonation at 1.0 second delay. The final detonation may be the beginning of a possible fourth group, or single isolated shot used near the roof of the drift. The duration of a group of detonations is about 125 to 175 ms. The separation between the first detonation of sequential groups is 250 to 450 ms. While no positive identification as to location and type of blast was made at the time the measurements were made, it is believed the blast was in a small 3 by 2.1 meter development drift. These blasts typically use 20 to 24 holes filled with explosives (figure 3-26 shows approximately 21 individual detonations, or holes). The holes are shot in concentric "wedges" (or groups); the central wedge is detonated first, with following wedges delayed by multiples of 25 milliseconds. This type of shot is sometimes done near the noon hour; data for figure 3-27 was taken at 11:35 a.m. The possibility that the signature shown came from the electrical pulse used in igniting the cap is ruled out. All caps in the entire blast are connected electrically in parallel and are ignited simultaneously by a single electrical impulse. The required delay is built into each cap. The magnetic signature shown in figure 3-27 probably originates from the movement of free ions in the expanding plasma produced by the detonating nitrate explosives.

Figure 3-28 shows a computer-drawn three-dimensional (3-D) view of the first two "wedges" fired. The time covered is 450 ms. This shows the inequality in intensity of each hole (which is to be expected as each hole is of different length and loaded differently).

### 3.5 Mine Noise Contour Maps

To give a better picture of how noise varied as a function of location, several contour maps are presented. Four frequencies were selected, 2 kHz, 10 kHz, 20 kHz and 60 kHz, and from these data four contour maps were produced. Each map is produced by selecting a given frequency, say 2 kHz, and then recording the amplitude measured at each location in the mine on a map. Lines of constant magnetic noise level are then drawn on the map. Areas of high or low noise level can then be more easily located. It is acknowledged that eleven measurement locations are not enough locations to provide a detailed map, accurate enough to produce reliable extrapolation of noise intensities at areas far from locations actually measured. The intent is to give a feeling of the overall noise distribution using available information.

Figures 3-29, 3-30, 3-31 and 3-32 show Grace Mine noise contour maps for frequencies 2 kHz, 10 kHz, 20 kHz, and 60 kHz, respectively. Every map shows an area of high noise centered approximately on the crusher room. Note also that the noise tends to follow the powerlines (through area J) to some extent.

### 3.6 Miscellaneous Measurements

#### 3.6.1 Electric Field

An active dipole, 1.93 meters long, was used as a sensor on the second day while in area D (crusher access drift). This dipole has not been calibrated, nor have any system nonlinearities in gain vs. frequency been removed by a correction curve. All field strength information is therefore qualitative only. Figure 3-33 shows unprocessed data results obtained with the dipole ends pointed across (perpendicular to) the drift. Measurements taken with the dipole

pointed vertically (up-down) and in the direction of (parallel to) the drift gave spectra that were 10 or more dB lower than figure 3-33. Maximum noise pickup was found a few tens of meters away along the drift under some steel reinforcing ribs. The noise spectrum has the same shape as figure 3-33 and is 2 dB higher.

Because of the relative nature of the electric field measurements, the principal conclusions that can be drawn are restricted to: (1) an electric noise field exists in location D; (2) it is primarily a train of spikes, similar to the magnetic field noise, occurring at an average rate of 360 times per second; and (3) the electric field is strongest for horizontal dipole orientation across (perpendicular to) the drift.

### 3.6.2 Measurement of Voltage Between "Roof Bolts"

A single roof-support-bolt measurement was performed at location D on the second day. The separation between the two bolts was 10 meters, and the voltage was measured using non-shielded copper wire clipped to the bolts. Figure 3-34 shows the resulting spectrum. No receiver system noise curve is available for this spectrum. However, since the characteristic 360 Hz harmonic structure extends out to about 40 kHz, values out to 40 kHz are probably not obscured by system noise. It is not possible to say that the voltage measured between bolts was induced by any single mechanism. It may be any combination of electric field and magnetic field acting on the copper wires connected to the bolts, as well as by any potential produced by current flow between the bolts. To enhance electric field effects, a measurement was made with a single wire (a "monopole"). The resulting noise spectrum is 10 to 15 dB higher in the range from 1 kHz to 30 kHz than the spectrum shown in figure 3-34. This is probably due to the high input impedance ( $10^8$  ohms) of the receiver. This effect has been found in other mines.

## 3.7 Intercomparison of Magnetic-Field Noise in Different Mines

### 3.7.1 Summary of 1 to 3 kHz Data

Figure 3-35, lower curve, is a summary of magnetic field strength at power-line harmonic frequencies observed within Grace. Plotted are the logarithmic averages of the six highest powerline harmonics. Average fields at E, F, G, H, and I are plotted as a function of distance from the crusher room. Point C is crusher room substation data taken with the antenna about 3 meters from the control panels.

The six frequencies chosen are between 1020 Hz and 2940 Hz, but are not, in all cases, the third through eight harmonics of 360 Hz, which were the frequencies of maximum energy in Robena No. 4 Mine. The frequencies chosen are close enough to make a valid comparison between noise levels in Robena and Grace.

The Grace noise (as shown by the lower approximate data trend curve) is 10 to 20 dB lower than the Robena noise up to 100 meters. Beyond 100 meters, the Grace noise falls off much faster than the Robena noise. Two factors may contribute to this rapid fall off;

- (1) The Robena noise comes primarily from a line source (the trolley-rail transmission-line) whereas the Grace noise comes primarily from a point source in the crusher room.
- (2) The geological geometry and rock types are different. In Grace, propagation is entirely through dry diabase rock, 15 to 45 meters below an ore body containing 40 percent magnetite and 60 percent chlorite. In Robena, propagation is through coal several meters thick sandwiched between shale.

### 3.7.2 Magnetic-Field Spectra 3 kHz to 180 kHz

In addition to the low-frequency comparison given in this section, spectral plots to 180 kHz taken from several mines can give some idea as to relative noise levels in the different mines. The spectra have  $\pm 2$  dB uncertainty from 3 to 180 kHz, but are shown to 200 kHz. Spectra of electrically noisy pieces of equipment in four different mines are shown superimposed on figure 3-36. There may have been noisier equipment, but those selected were: (1) a LHD in Grace Mine, (2) a shuttle buggy and continuous miner combination in McElroy Mine, (3) an unidentified machine in a longwall section in Itmann #3 Mine, and (4) a car pull in Robena Mine (this curve extends only to 100 kHz). As might be expected, machines which depend on electrical power for basic work force do make more electrical noise than diesel-powered equipment which only has ancillary electric systems. Also, although the spacing between measurement system antenna and source were approximately the same, the spacing makes a crucial ( $d^{-3}$ ) difference; therefore these curves are somewhat qualitative, even though the measurement uncertainty is less than 2 dB.

A similar comparison of noise levels in four different mines, away from noise sources, but near transmission lines, are shown in figure 3-37. Measurement system noise is indicated by showing dashed curves over the portion of the spectrum where system noise is 1 dB or closer to measured mine noise.

The results show that although electromagnetic noise levels in Grace Mine are generally somewhat lower than in mines with other types of equipment, the levels adjacent to noisy sources are comparable to levels near sources in other mines in some cases. The noise levels do not decrease monotonically with frequency in this mine.

<u>Letter Designation</u>	<u>Description</u>
A	Development foreman office
B	601 intersection
C	crusher substation
D	crusher access drift
E	603 intersection
F	606E entry, dinner area
G	jumbo-drilling face
H	608E fanhole drill
I	No. 2 mine transfer drift
J	No. 6 cross drift substation
K	shop office

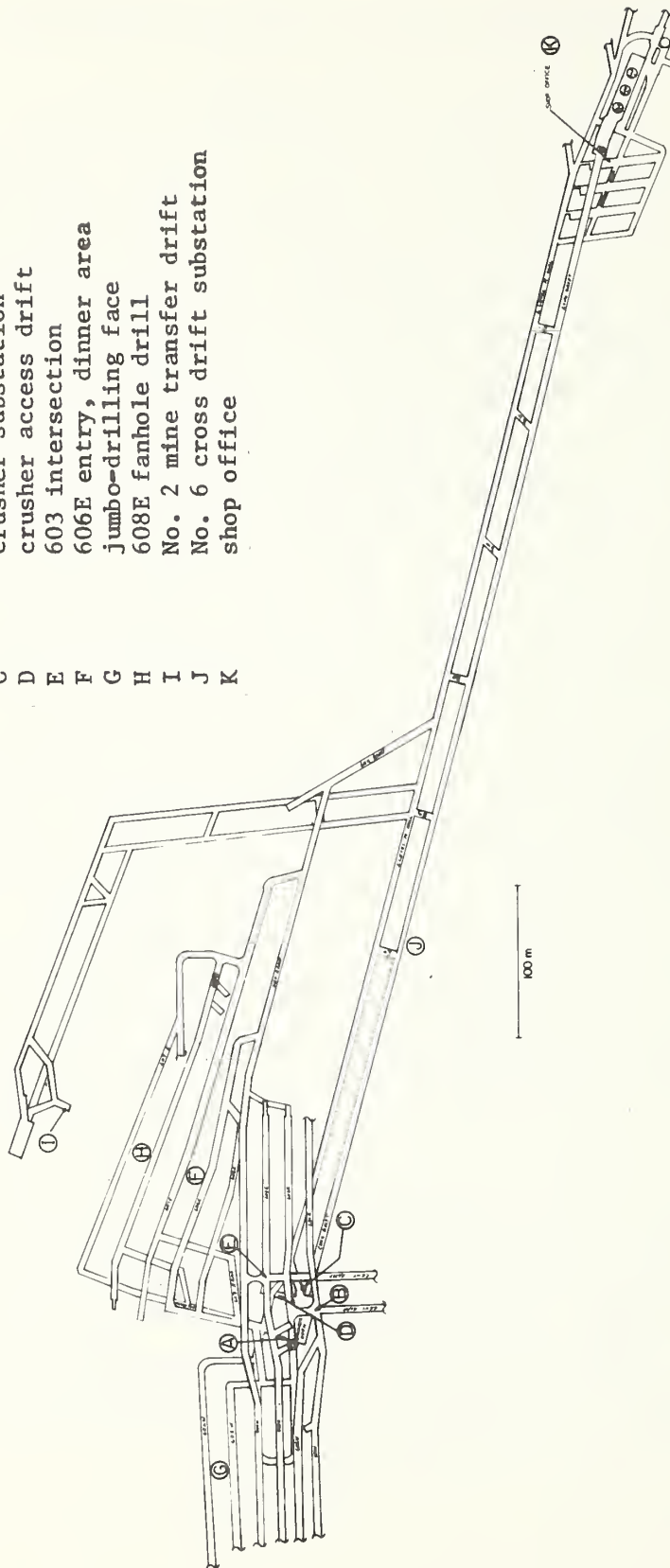


Figure 3-1 Simplified map of Grace Mine where measurements were made.



Letter Designation	Description
A	Development foreman office
B	601 intersection
C	crusher substation
D	crusher access drift
E	603 intersection
F	606E entry, dinner area
G	jumbo drilling face
H	608E fanhole drill
I	No. 2 mine transfer drift
J	No. 6 cross drift substation
K	shop office

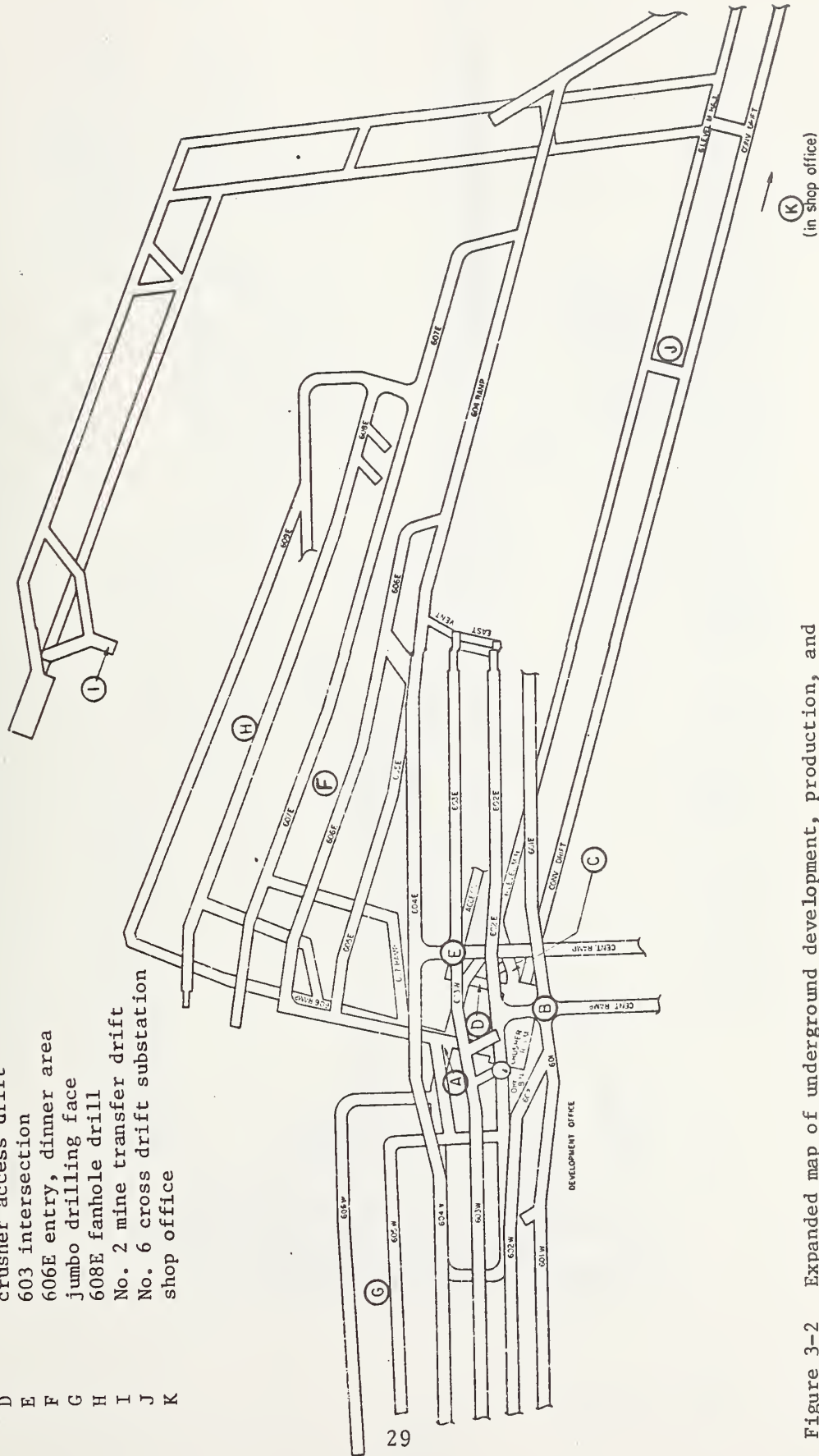


Figure 3-2 Expanded map of underground development, production, and crusher-room areas.

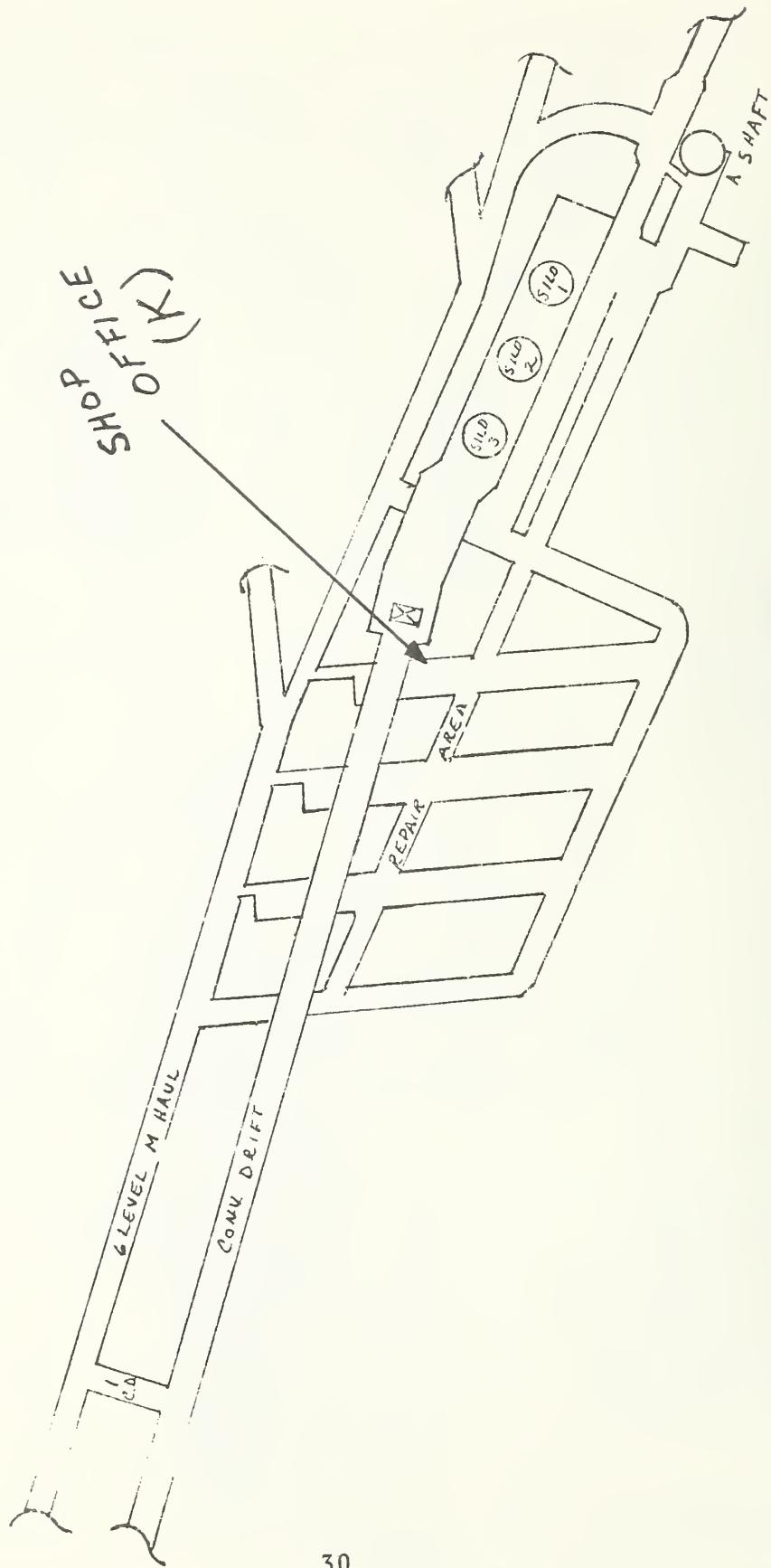


Figure 3-3 Expanded map of underground workshop and lunchroom area.

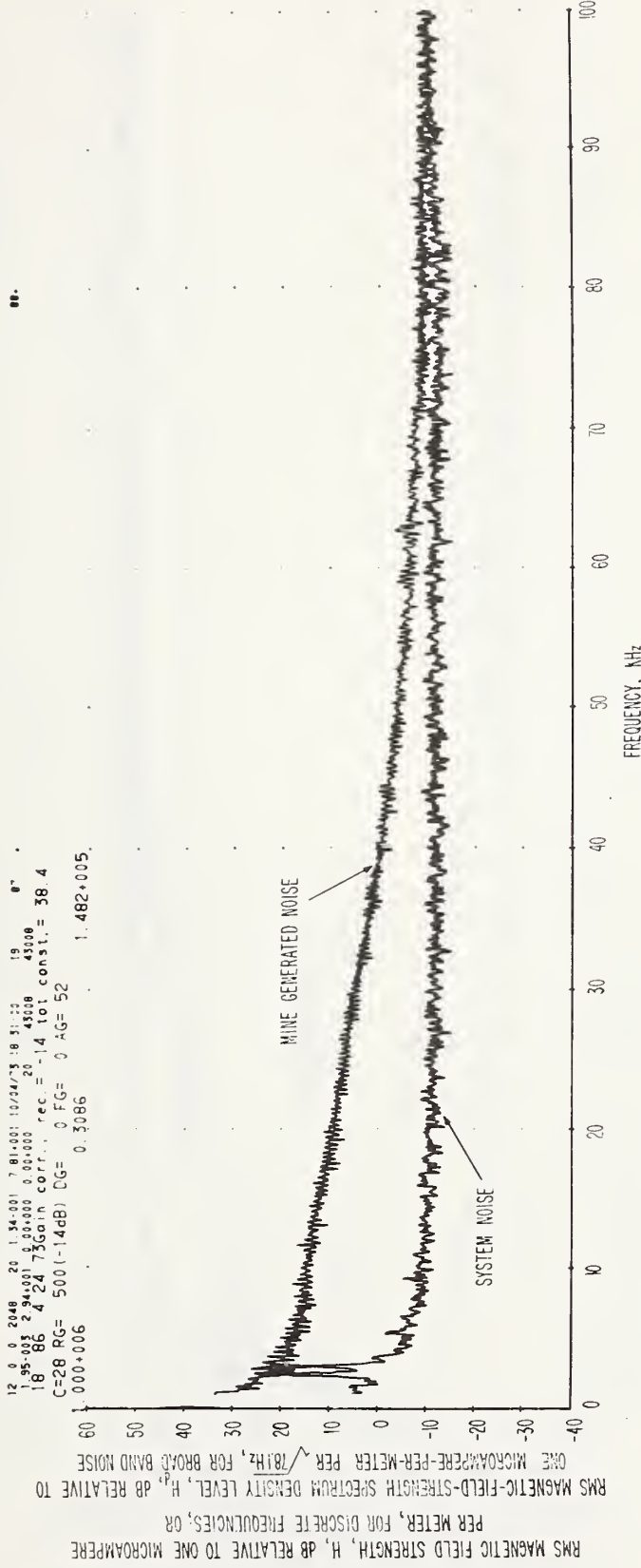


Figure 3-4 Spectrum of magnetic field strength obtained on a loop antenna 1 kHz to 100 kHz, Grace Mine, underground, development foreman office, antenna sensitive axis vertical, 11:35 a.m., April 24, 1973. Area noise before explosion. Spectral resolution is 78.1 Hz.

12 6 0 2048 20 1.34-001 7.81+001 10/04/73 10.51 40 47 227  
 46 86 4 24 736000 0.00+000 0.00+000 43000 43000  
 C=28 RG= 200 (-6dB) DG= 0 FG= 0 AG= 52  
 0.000+009 0.3086 1.444+008

RMS MAGNETIC FIELD STRENGTH, H<sub>1</sub>, DB RELATIVE TO ONE MICROAMPERE PER METER, FOR DISCRETE FREQUENCIES, OR RMS MAGNETIC-FIELD-STRENGTH SPECTRUM DENSITY LEVEL, H<sub>1</sub>, DB RELATIVE TO ONE MICROAMPERE-PER-METER PER  $\sqrt{781\text{Hz}}$ , FOR BROAD BAND NOISE

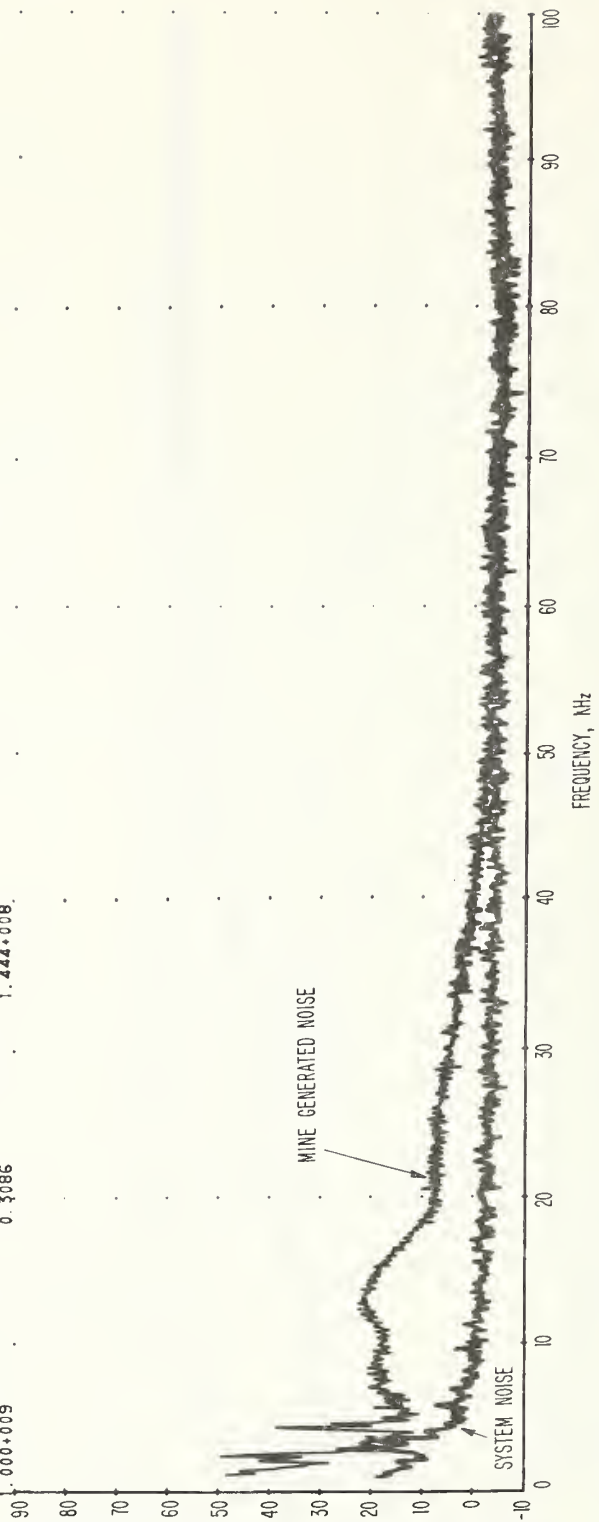


Figure 3-5 Spectrum of magnetic field strength obtained on a loop antenna 1 kHz to 100 kHz, Grace Mine, underground crusher substation, antenna sensitive axis vertical, 4:30 p.m, April 24, 1973. Crusher is not operating. Spectral resolution is 78.1 Hz.

12 0 0 2048 20 1.54-001 7.81-001 10/04/73 18 51:00 45 222  
 1.95-003 -4.24-001 0.00-000 0.00-000 20 43008 43008  
 45 86 4 24 73Gain corr. rec. = -26 tot const. = 26.4  
 C=26 RC= 2000 (-26dB) DG= 0 FG= 0 AG= 52  
 0.000+007 0.3086 1.471+006.

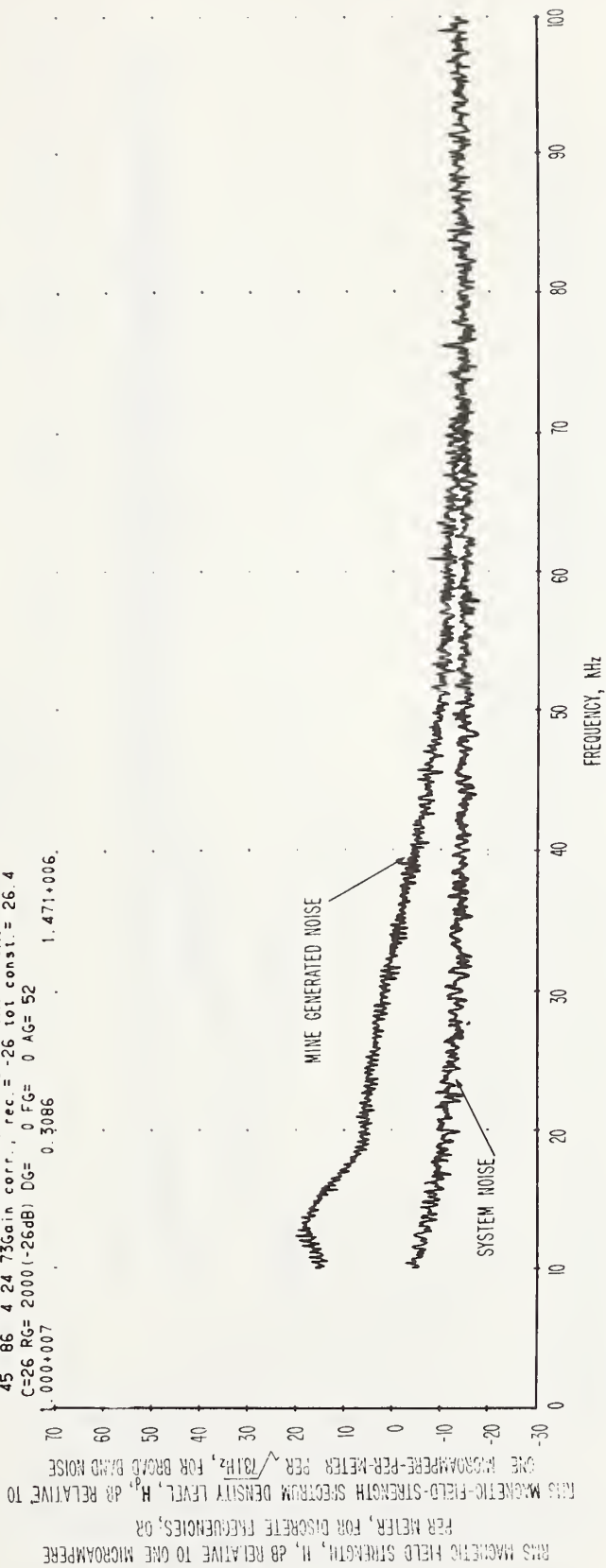


Figure 3-6 Spectrum of magnetic field strength obtained on a loop antenna 10 kHz to 100 kHz, Grace Mine, underground, crusher substation, antenna sensitive axis vertical, 4:30 p.m, April 24, 1973. Crusher is not operating. Spectral resolution is 78.1 Hz.

12 0 0 2040 20 1.54+001 7.01+001 10/04/73 18 52.26 48 232  
 1.95+003 -4.40+001 0.00+000 0.00+000 20 43000 43000  
 4.7 86 4 24 75Gain corr., rec. = -26 tot const. = 26.4  
 C=26 RG= 2000 (-26dB) DG= 0 FG= 0 AG= 52  
 000+007 0.3086 1.254+006.

235.

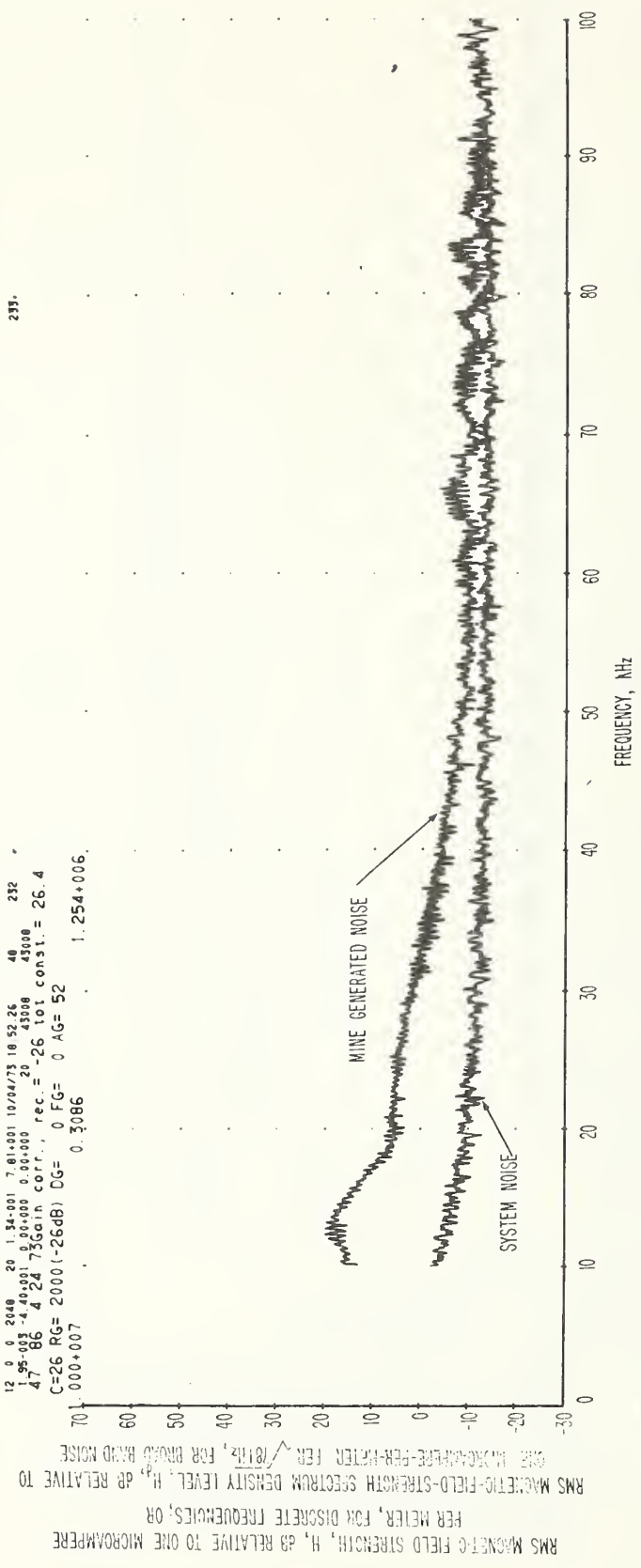


Figure 3-7 Spectrum of magnetic field strength obtained on a loop antenna 10 kHz to 100 kHz, Grace Mine, underground, crusher substation, antenna sensitive axis vertical, 4:35 p.m., April 24, 1973. Crusher is operating. Spectral resolution is 78.1 Hz.

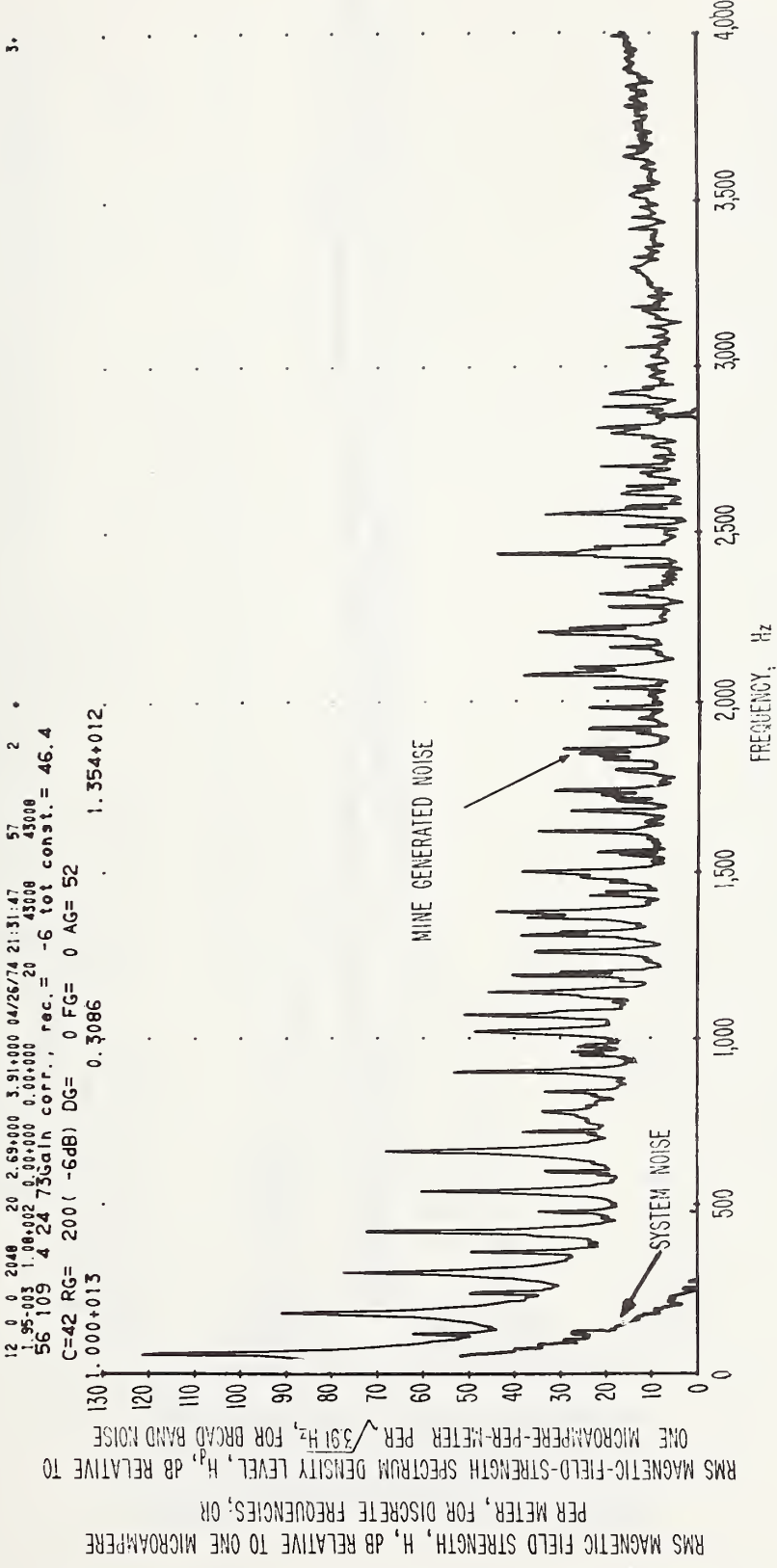


Figure 3-8 Spectrum of magnetic field strength obtained on a loop antenna 40 Hz to 4 kHz, Grace Mine, underground, crusher substation, antenna sensitive axis vertical, 4:30 p.m., April 24, 1973. Crusher is working. Spectral resolution is 3.91 Hz.

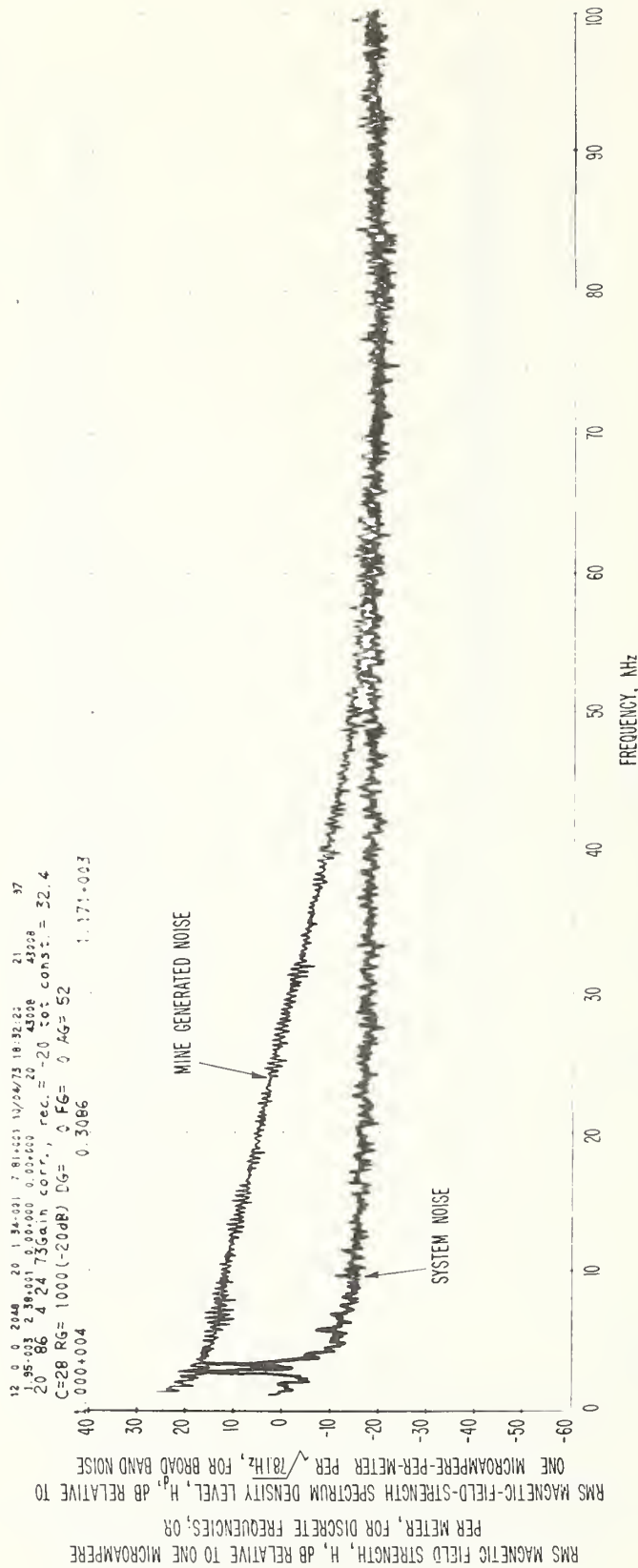


Figure 3-9 Spectrum of magnetic field strength obtained on a loop antenna 1 kHz to 100 kHz, Grace Mine, underground, crusher access drift, antenna sensitive axis vertical, 12:00 noon, April 24, 1973. Crusher is not operating. Explosion. Spectral resolution is 78.1 Hz.



12 0 0 2048 20 1.54+001 7.81+001 10/04/75 18:59:48 58 202  
 1.95-003 -2.97+001 0.00+000 0.00+000 20 45008 45008  
 57 86 4.26 736gain corr., rec. = -20 tot const. = 32.4  
 C=25 RG= 1000 (-20dB) DG= 0 FG= 0 AG= 52  
 1.000+003 0.3086 8.984+002.

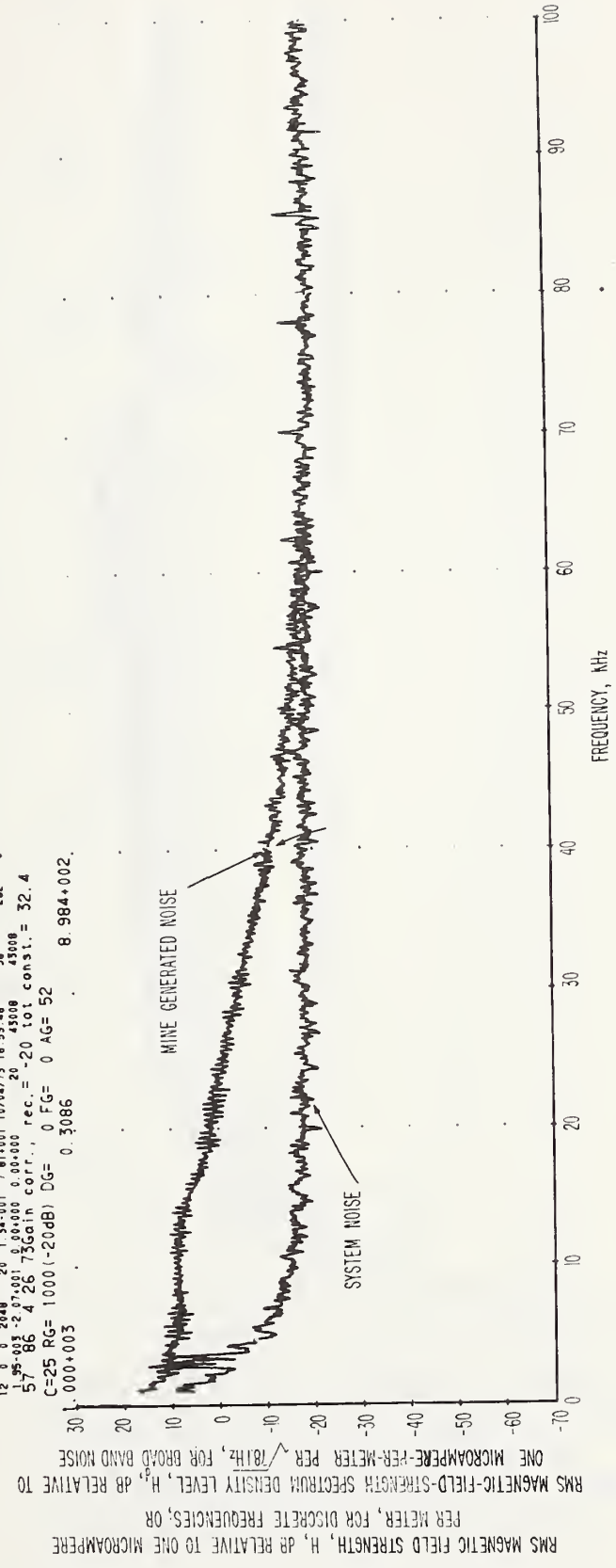


Figure 3-10 Spectrum of magnetic field strength obtained on a loop antenna 1 kHz to 100 kHz. Grace Mine, underground, crusher access drift, antenna sensitive axis vertical, 10:27 a.m., April 26, 1973. Crusher is operating. Two days later. Spectral resolution is 78.1 Hz.

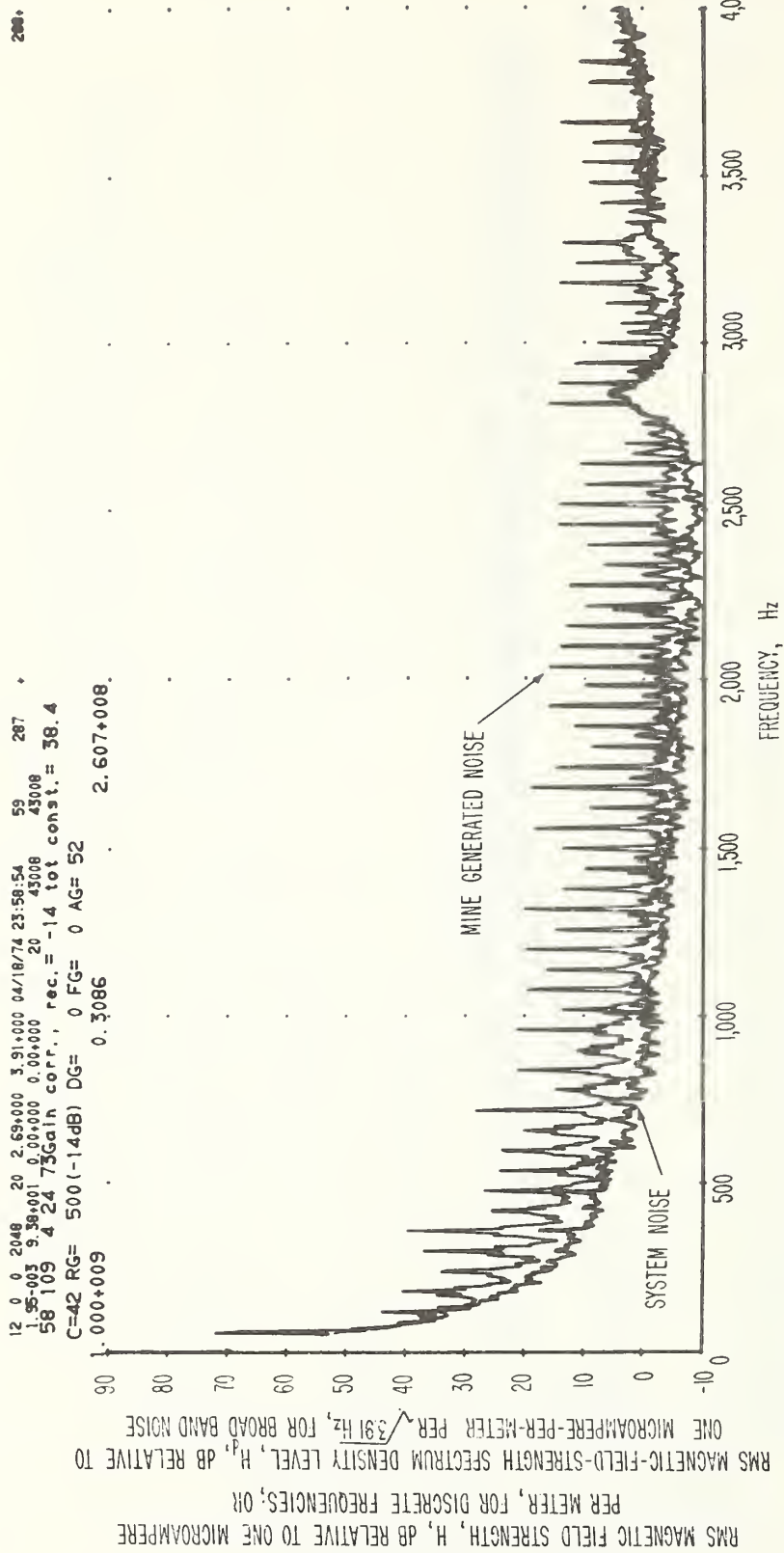


Figure 3-11 Spectrum of magnetic field strength obtained on a loop antenna 40 Hz to 4 kHz, Grace Mine, underground, crusher access drift, antenna sensitive axis vertical, 4:47 p.m, April 24, 1973. Crusher is working. Spectral resolution is 3.91 Hz.

12 0 0 2048 20 1.34-001 7.01-001 10/04/73 10 36:35 27 12" 1  
 25-003 2.53-001 3.00-000 0.00-000 20 43000 43000  
 26 86 4 24 750gain corr., rec. = -20 tot const. = 32.4  
 C=28 RG= 1000(-20dB) DG= 0 FG= 0 AG= 52  
 000+004 0.3086 1.264+003

:20.

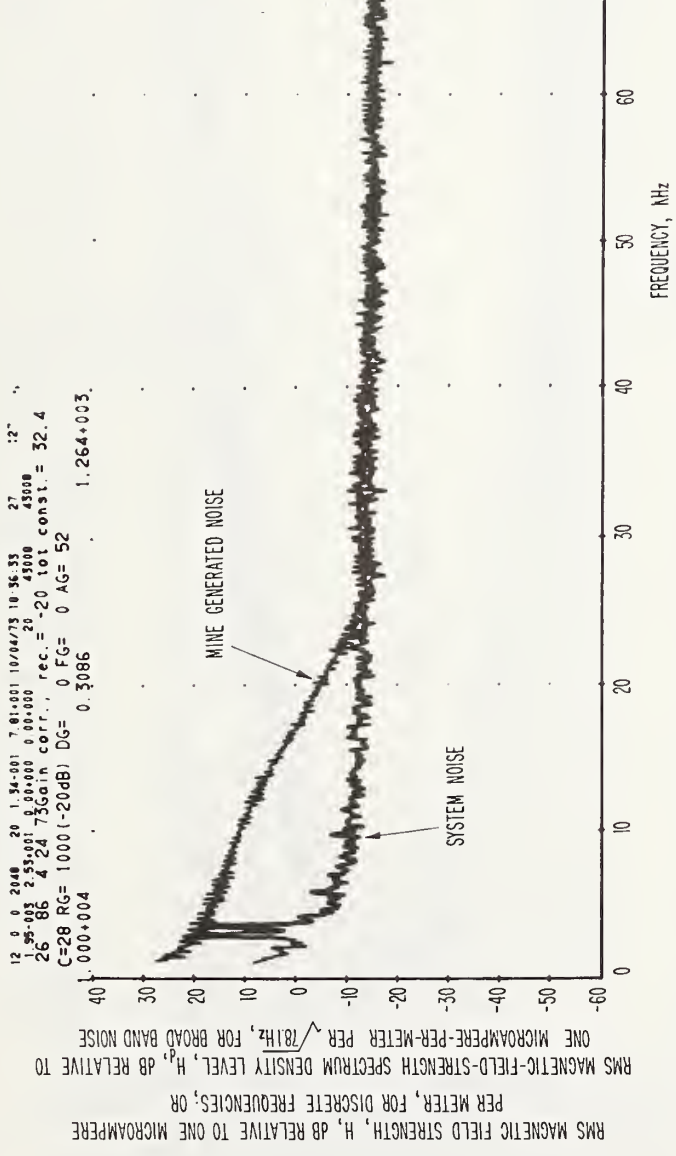


Figure 3-12 Spectrum of magnetic field strength obtained on a loop antenna 1 kHz to 100 kHz, Grace Mine, underground, intersection 603, antenna sensitive axis vertical, 12:55 p.m., April 24, 1973. Production area. Spectral resolution is 78.1 Hz.

12 6 6 2040 20 1.34+001 7.81+001 10/04/73 18 22 56 32  
 1.75+008 -2.17+001 0.00+000 0.00+000 45000  
 86 4.24 73 Gain corr., rec. = -34 Tot const. = 18.4  
 C=26 RG= 5000 (-34dB) DG= 0 FG= 0 AG= 52  
 .000+008 0.3086 5.239+007.

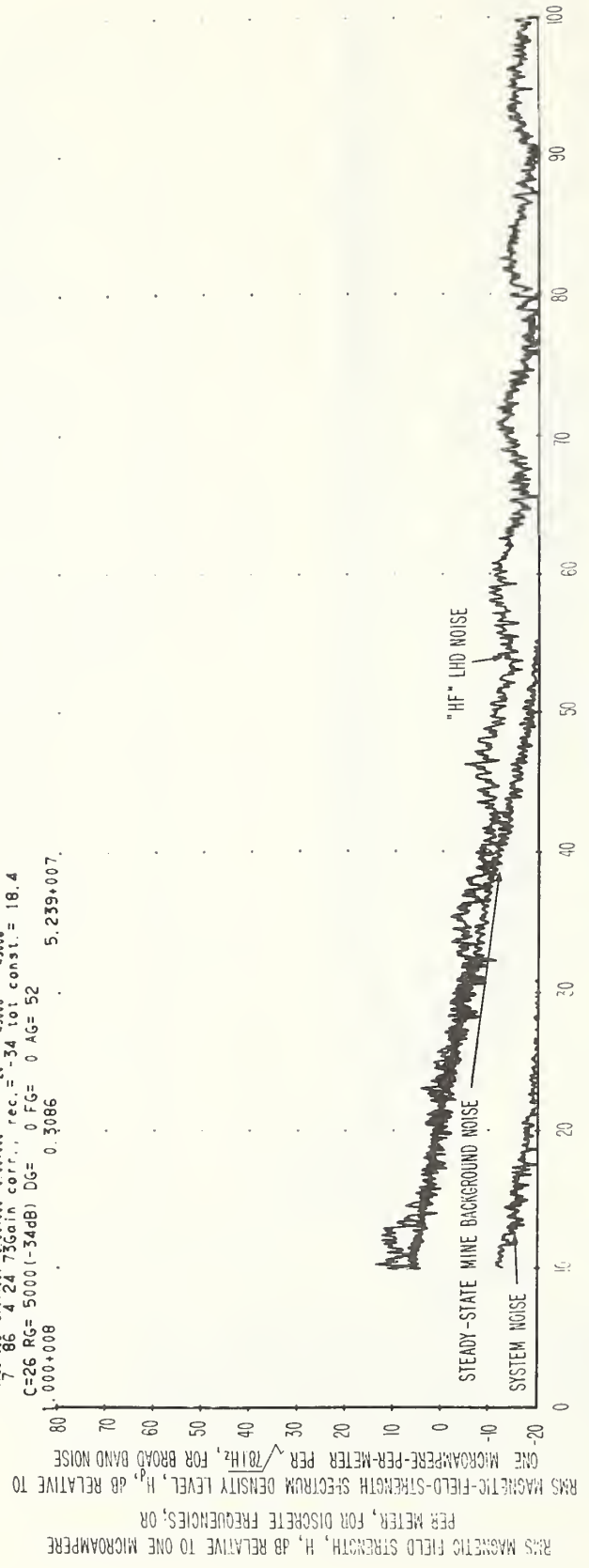


Figure 3-13 Spectrum of magnetic field strength obtained on a loop antenna 10 kHz to 100 kHz, Grace Mine, underground, entry and dining area 606E, antenna sensitive axis vertical, 10:45 a.m., April 24, 1973, Empty V-8, diesel LHD passed by. Spectral resolution is 78.1 Hz.

12 0 0 2048 20 1.34-001 7.81+001 10/04/73 18 25.01 11 47  
 1.95-003 -4.32-001 0.05+000 0.00+000 23 45008 43008  
 10 86 4 24.75Gain corr., rec. = -14 101 const. = 38.4  
 C=28 RG= 500 (-14dB) DG= 0 FG= 0 AG= 52  
 1.000+008 0.3086 3.504+007.

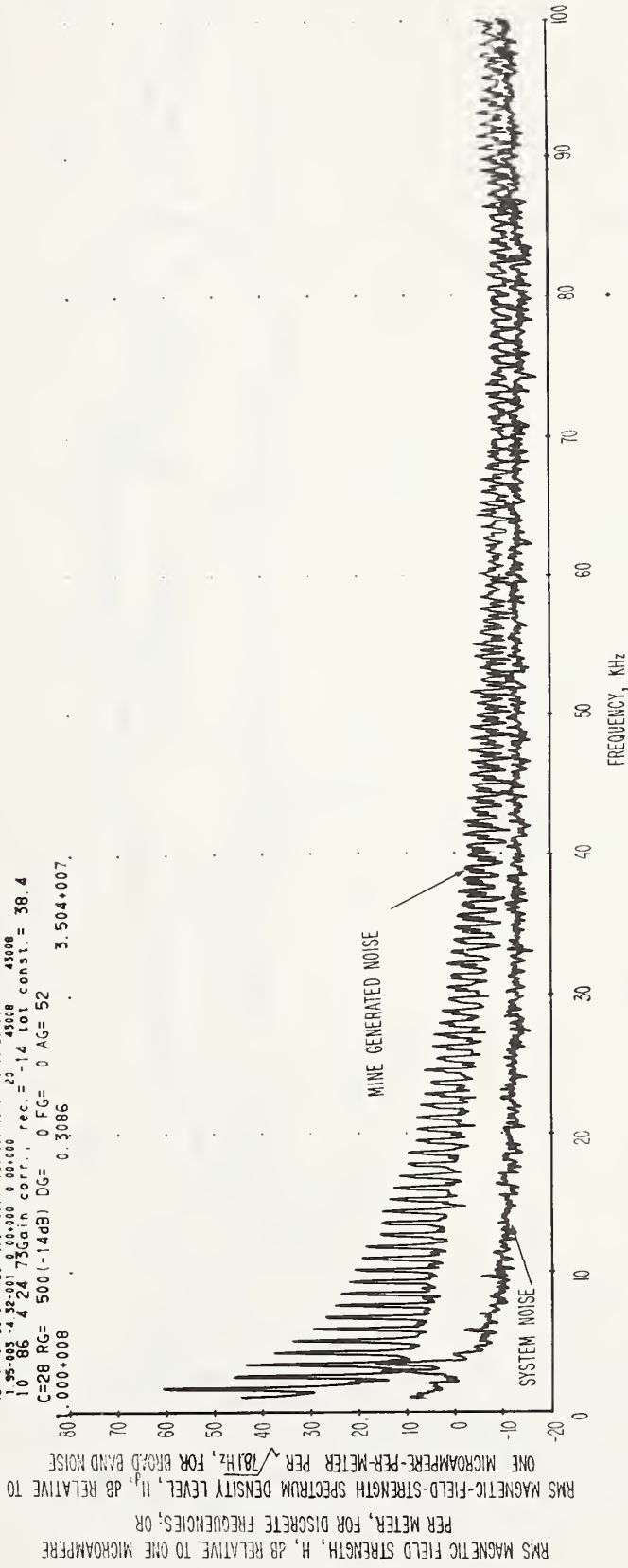


Figure 3-14 Spectrum of magnetic field strength obtained on a loop antenna 1 kHz to 100 kHz, Grace Mine, underground, entry and dining area 606E, antenna sensitive axis vertical, 11:55 a.m., April 24, 1973. V-8 diesel LHD nearby. Spectral resolution is 78.1 Hz.

12 0 0 2048 20 2.69+000 3.91+000 04/18/74 23:46:05 41 197 \*  
 1.95-003 9.11+001 0.00+000 0.00+000 20 43008 43008  
 40 109 4 24 75Gain corr., rec. = -14 tot const. = 38.4  
 C=42 RG= 500(-14dB) DG= 0 FG= 0 AG= 52  
 1.000+009 0.3086 2.362+008

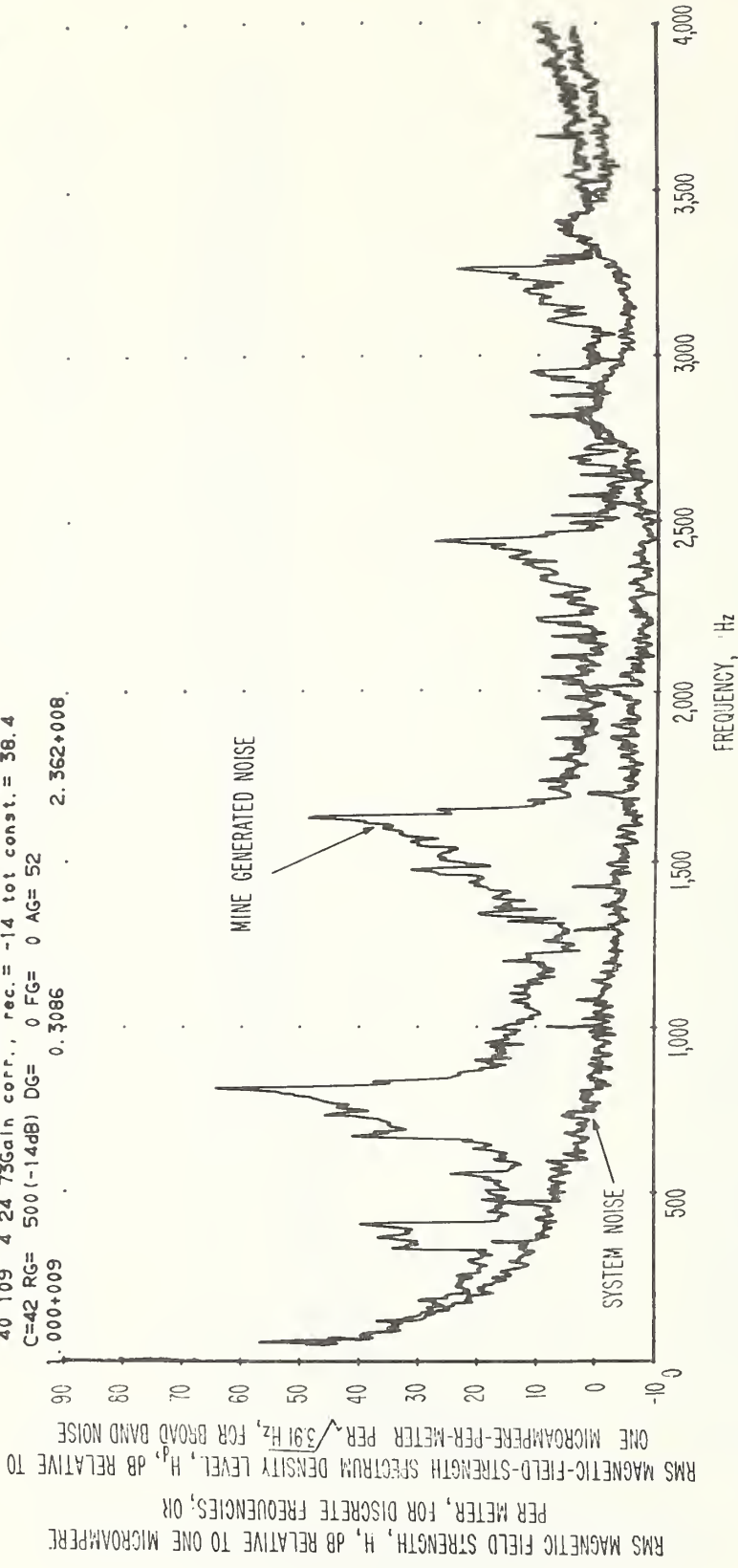


Figure 3-15 Spectrum of magnetic field strength obtained on a loop antenna 40 Hz to 4 kHz, Grace Mine, underground, entry and dinner area 606E, antenna sensitive axis vertical, 11:56 a.m., April 24, 1973. Loaded LHD. Spectral resolution is 3.91 Hz.

12 0 0 2048 20 1.34-001 7.81-001 10/24/73 18 33 40 25 107  
 1.95-003 2.63-001 0.00-000 0.00-000 20 43008 43008  
 22 86 4 24 73Gain corr., rec. = -34 101 const. = 18.4  
 C=28 RG= 5000(-34dB) DG= 0 FG= 0 AG= 52  
 1.000\*002 0.3086 1.665\*001.

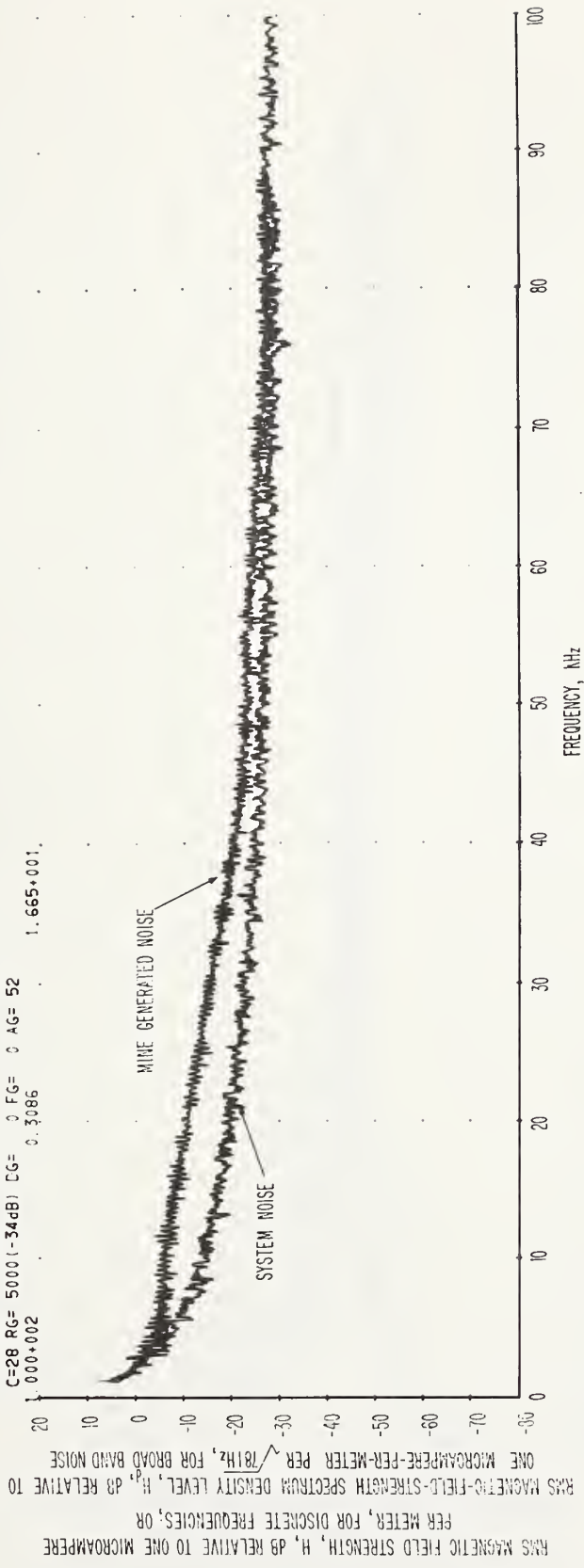


Figure 3-16 Spectrum of magnetic field strength obtained on a loop antenna 1 kHz to 100 kHz, Grace Mine, underground, 9.2 m from Jumbo drill working face, antenna sensitive axis vertical, 12:25 p.m., April 24, 1973. Drill operating. (No change in figure whether one drill bit or two drill bits are being used.) Spectral resolution is 78.1 Hz.

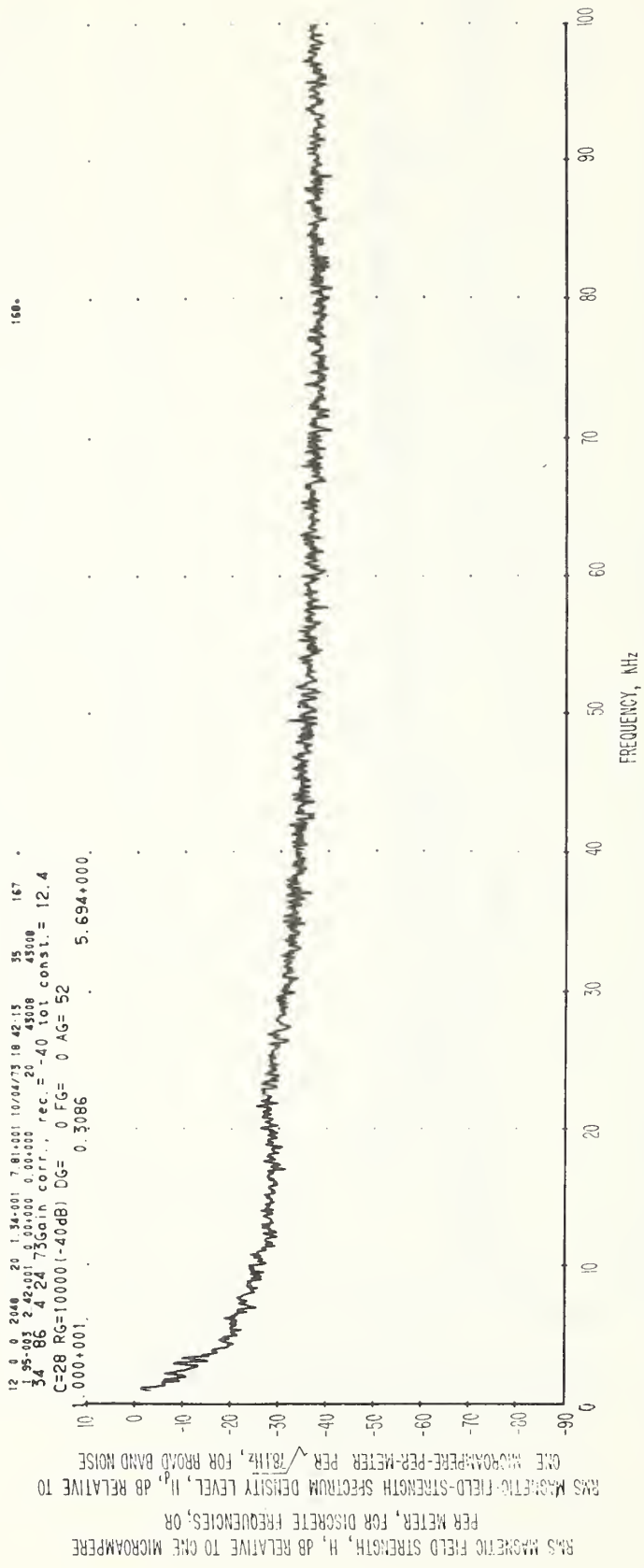


Figure 3-17 Spectrum of magnetic field strength obtained on a loop antenna 1 kHz to 100 kHz, Grace Mine, underground, Number 2 mine. transfer drift, antenna sensitive axis vertical, 2:22 p.m., April 24, 1973. Power-line harmonics. Spectral resolution is 78.1 Hz.



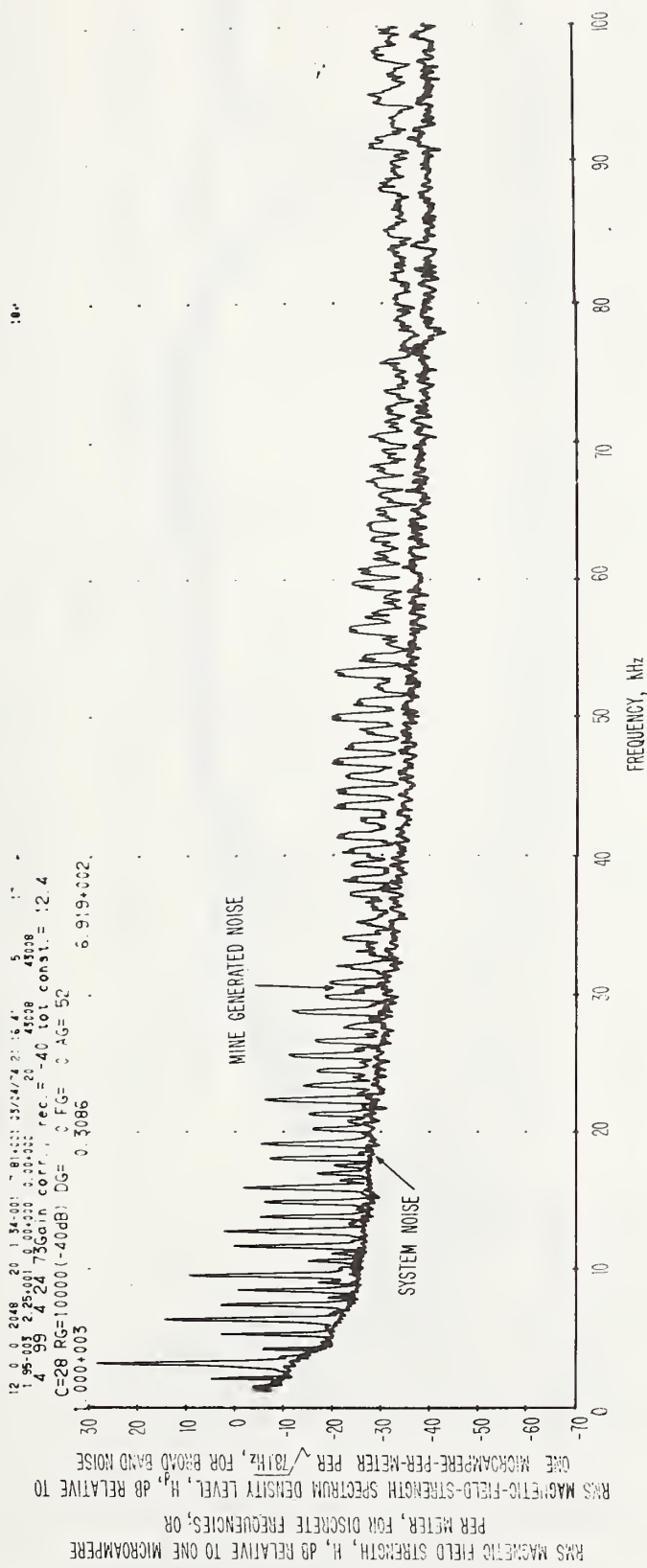


Figure 3-18 Spectrum of magnetic field strength obtained on a loop antenna 1 kHz to 100 kHz, Grace Mine, underground, Number 2 mine transfer drift, antenna sensitive axis vertical, 2:22 p.m., April 24, 1973. Huge V-10 diesel LHD nearby. Spectral resolution is 78.1 Hz.

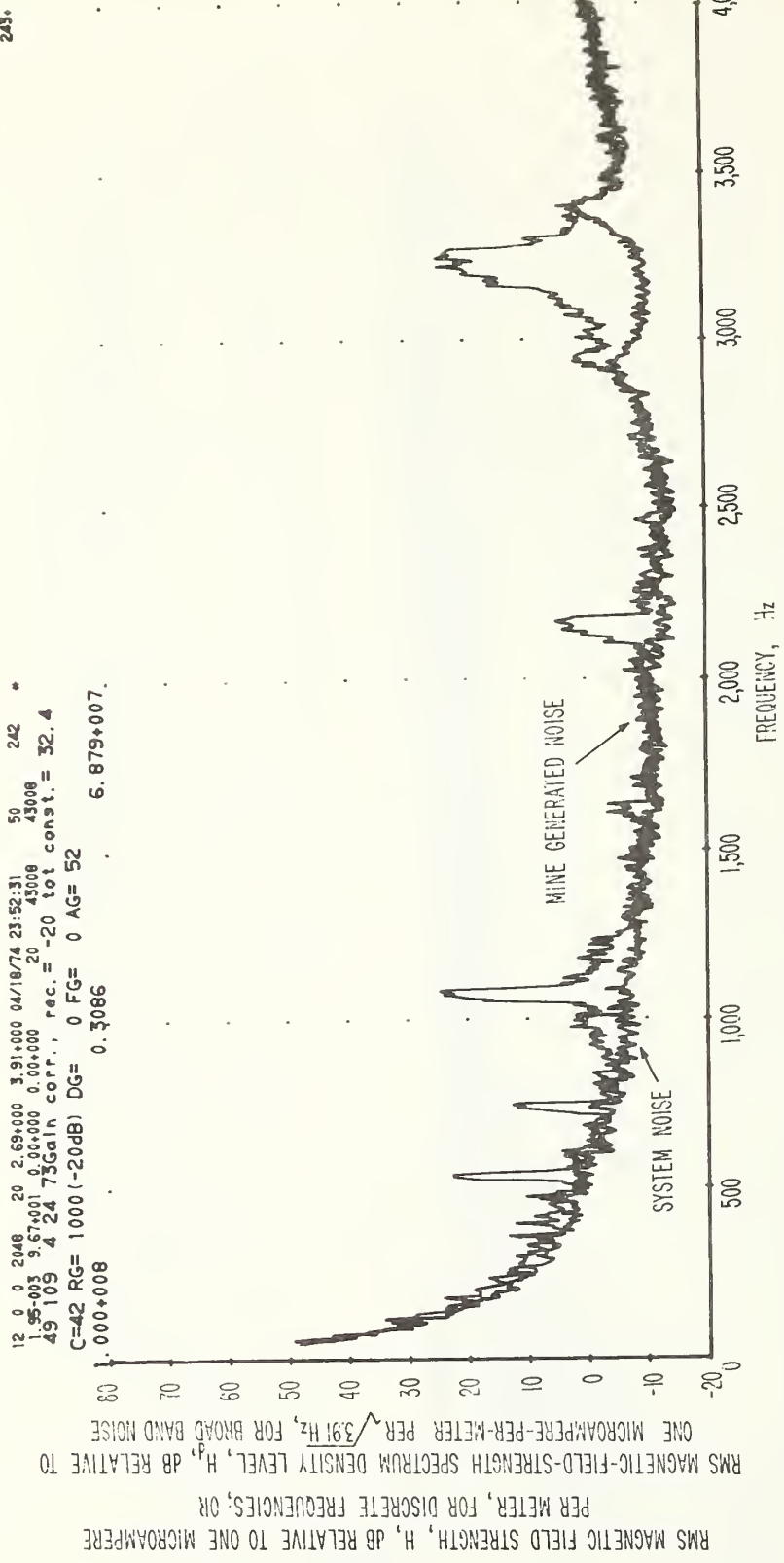


Figure 3-19 Spectrum of magnetic field strength obtained on a loop antenna 40 Hz to 4 kHz, Grace Mine, underground, Number 2 mine transfer drift, antenna sensitive axis vertical, 2:20 p.m., April 24, 1973. V-10 LHD. Spectral resolution is 3.91 Hz.

12 0 0 2048 20 2.69+000 3.91+000 04/18/74 23:53:14 51 247  
 1.95-003 9.45+001 0.00+000 0.00+000 20 43008 43008  
 50 109 4 24 73gain corr., rec. = -40 tot const. = 12.4  
 C=42 RG=10000 (-40dB) DG= 0 FG= 0 AG= 52  
 1.000+006 0.3086 6.657+005.

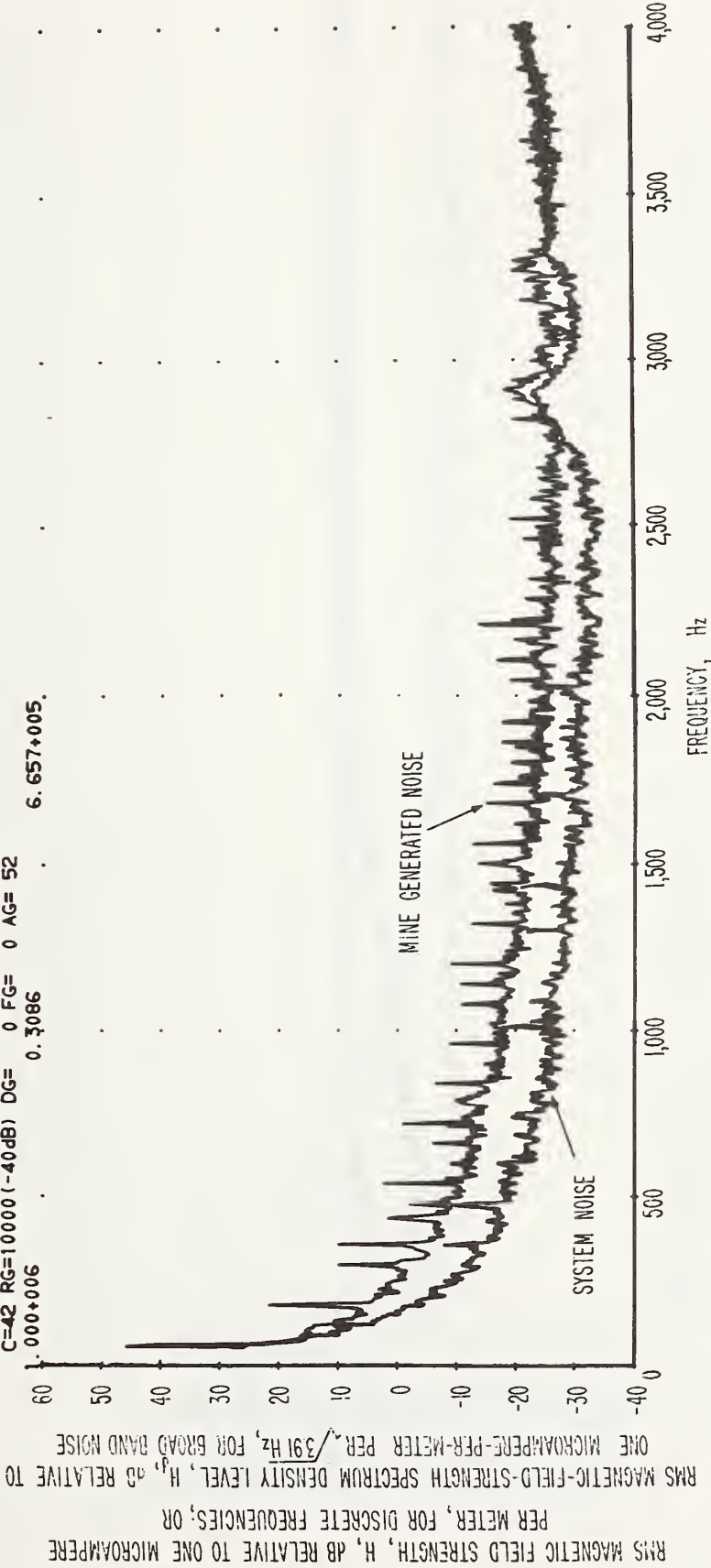


Figure 3-20 Spectrum of magnetic field strength obtained on a loop antenna 40 Hz to 4 kHz, Grace Mine, underground, Number 2 mine transfer drift, 2:22 p.m., April 24, 1973. V-10 LHD is not in vicinity. Spectral resolution is 3.91 Hz.

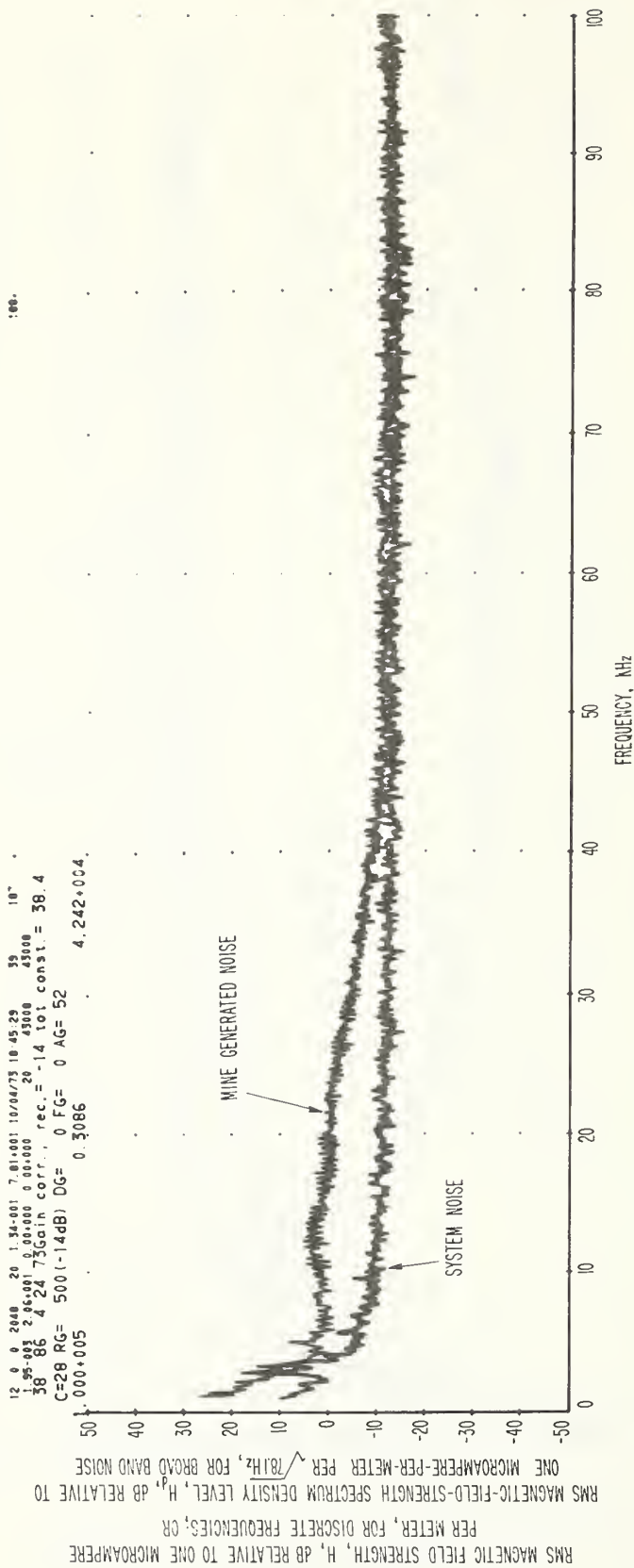


Figure 3-21 Spectrum of magnetic field strength obtained on a loop antenna 1 kHz to 100 kHz, Grace Mine, underground, Number 6 crossdrift substation, antenna sensitive axis vertical, 3:10 p.m., April 24, 1973. Spectral resolution is 78.1 Hz.

12 0 0 2048 20 1.34-001 7.81+001 10/04/73 18.47-07 41 :57  
 1.95-003 2.32+001 0.00+000 0.00+000 20 43008 43008  
 40 86 4 24 73Gain corr., rec.= -26 tot const.= 26.4  
 C=28 RC= 2000 (-26dB) DG= 0 FG= 0 AG= 52  
 000+005 0.3086 7.752+004.

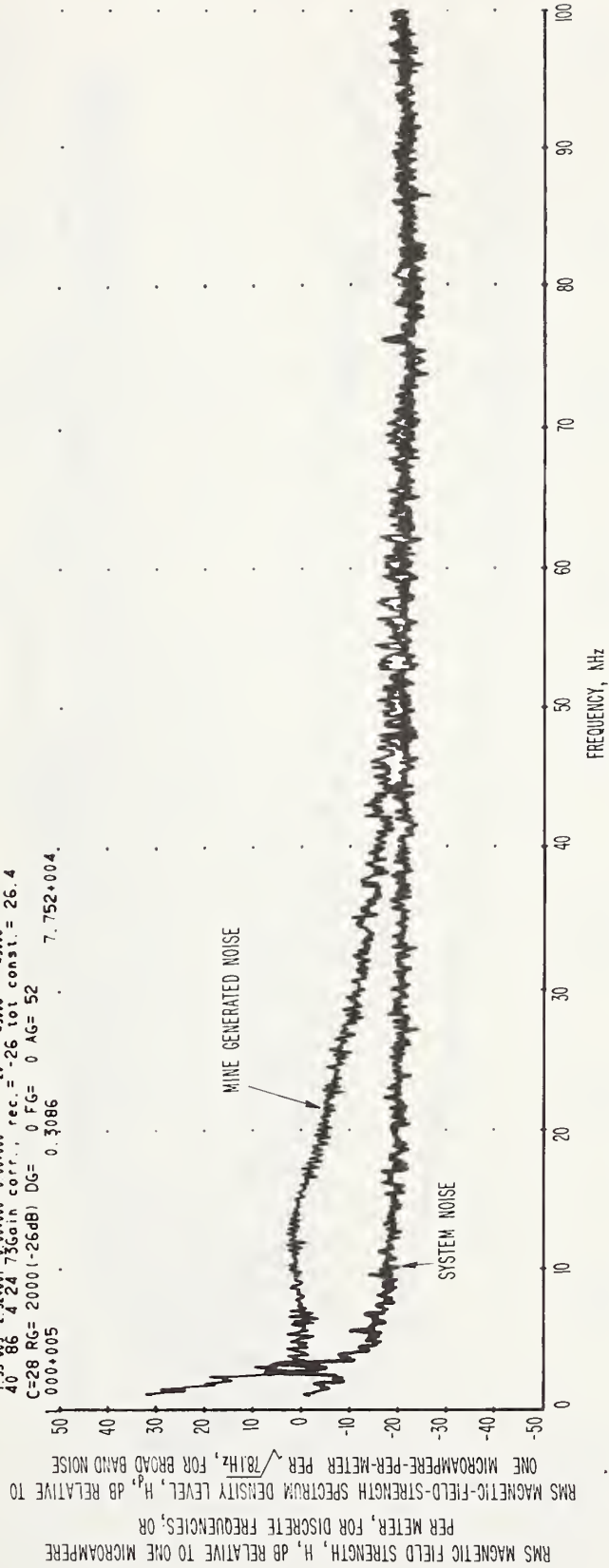


Figure 3-22 Spectrum of magnetic field strength obtained on a loop antenna 1 kHz to 100 kHz, Grace Mine, underground, shop office, antenna sensitive axis vertical, 3:50 p.m., April 24, 1973. LHD's being refueled meters distant, fluorescent light area. Spectral resolution is 78.1 Hz.

12 0 0 2048 20 2.69+000 3.91+000 04/18/74 23:55:21 54 262 \*  
 1.55-003 9.68+001 0.00+000 0.00+000 20 43008 43008  
 53 109 4 24 75Gain corr., rec. = -26 tot const. = 26.4  
 C=42 RG= 2000 (-26dB) DG= 0 FG= 0 AG= 52  
 0.000+008 0.3086 3.727+007.

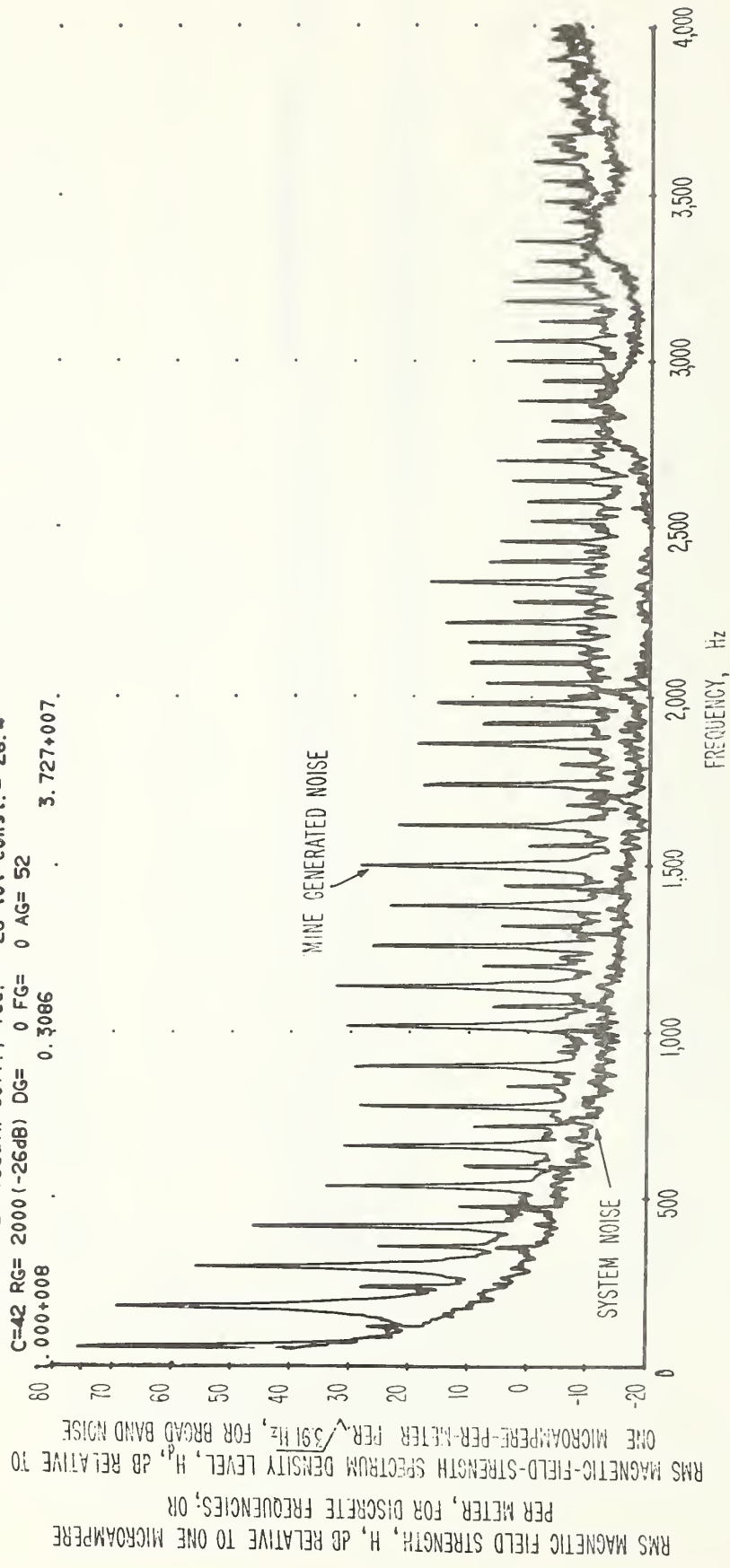


Figure 3-23 Spectrum of magnetic field strength obtained on a loop antenna 40 Hz to 4 kHz, Grace Mine, underground, shop office, antenna sensitive axis vertical, 3:50 p.m., April 24, 1973. Fluorescent lights. Spectral resolution is 3.91 Hz.

12 0 0 2000 20 5.38-001 1.95+001 09/25/73 22:13:57 14 62 "  
 1.95-003 5.62+000 0.00+000 20 43000 43000  
 13 81 4 24 73Gain corr., rec. = -20 tot const. = 32.4  
 C=21 RG= 1000(-20dB) DG= 0 FG= 0 AG= 52  
 1.000+006 0.3086 5.708+005

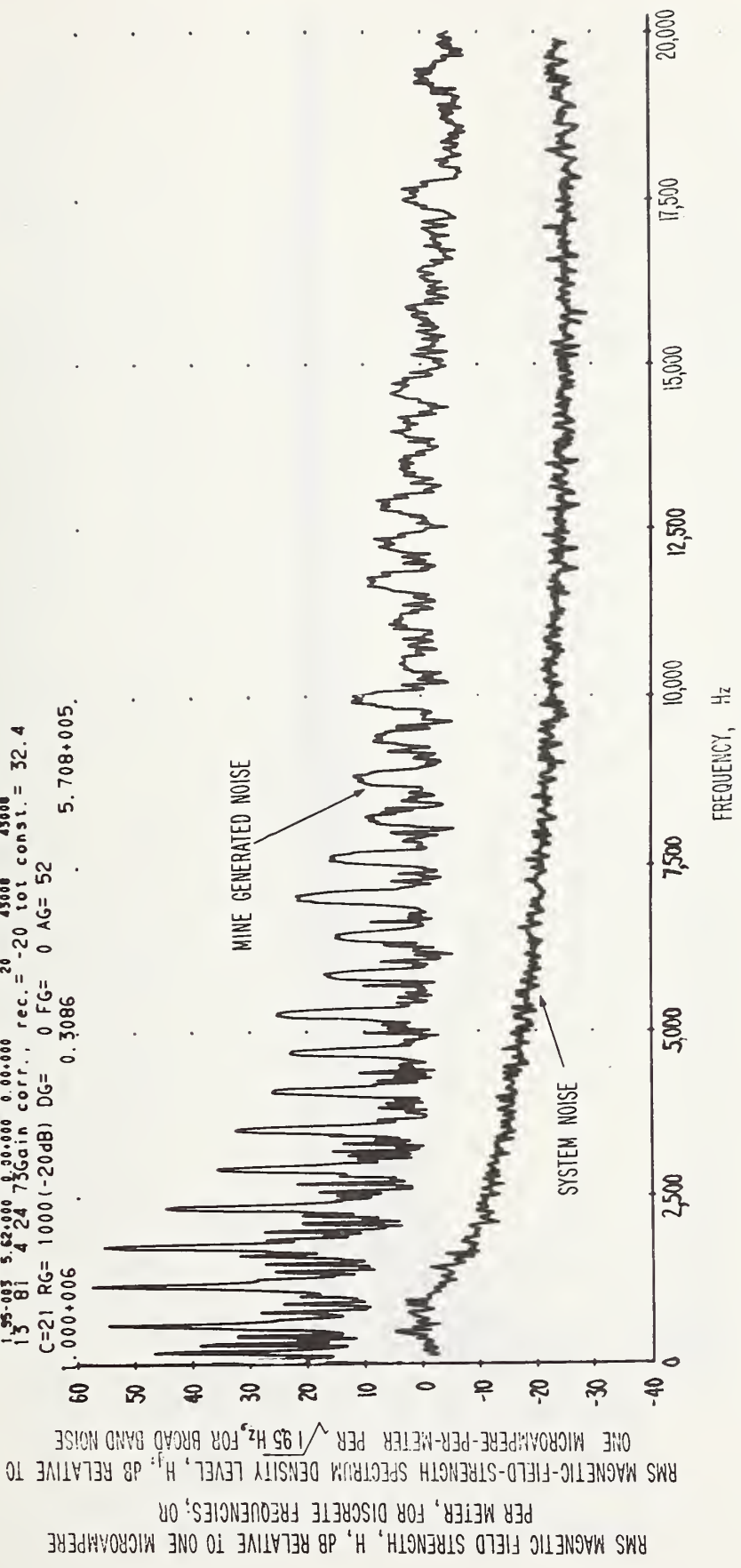


Figure 3-24 Spectrum of magnetic field strength obtained on a loop antenna 1 kHz to 20 kHz, Grace Mine, underground, LHD diesel vehicle passing by the shop lunchroom area, antenna sensitive axis vertical, 4:30 p.m., April 24, 1973. Spectral resolution is 19.5 Hz.

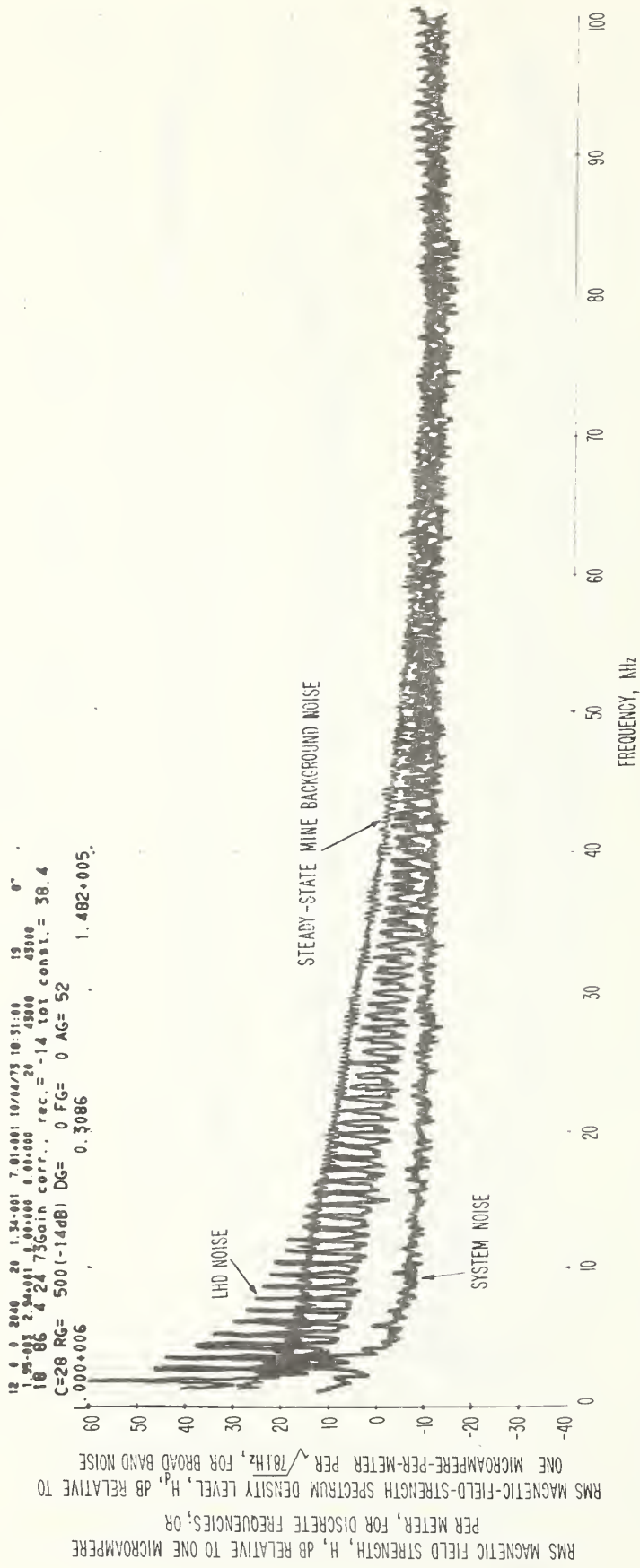


Figure 3-25 Spectrum of magnetic field strength obtained on a loop antenna 10 kHz to 100 kHz, Grace Mine, under ground, composite of highest steady-state background noise and highest LHD spectra, April 24, 1973. Spectral resolution is 78.1 Hz.



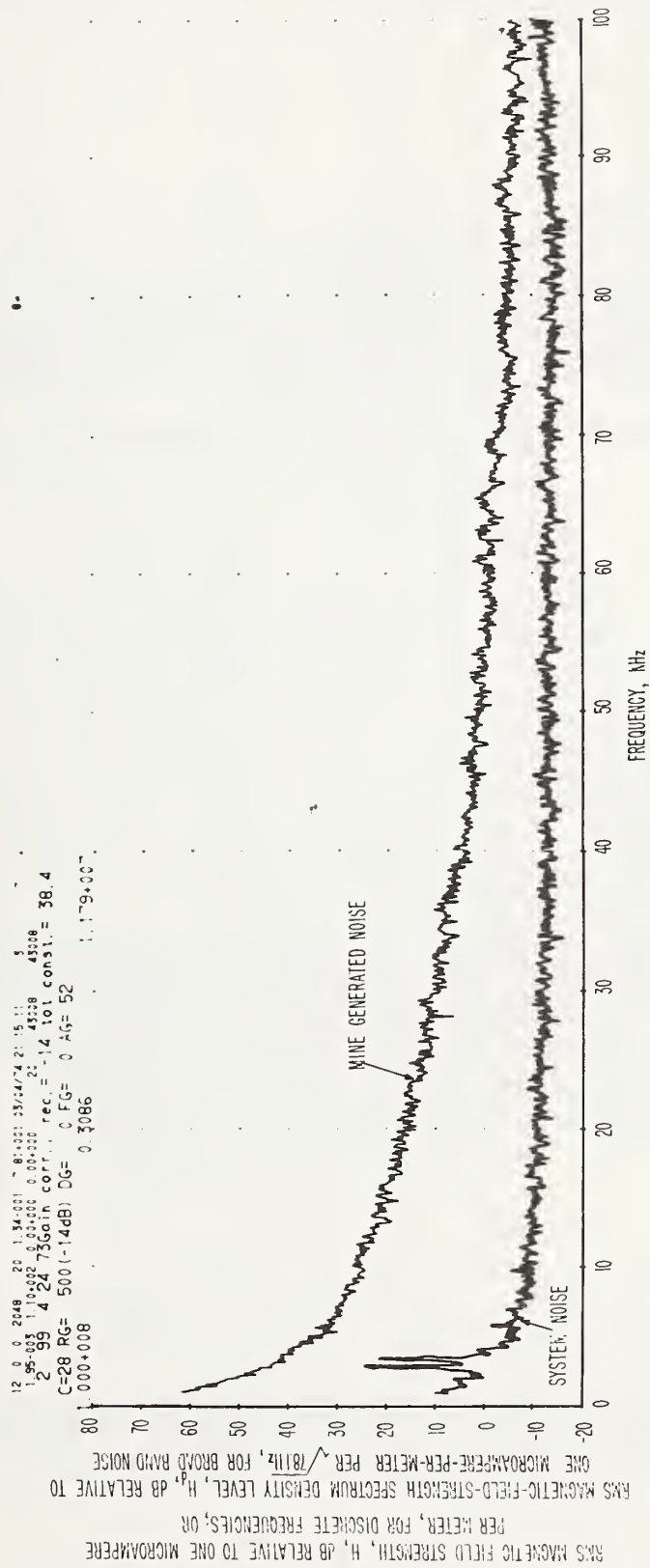


Figure 3-26 Spectrum of magnetic field strength obtained on a loop antenna 1 kHz to 100 kHz, Grace Mine, underground, development foreman office, antenna sensitive axis vertical, 11:35 a.m., April 24, 1973. Explo-sion. Spectral resolution is 78.1 Hz.

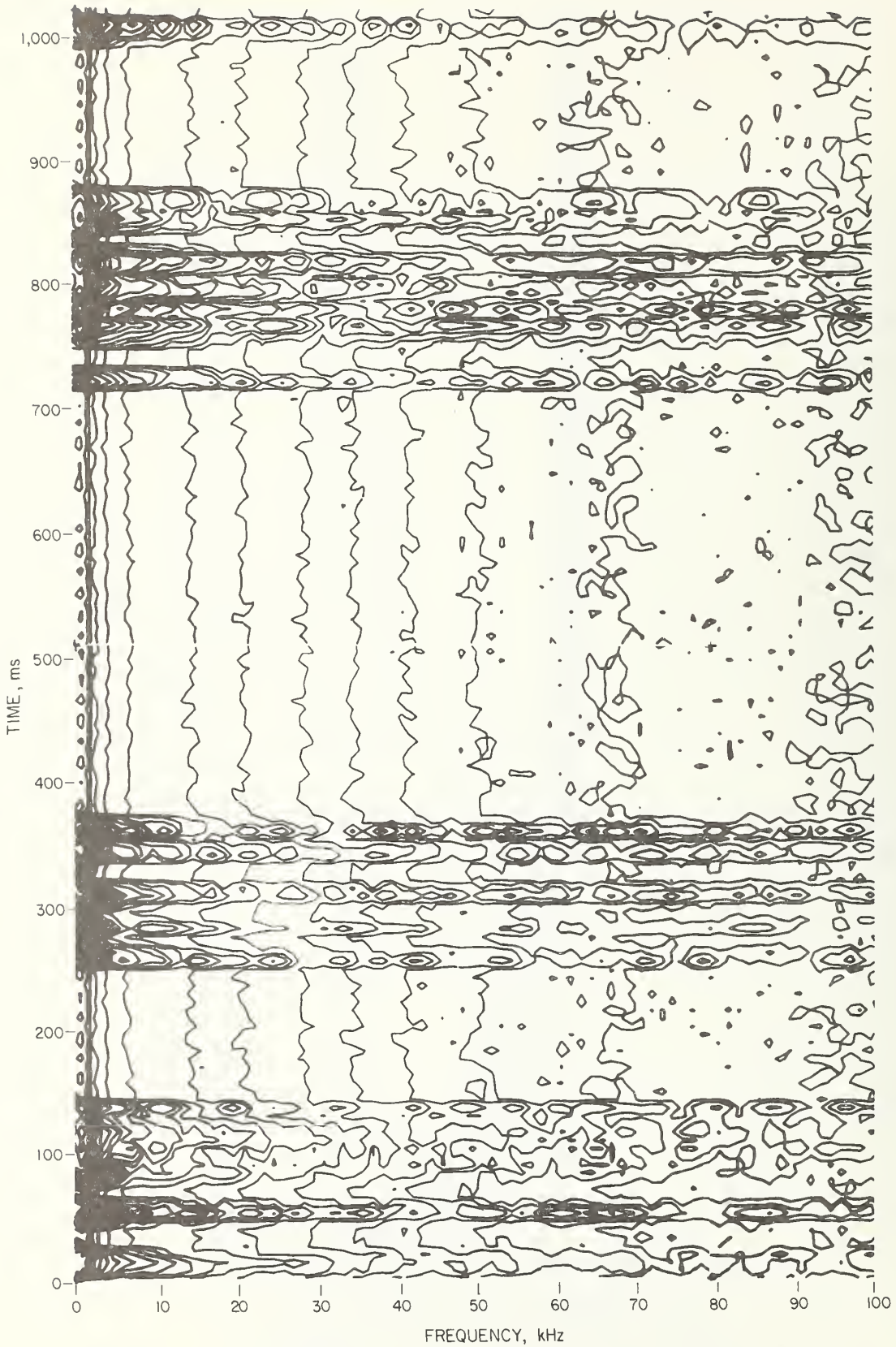


Figure 3-27 Contour map showing noise generated from a group of denonations comprising a "shot," as a function of time.

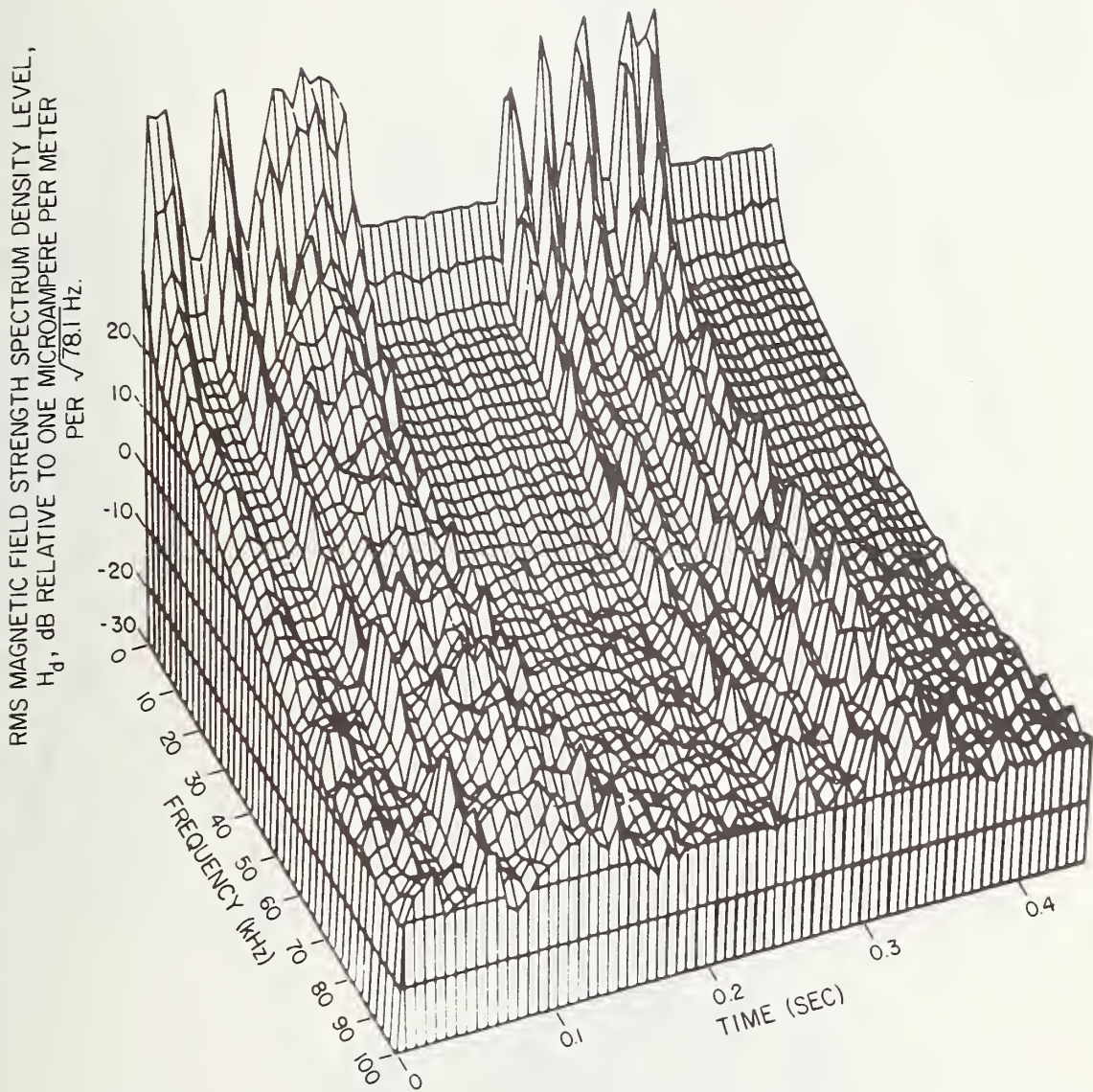


Figure 3-28 Three-dimensional view of two detonations from a larger group comprising a "shot."

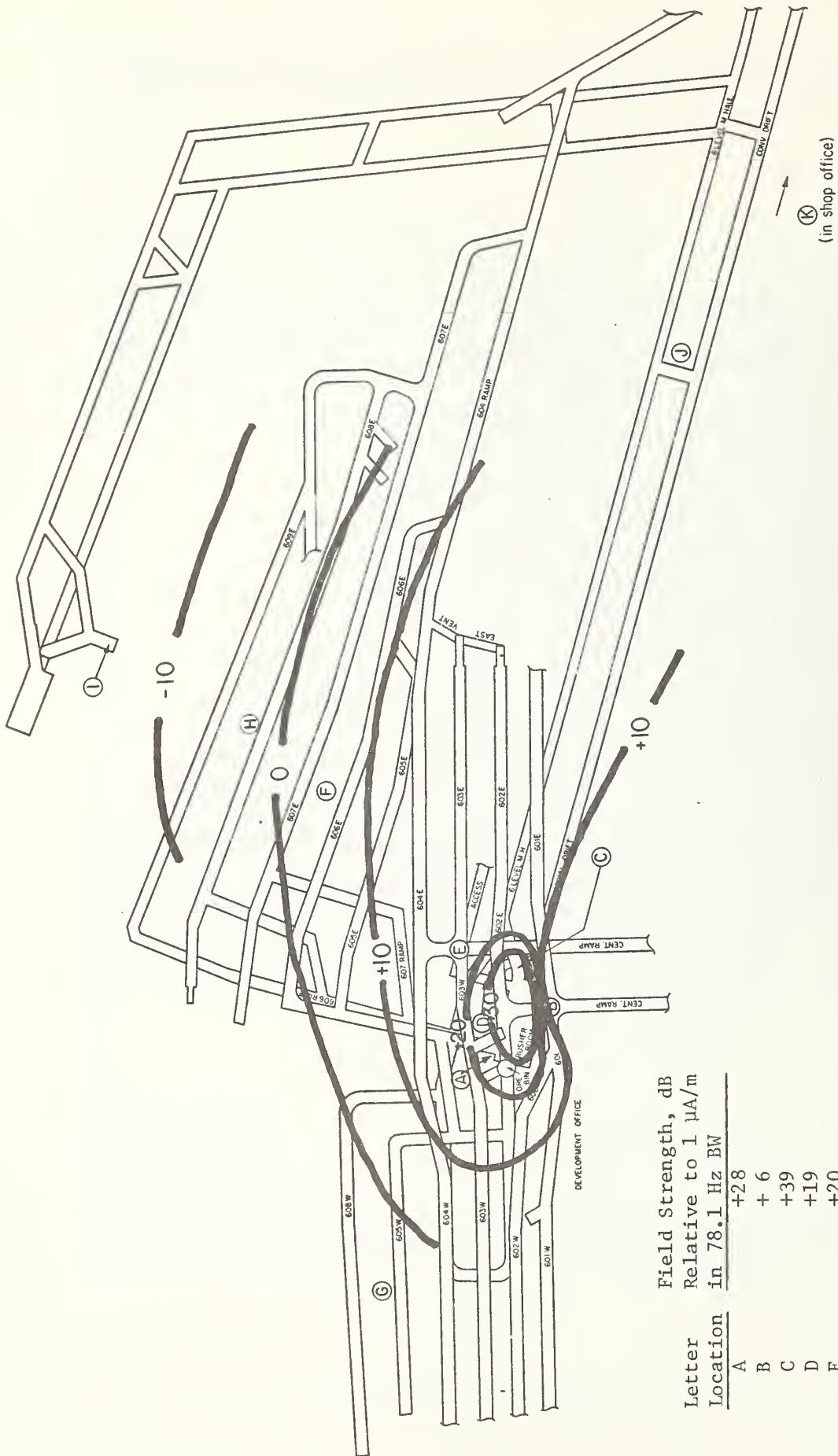
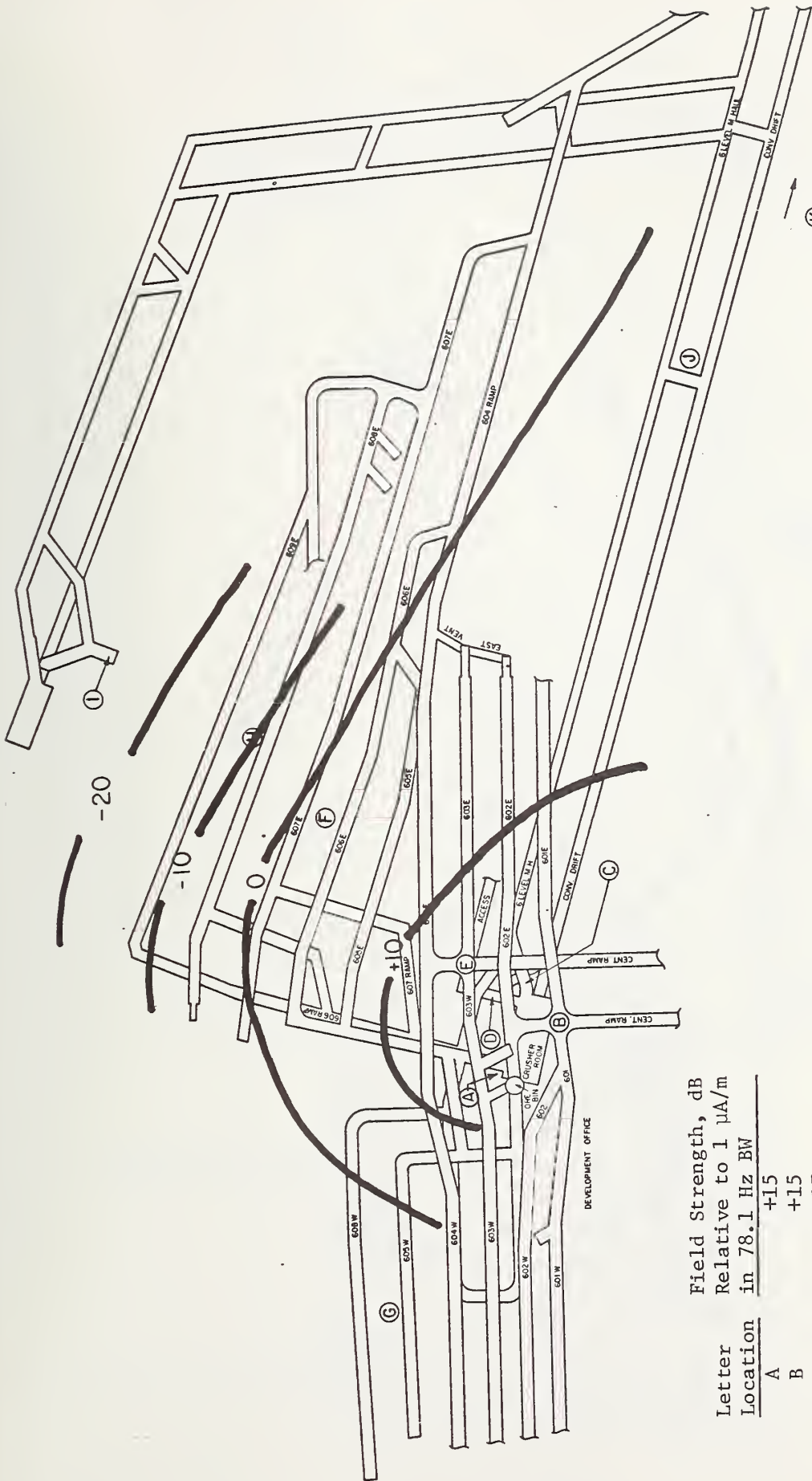


Figure 3-29 Grace Mine, contour map of largest measured power-line magnetic-noise field-strength for 2 kHz.

Letter Location	Field Strength, dB Relative to 1 $\mu\text{A}/\text{m}$ in 78.1 Hz BW
A	+28
B	+6
C	+39
D	+19
E	+20
F	+10
G	-3
H	-2
I	-18
J	+16
K	+19



Letter Location	Field Strength, dB Relative to 1 $\mu\text{A}/\text{m}$ in 78.1 Hz BW
A	+15
B	+15
C	+17
D	+11
E	+11
F	+ 6
G	- 6
H	-14
I	-25
J	+ 2
K	+ 1

Figure 3-30 Grace Mine, noise contour map for 10 kHz.

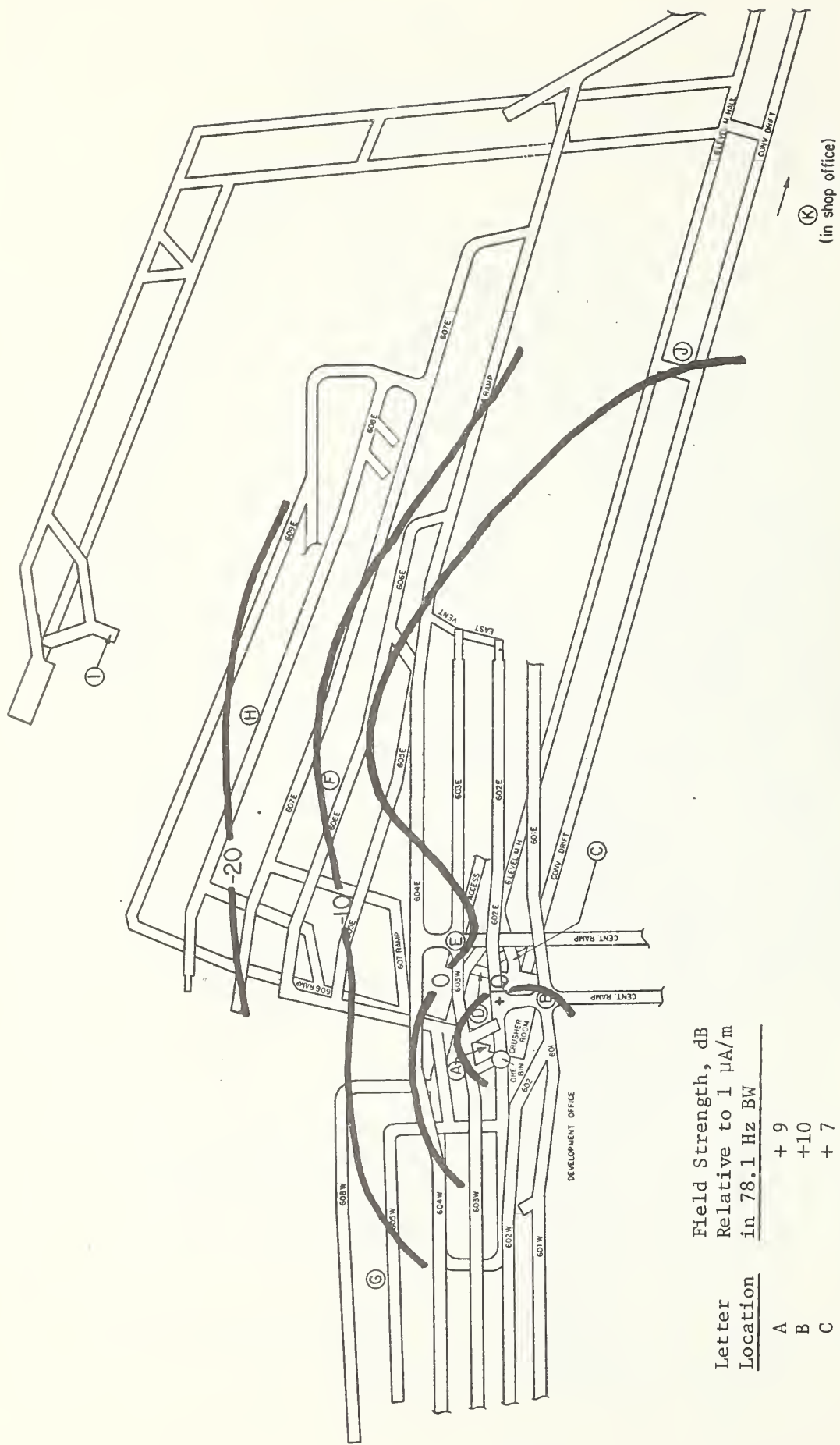


Figure 3-31 Grace Mine, noise contour map for 20 kHz.

Letter Location	Field Strength, dB Relative to 1 $\mu$ A/m in 78.1 Hz BW
A	+ 9
B	+10
C	+ 7
D	+ 5
E	- 5
F	+ 1
G	-11
H	-21
I	-28
J	0
K	- 5

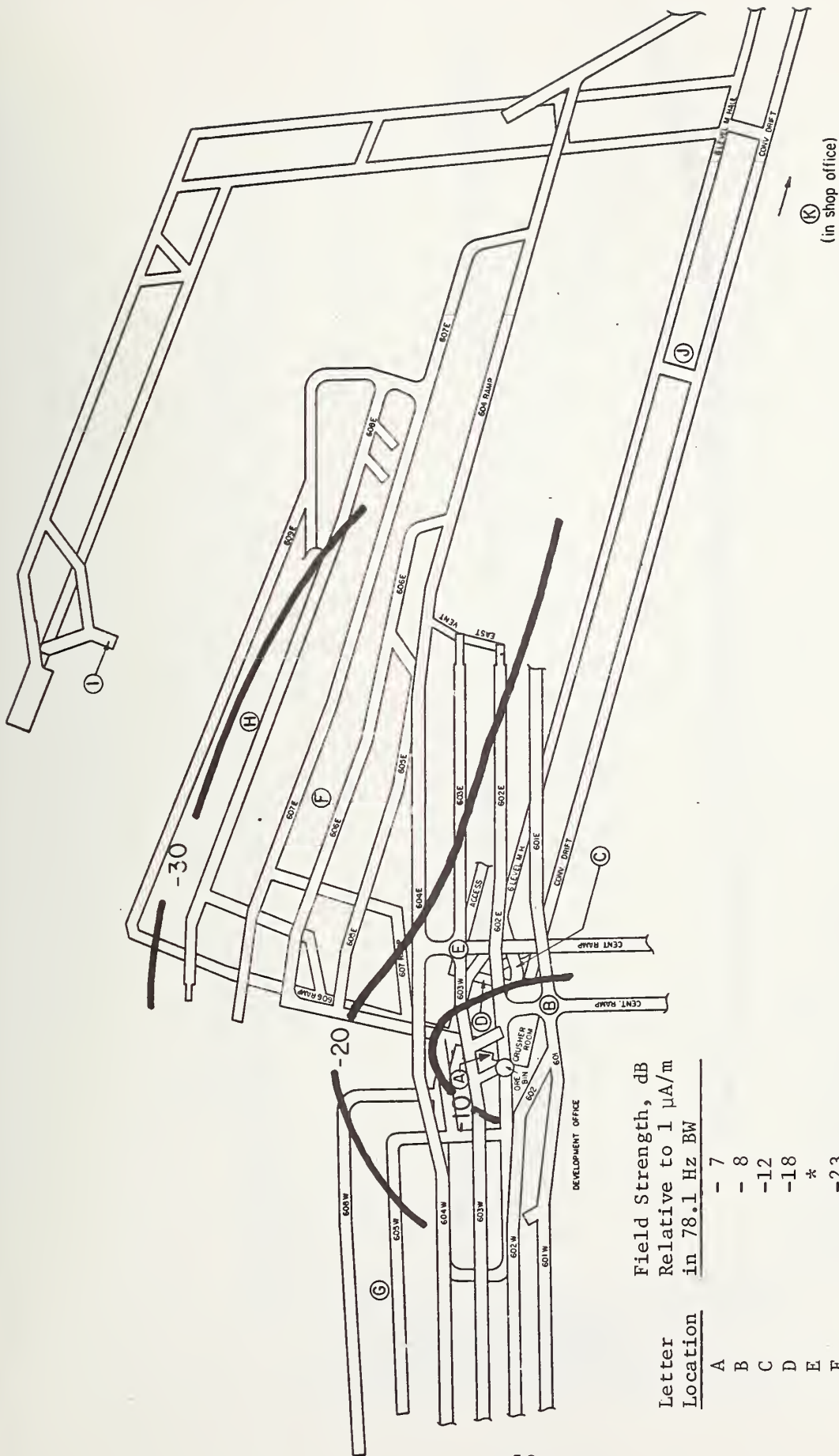


Figure 3-32 Grace Mine, noise contour map for 60 kHz.

\*Predominately system noise

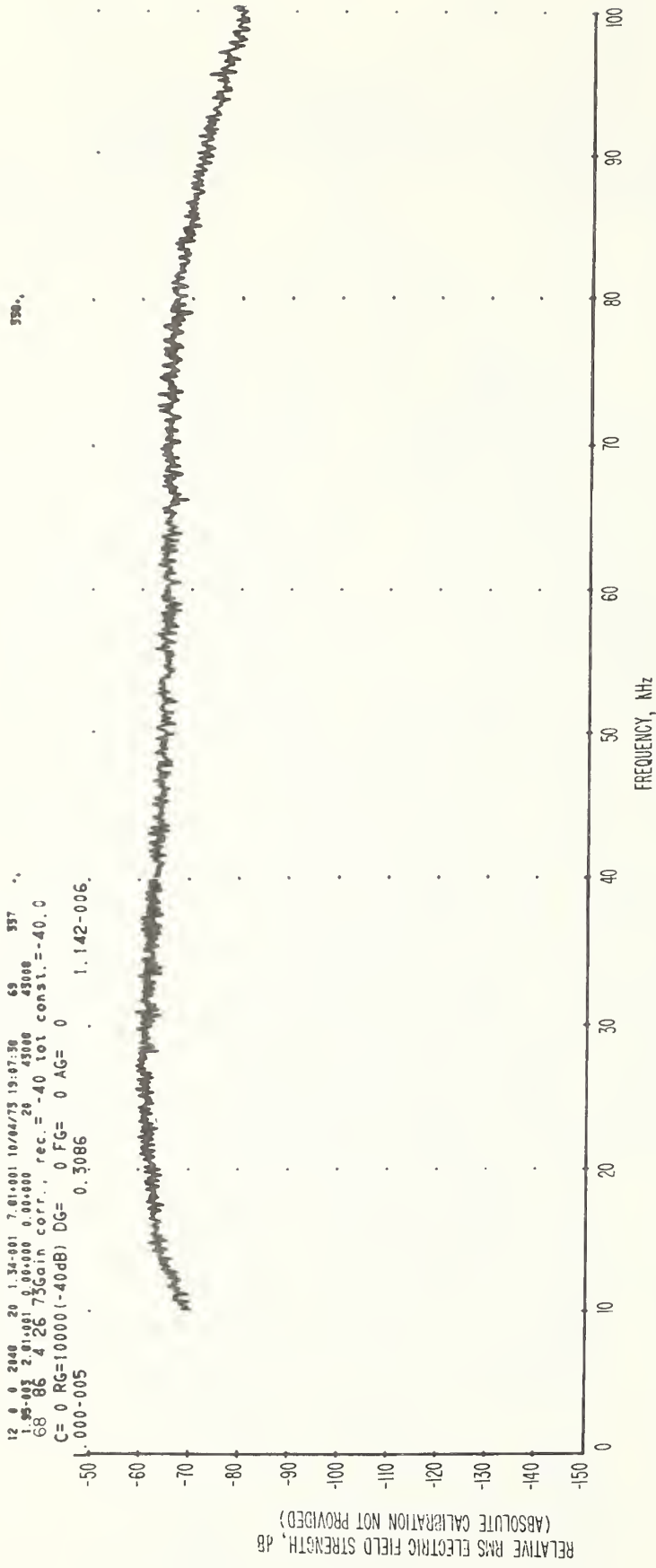


Figure 3-33 Spectrum (unprocessed) of electric field strength obtained with an active dipole 10 kHz to 100 kHz, Grace Mine, underground, crusher access drift, dipole ends perpendicular to the drift, 11:05 a.m., April 26, 1973. Spectral resolution is 78.1 Hz.



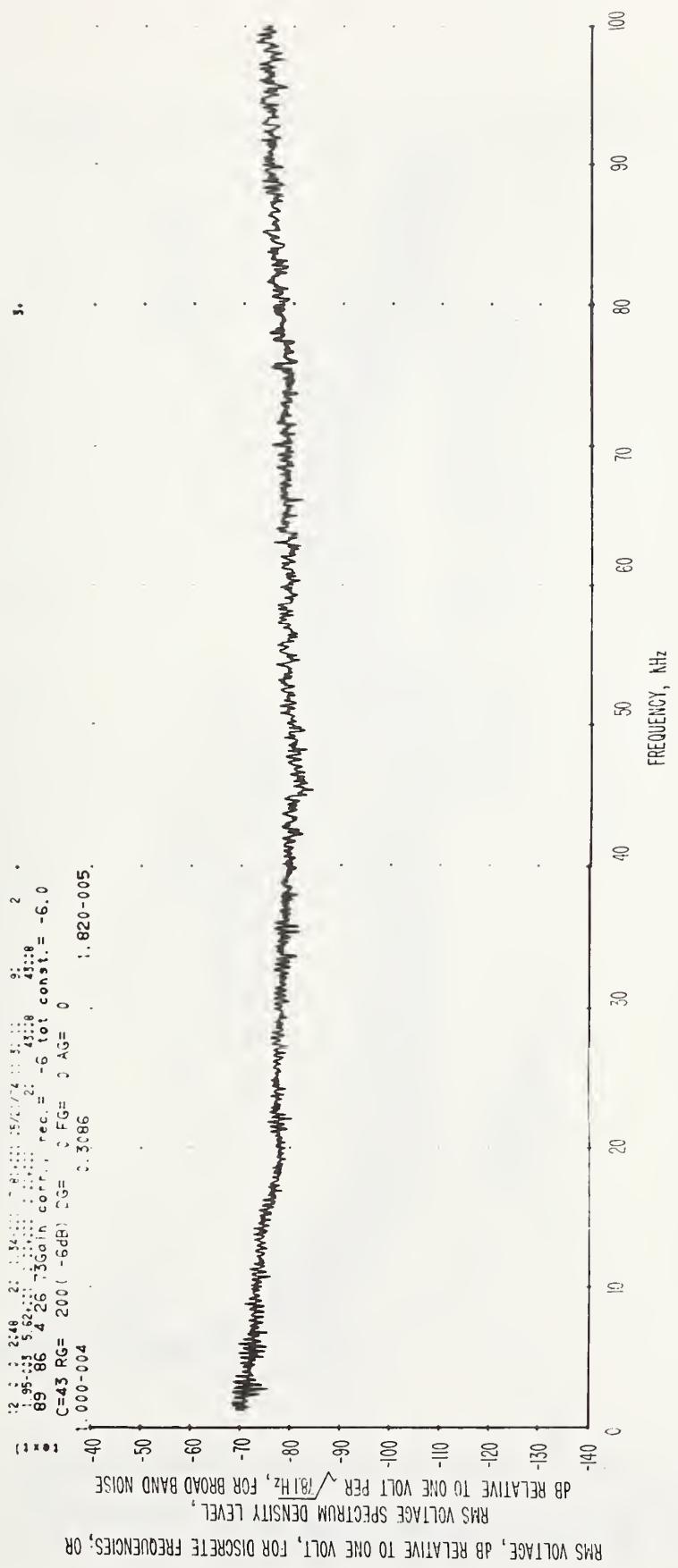


Figure 3-34 Voltage spectrum obtained with a monopole attached to two roof bolts,  
 10 meter separation, 10 kHz to 100 kHz, Grace Mine, underground,  
 11:35 a.m., April 26, 1973. Spectral resolution is 78.1 Hz.

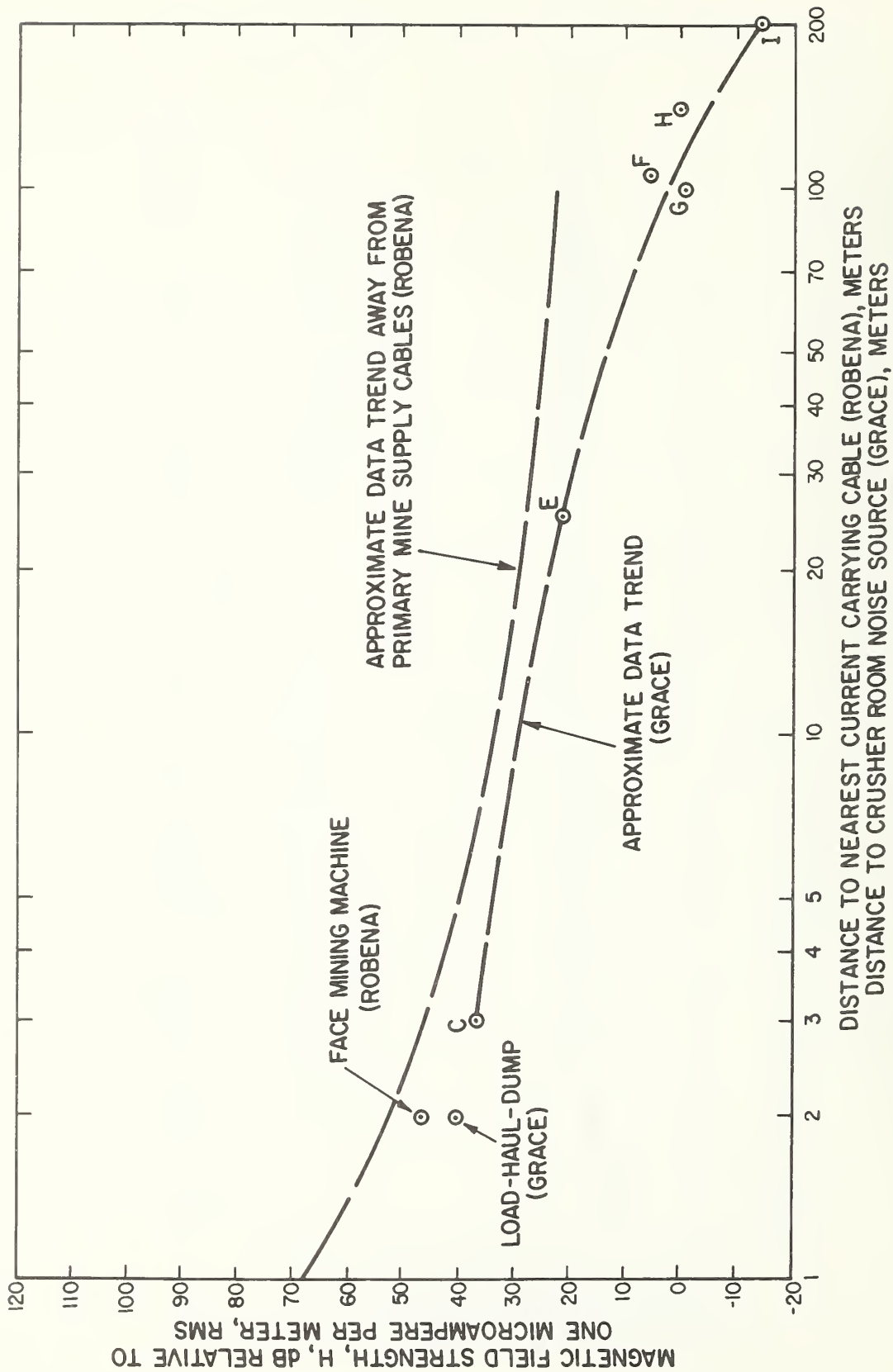


Figure 3-35 Comparison of magnetic field strengths of Grace and Robena Mines as a function of distance from noise source.

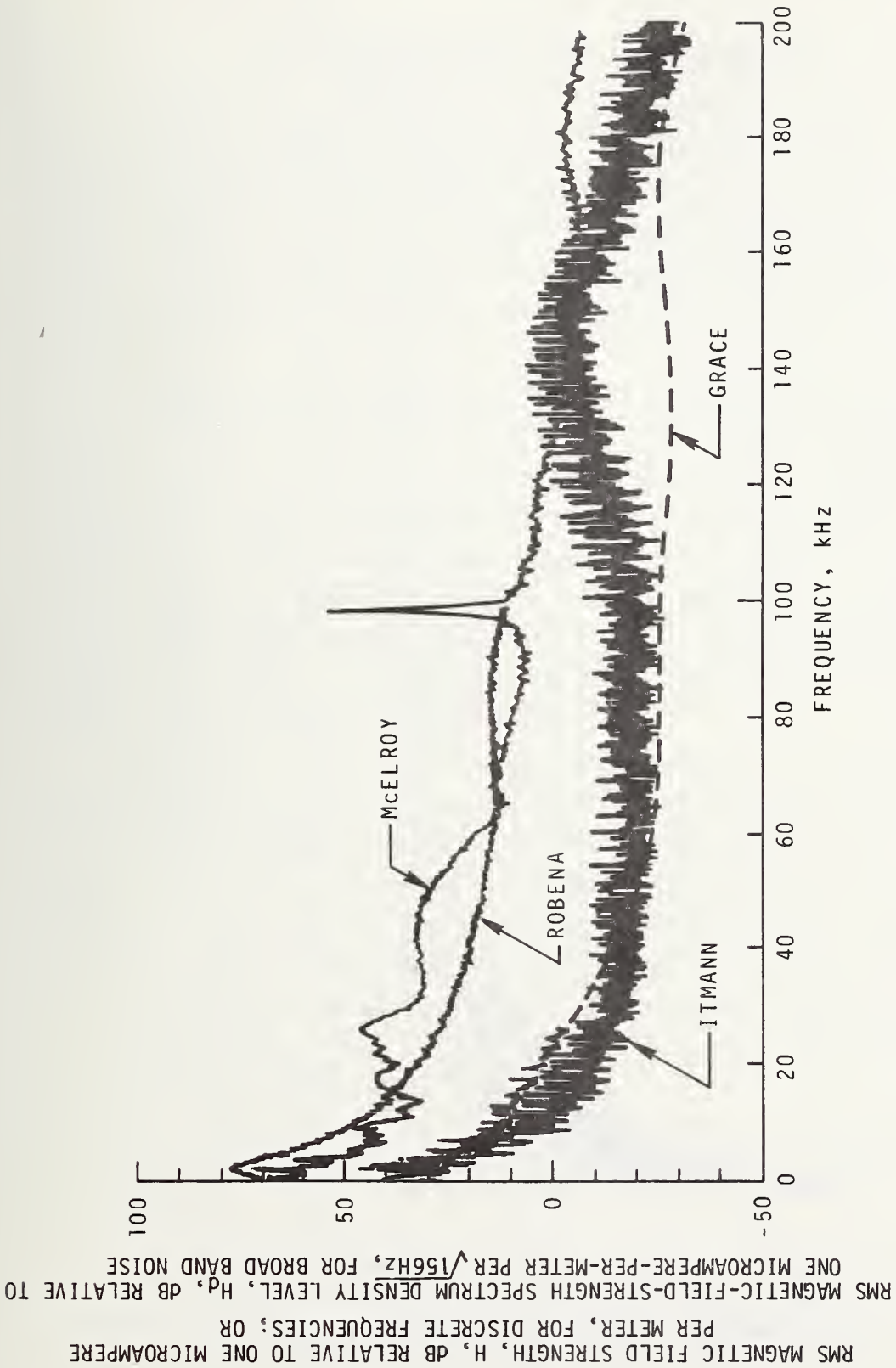


Figure 3-36 Comparison of E-M noise levels near operating machinery from four mines. Vertical magnetic-field components are shown. Broken sections of the curves represent system noise.

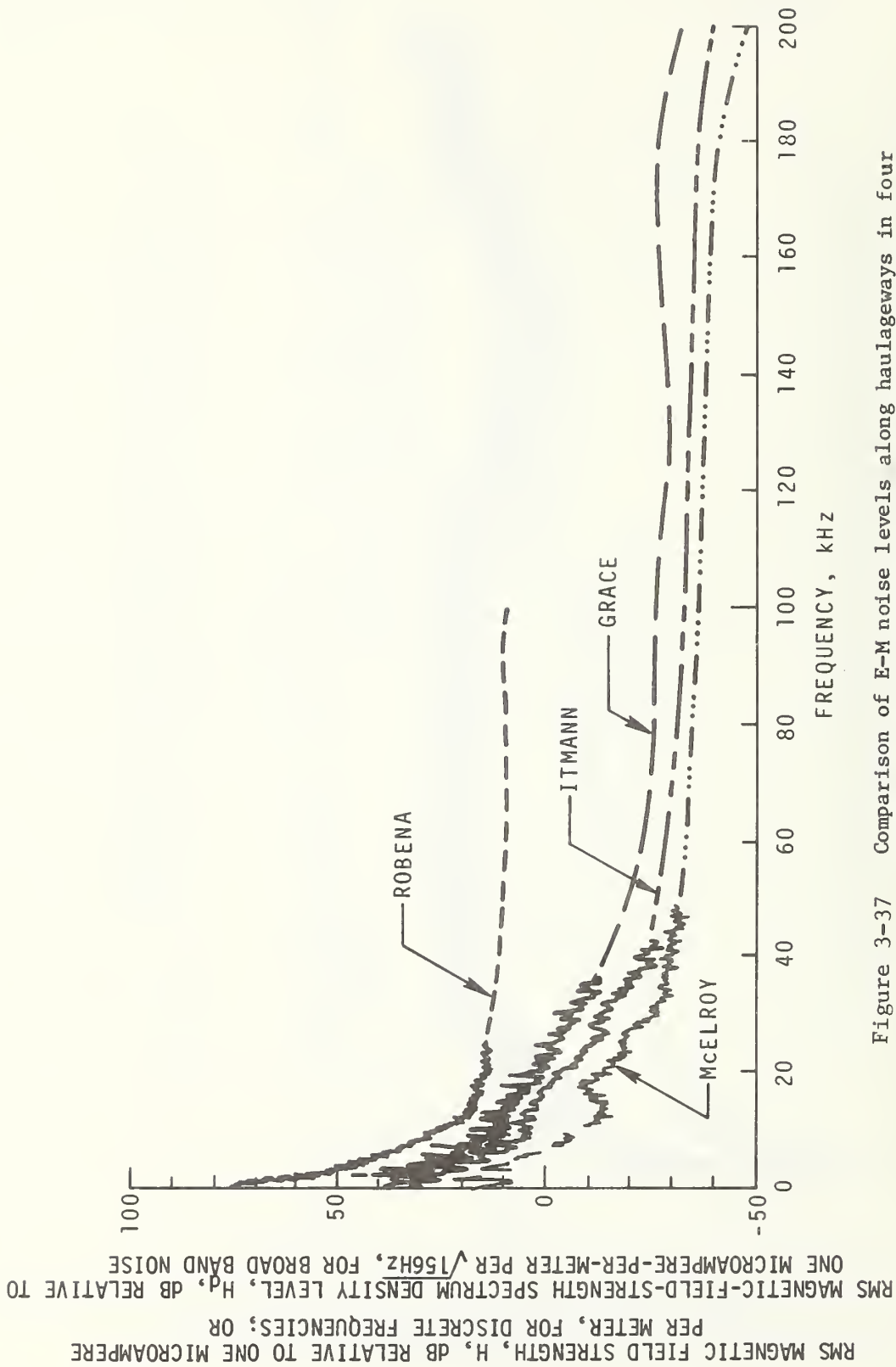


Figure 3-37 Comparison of E-M noise levels along haulageways in four mines. Vertical magnetic-field components are shown. Broken sections of the curves represent measurement-system noise levels.

## 4. AMPLITUDE PROBABILITY DISTRIBUTION MEASUREMENT RESULTS

### 4.1 Introduction and Uncertainties

Statistical representations are required since the variations of field strength are, in general, random. The amplitude probability distribution (APD) of the received noise envelope is one of the most useful statistical descriptions of the noise process for the design and evaluation of a telecommunications system operating in a noisy environment [3,4,6].

By plotting the cumulative APD on Rayleigh graph paper, one can show clearly the fraction of time that a noise envelope exceeds various levels. Rayleigh graph paper is chosen with scales such that a Rayleigh distribution (i.e., envelope distribution of Gaussian noise) plots as a straight line with slope of  $-1/2$ . Noise with rapid large changes in amplitude (e.g., impulsive noise) then has a much steeper slope, typically  $-4$  or  $-5$ , depending on the impulsiveness of the noise and the receiver bandwidth.

With the exception of the roof-support bolt measurements, all APD measurements are reported in absolute quantities.

The estimated limits of error for the APD noise measurements are  $\pm 5$  dB. Several sources of error that are critical to the overall accuracy of our measurements are listed below:

1. Use of a discrete, digital level counter (levels are 6 dB apart) contributes  $\pm 1$ -dB quantization error limit. One-decibel step attenuators are used to achieve the  $\pm$  one decibel.
2. The system, i.e., recording, data transcribing, and data processing, has a calibration uncertainty of  $\pm 0.5$  dB [3].

3. The estimated uncertainty involved in using the portable and the laboratory tape recorders for record and playback is  $\pm 0.5$  dB due to harmonic distortion, flutter, dropout, cross-talk, etc.

4. The gain instability during measurements, gain changes between measurements and calibration, and the non-linearity of electromagnetic interference and field strength (EIFS) meters and mixers, all combined, contribute  $\pm 0.5$  dB uncertainty.

5. The gain instability and non-linearity of the digital level counter, the tuned frequency converter, the amplifier, and attenuators, all combined, contribute  $\pm 0.5$  dB uncertainty.

6. Connector losses and BNC cable losses, particularly at higher frequencies above 100 kHz, contribute  $\pm 2.0$  dB uncertainty.

Some additional uncertainty beyond the stated measurement system uncertainty is caused by the in-mine environment. Care was taken to provide at least one meter separation from metallic objects wherever possible. However, coal, rock, or earth was sometimes immediately adjacent to a loop antenna. In all observed cases, this had no effect at frequencies up to 1 MHz. Above 1 MHz, earth and other reflections did in some cases cause  $\pm 1$  dB variations, even with a shielded, balanced loop antenna. An estimate is that an additional  $\pm 5$  dB uncertainty might be advisable. However, due to the complexity of the shielded loop in the mine environment, this uncertainty cannot be rigorously bounded without substantial additional analysis.

## 4.2 Measurement Results

APD measurements were made on April 24, 1973, during operation in the Grace Iron Mine located near Morgantown, south of Reading, Pennsylvania. Descriptions of Grace Mine are given in section 1.2. APD measurements were made at three locations. The first set of APD measurements of eleven different frequencies was made at the development foreman office, which is identified as A in figure 3-2. The second set of APD measurements of eight different frequencies was made at the electrical substation of the crusher, which is identified as C in figure 3-2. In these two sets of APD measurements, only the vertical component of magnetic field was measured. The third set of APD measurements was made at the shop office, which is identified as K in figure 3-3. Here two orthogonal components of magnetic field were measured: the vertical component of magnetic field was measured at thirteen different frequencies and the horizontal component (E-W) was measured at ten different frequencies.

Predetection bandwidth is either 1 kHz or 1.2 kHz as indicated on each APD.

Figures 4-1 through 4-11 show the APD's of magnetic field noise measured at the development foreman office (location A in figure 3-2). Only the vertical component of magnetic field was measured at eleven frequencies ranging from 10 kHz to 32 MHz. These frequencies are 10 kHz, 30 kHz, 70 kHz, 130 kHz, 160 kHz, 250 kHz, 1 MHz, 2 MHz, 6 MHz, 14 MHz, and 32 MHz. Figure 4-12 through Figure 4-19 show the APD's of magnetic field noise measured at the crusher substation (location C in figure 3-2). Again only the vertical component of magnetic field was measured at eight frequencies, 10 kHz, 30 kHz, 70 kHz, 130 kHz, 500 kHz, 1 MHz, 2 MHz and

6 MHz. Figure 4-20 through 4-42 show the APD's of magnetic field noise measured at the shop office (location K in figure 3-3). Figures 4-20 through 4-32 show the APD's of the vertical component of magnetic field noise measured at thirteen different frequencies, 30 kHz, 70 kHz, 110 kHz, 130 kHz, 160 kHz, 205 kHz, 250 kHz, 500 kHz, 1 MHz, 2 MHz, 6 MHz, 14 MHz, and 32 MHz. Figures 4-33 through 4-42 show the APD's of the horizontal E-W component of magnetic field noise measured at ten different frequencies, 10 kHz, 30 kHz, 70 kHz, 130 kHz, 160 kHz, 250 kHz, 500 kHz, 1 MHz, 2 MHz and 6 MHz.

Air-cooled, V-8 diesel-powered, rubber-tired Load-Haul-Dump (LHD) vehicles with front-loading scoops of typically 5 cubic-yard capacity (1 cubic yard  $\approx$  0.75 m<sup>3</sup>) are used to pick up and haul iron ore to the underground crusher, and dump the ore into the crusher ore bin. Main sources of EM noise are considered to be located in the crusher room area (see Section 3.5). As stated in Section 3.3.3, the crusher substation contains two 500 KVA transformers for stepping three-phase voltage down to 480 volts. The crusher itself is run by a 150 horsepower, 4160 volt, 20.3 ampere, three-phase, wound-rotor motor. Crusher feeders, conveyers and other similar equipments in the area of the crusher are run from 480 volts with typical currents of 400 amperes. Thus the general nature of noise measured at the electrical substation of the crusher and at the development foreman office is essentially a train of power line related pulses as mentioned in Section 3.3.3. The shoulder in the APD curves taken at frequencies from 10 kHz to 130 kHz results from this train of pulses. In other cases where the train of pulses was not present, this shoulder is not present (see APD curves taken at frequencies above 130 kHz).



### 4.3 RMS and Average Values

The APD's are integrated to give average and rms values of the field strength, according to the equations

$$H_{\text{avg}} = - \int_0^{\infty} H \, dp(H)$$

and

$$H_{\text{rms}} = \left( - \int_0^{\infty} H^2 \, dp(H) \right)^{\frac{1}{2}},$$

where H represents the magnetic field strength of the noise, and p is the probability that the measured field strength exceeds the value H. These quantities are also dependent upon the measurement bandwidth, the length of the data run, and possibly other parameters. Finite series are actually used for the numerical integration. The rms and average values so arrived at are identified on each graph and are time averages (23 minutes) of these time-dependent parameters. If the tapes are played into ordinary rms-reading meters, the meter readings will vary 10 to 20 dB over fractions of a second, since the averaging time constant is, of course, much less than 23 minutes. The rms value is directly relatable to noise power. With these wide variations of field strength with time, the most suitable presentations are statistical ones.

### 4.4 Summary Curves

Excursions of field strength between 0.001 and 99 percent, as well as rms and average values, are shown in figures 4-43 through 4-46 for magnetic field noise on April 24, 1973. The predetection bandwidth for these APD measurements either is 1 kHz or is normalized to 1 kHz. Some long-term fluctuations in values occur because of different operating conditions during different times of the day.

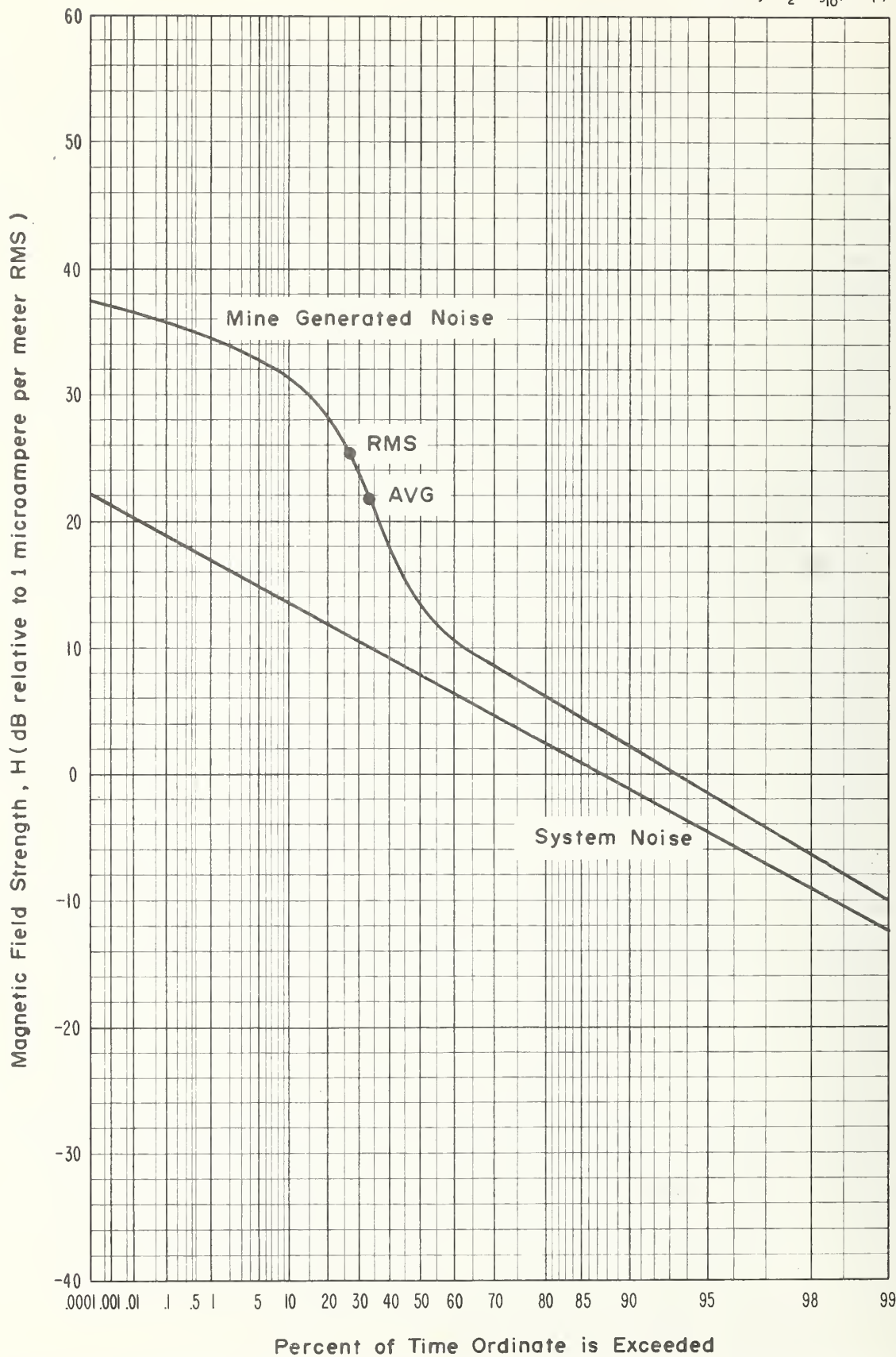


Figure 4-1 APD, 10 kHz, vertical component, 1.0 kHz predetection bandwidth, April 24, 1973, 10:00 a.m., development foreman office, Grace Mine.

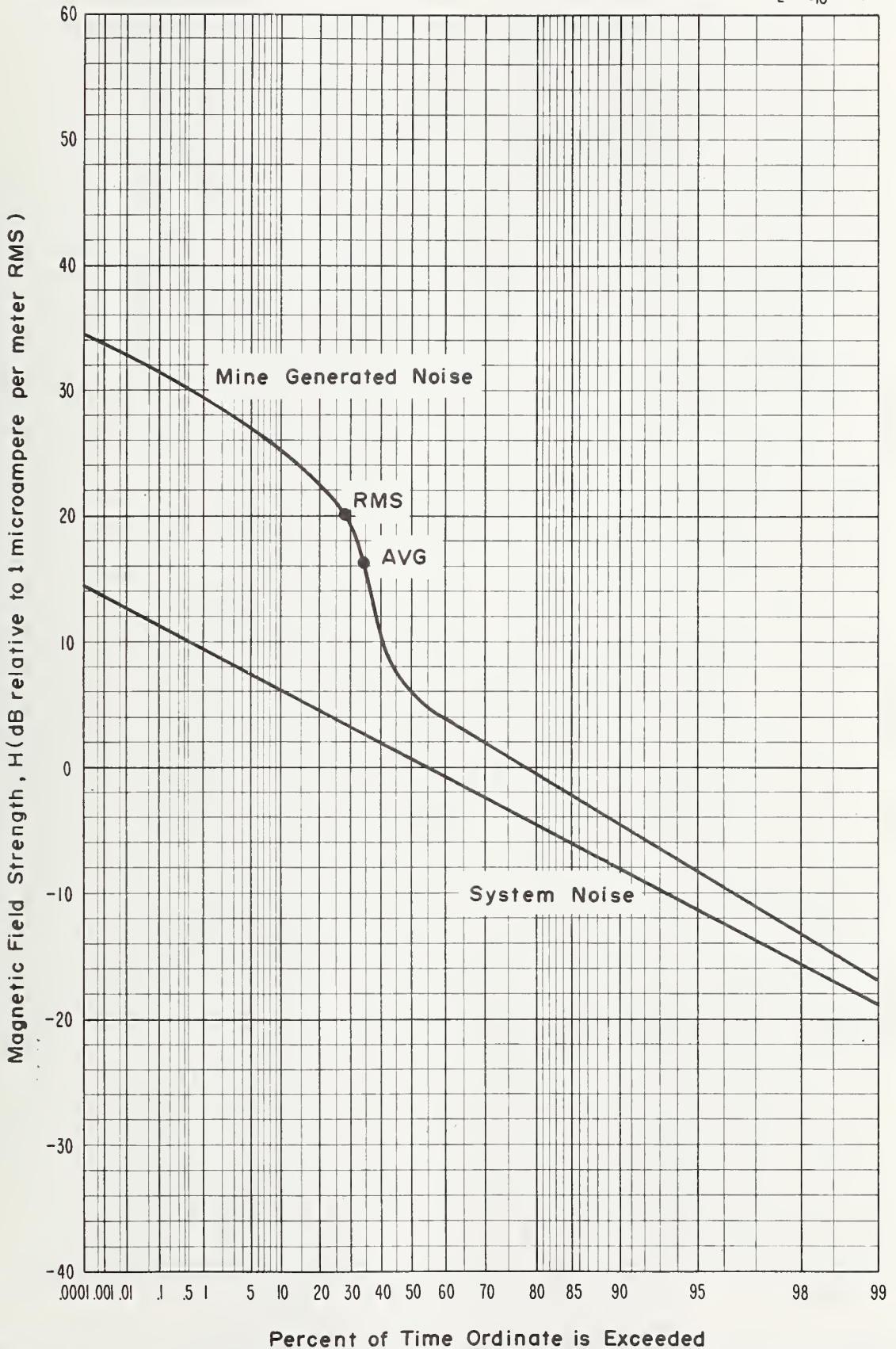


Figure 4-2 APD, 30 kHz, vertical component, 1.0 kHz predetection bandwidth, April 24, 1973, 10:36 a.m., development foreman office, Grace Mine.

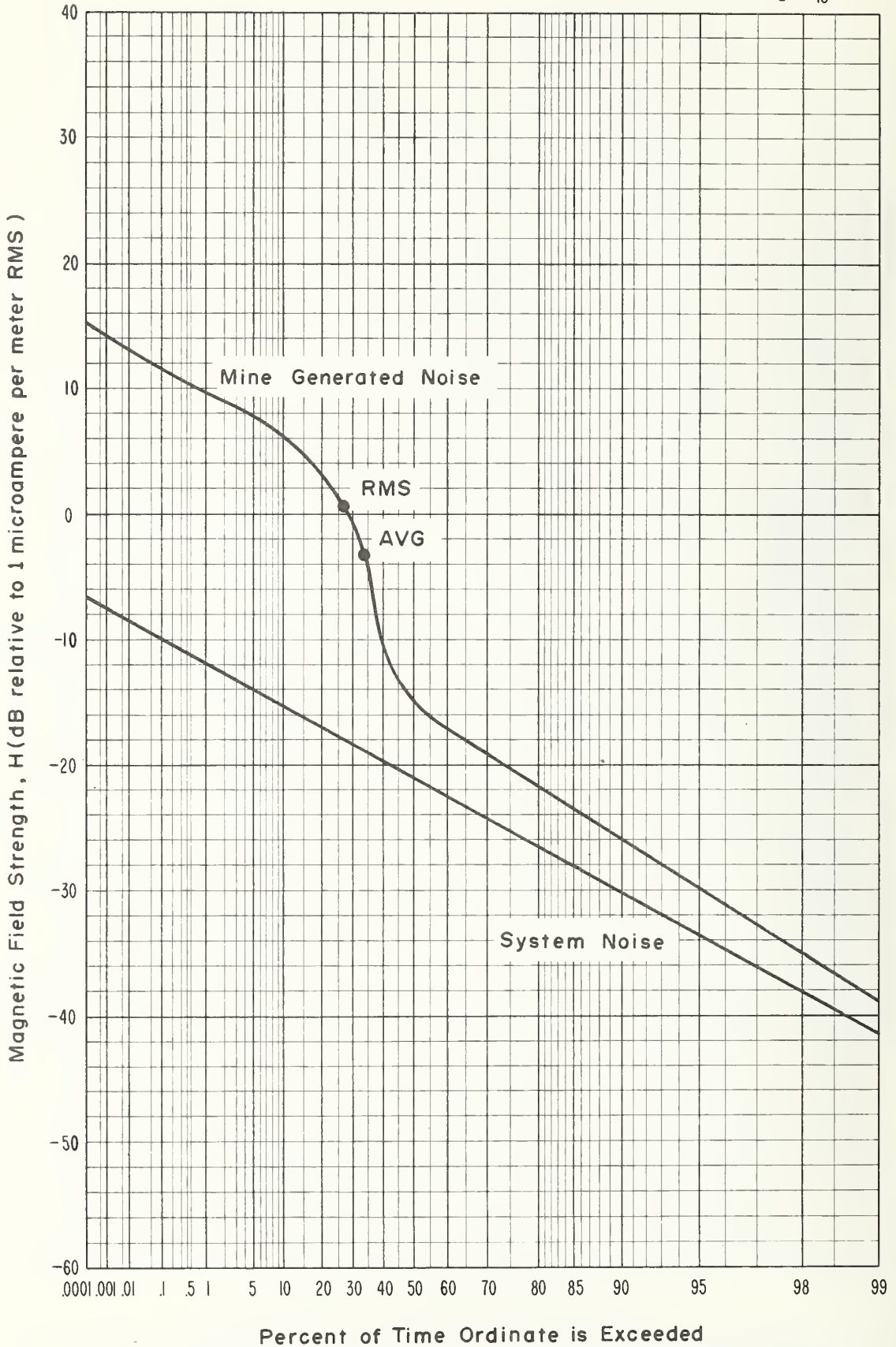


Figure 4-3 APD, 70 kHz, vertical component, 1.0 kHz predetection bandwidth, April 24, 1973, 11:05 a.m., development foreman office, Grace Mine.

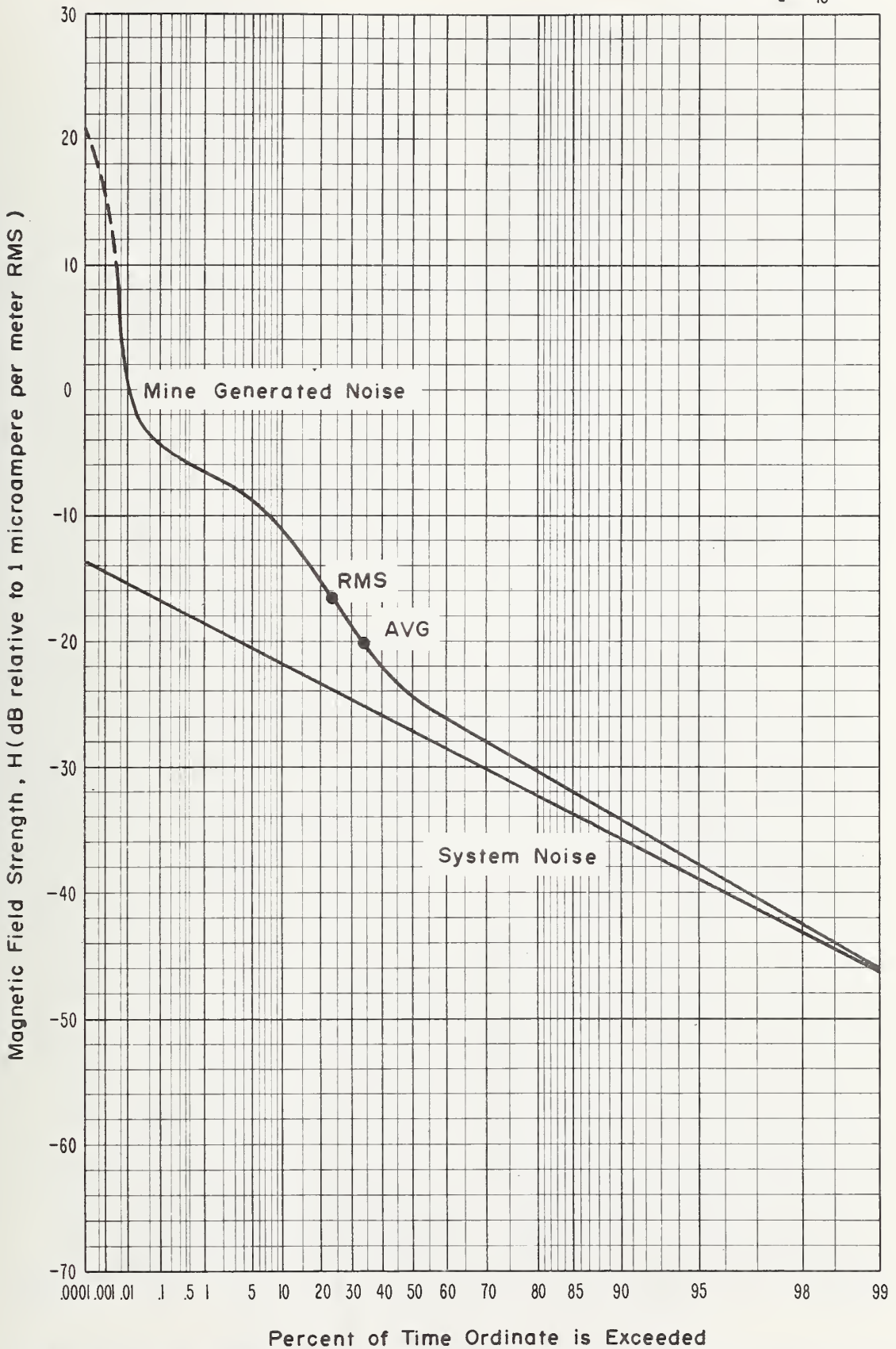


Figure 4-4 APD, 130 kHz, vertical component, 1.0 kHz predetection bandwidth, April 24, 1973, 11:44 a.m., development foreman office, Grace Mine.

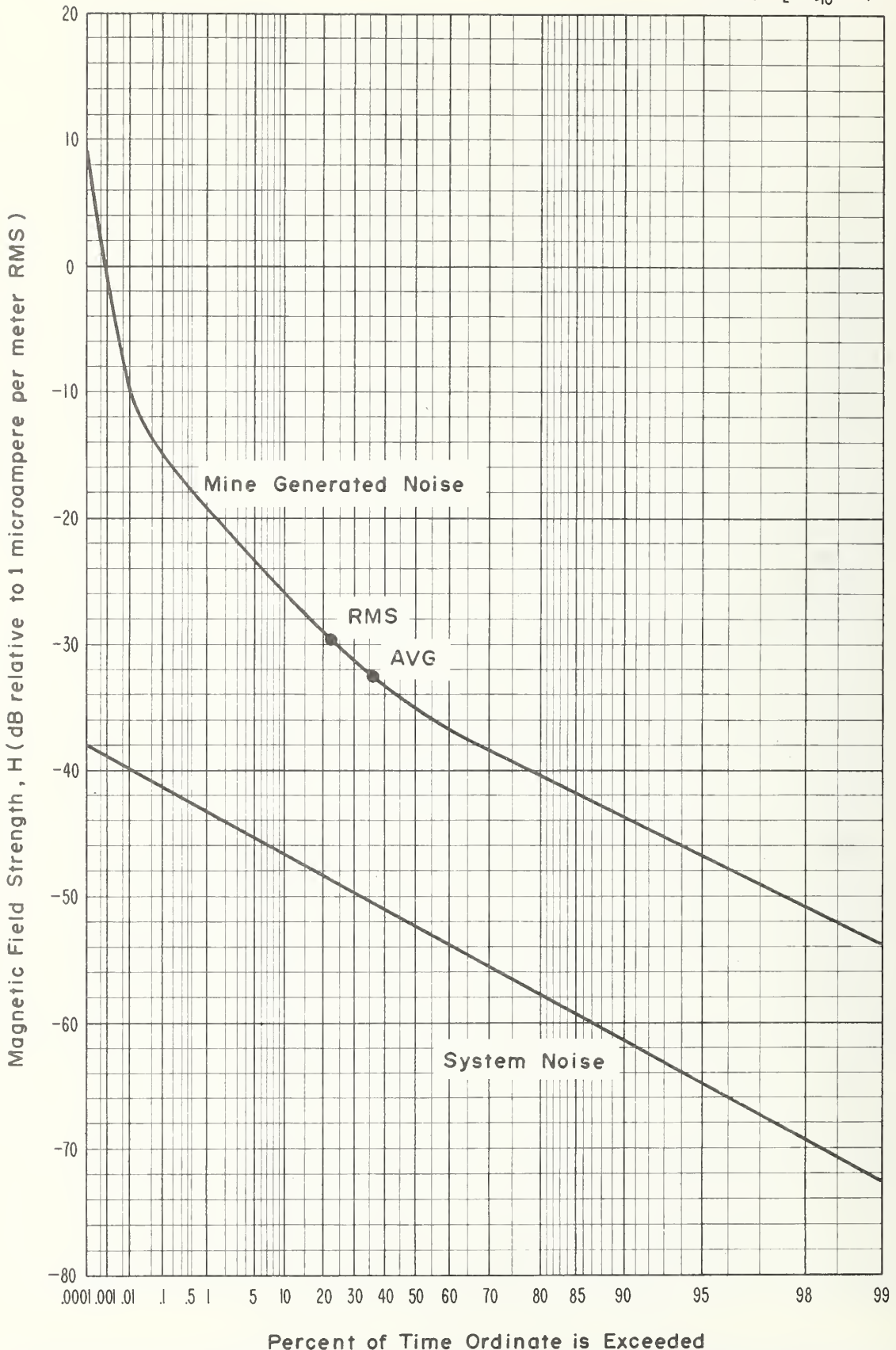


Figure 4-5 APD, 160 kHz, vertical component, 1.0 kHz predetection bandwidth, April 24, 1973, 12:10 p.m., development foreman office, Grace Mine.

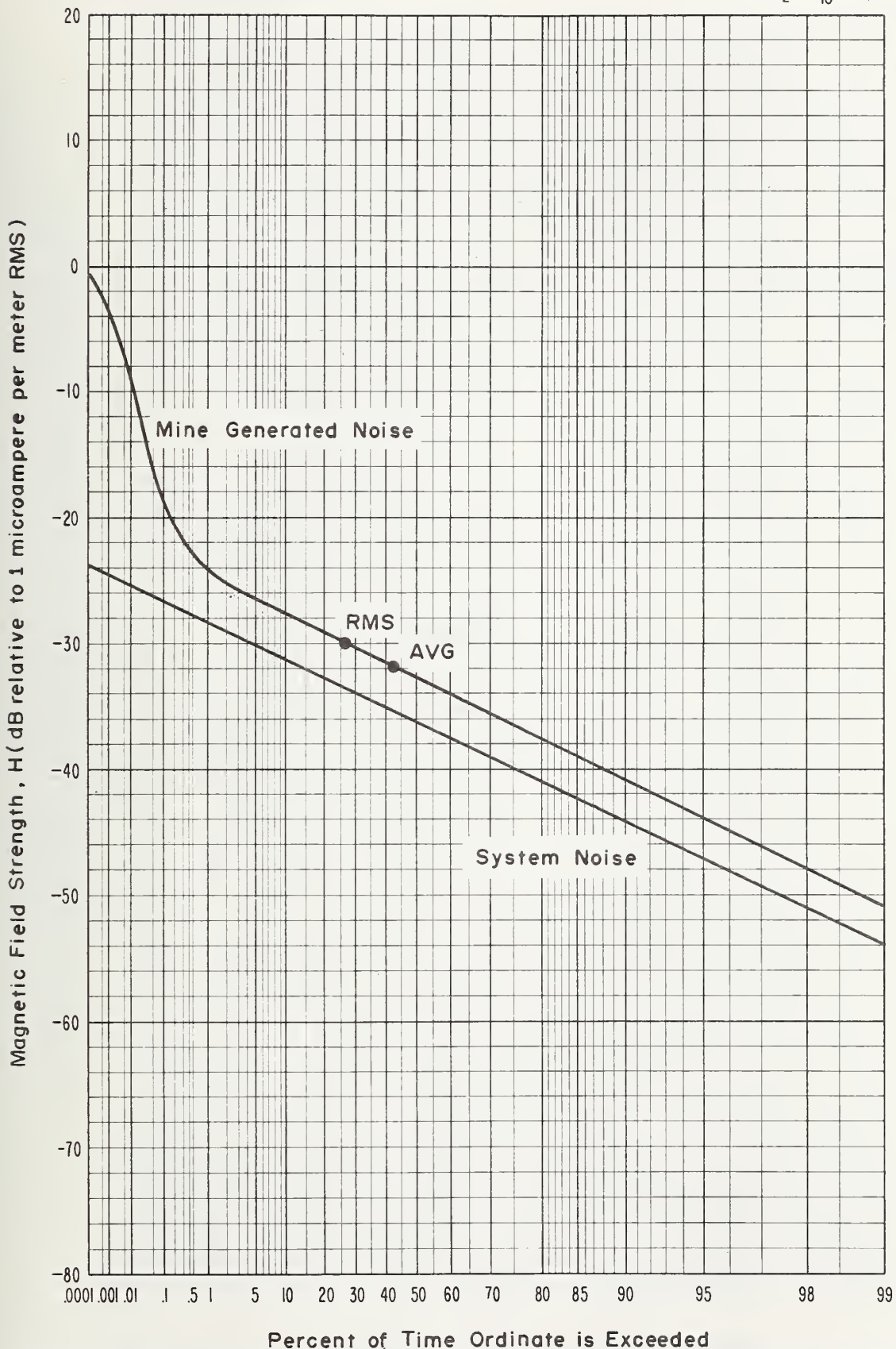


Figure 4-6 APD, 250 kHz, vertical component, 1.0 kHz predetection bandwidth, April 24, 1973, 12:40 p.m., development foreman office, Grace Mine.

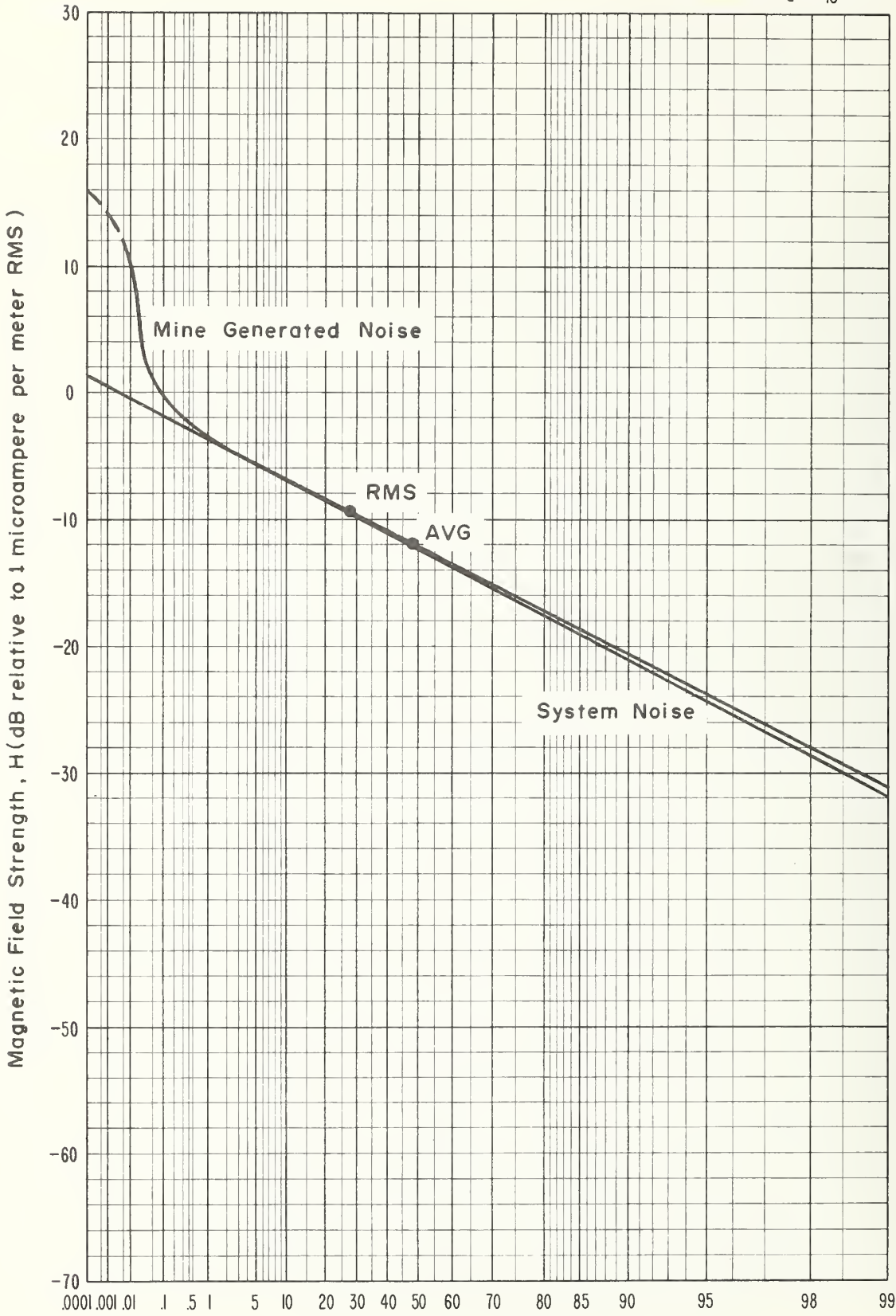


Figure 4-7 APD, 1 MHz, vertical component, 1.2 kHz predetection bandwidth, April 24, 1973, 10:36 a.m., development foreman office, Grace Mine.



Linear by  $-\frac{1}{2} \log_{10}(-\ln p)$

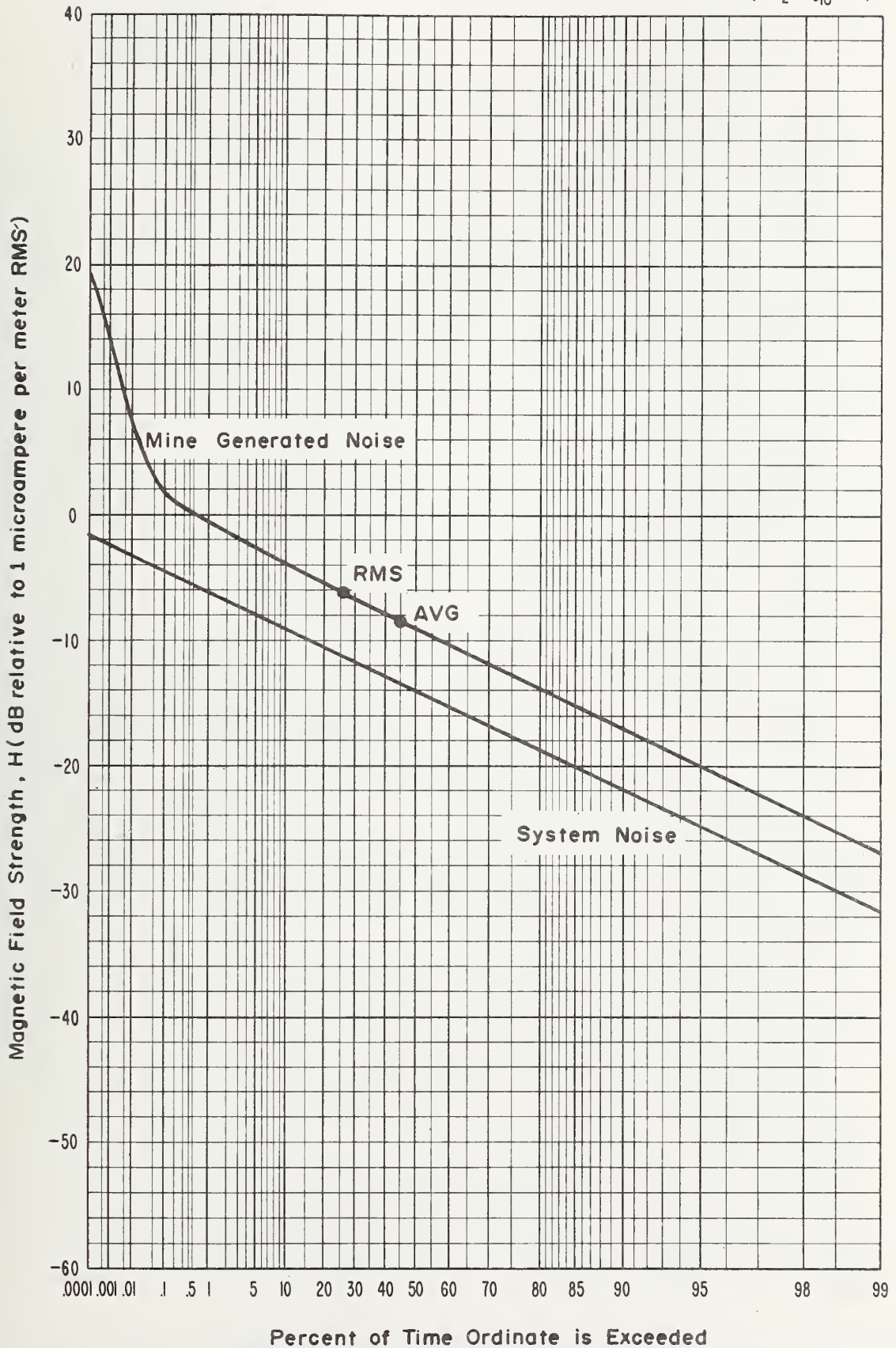
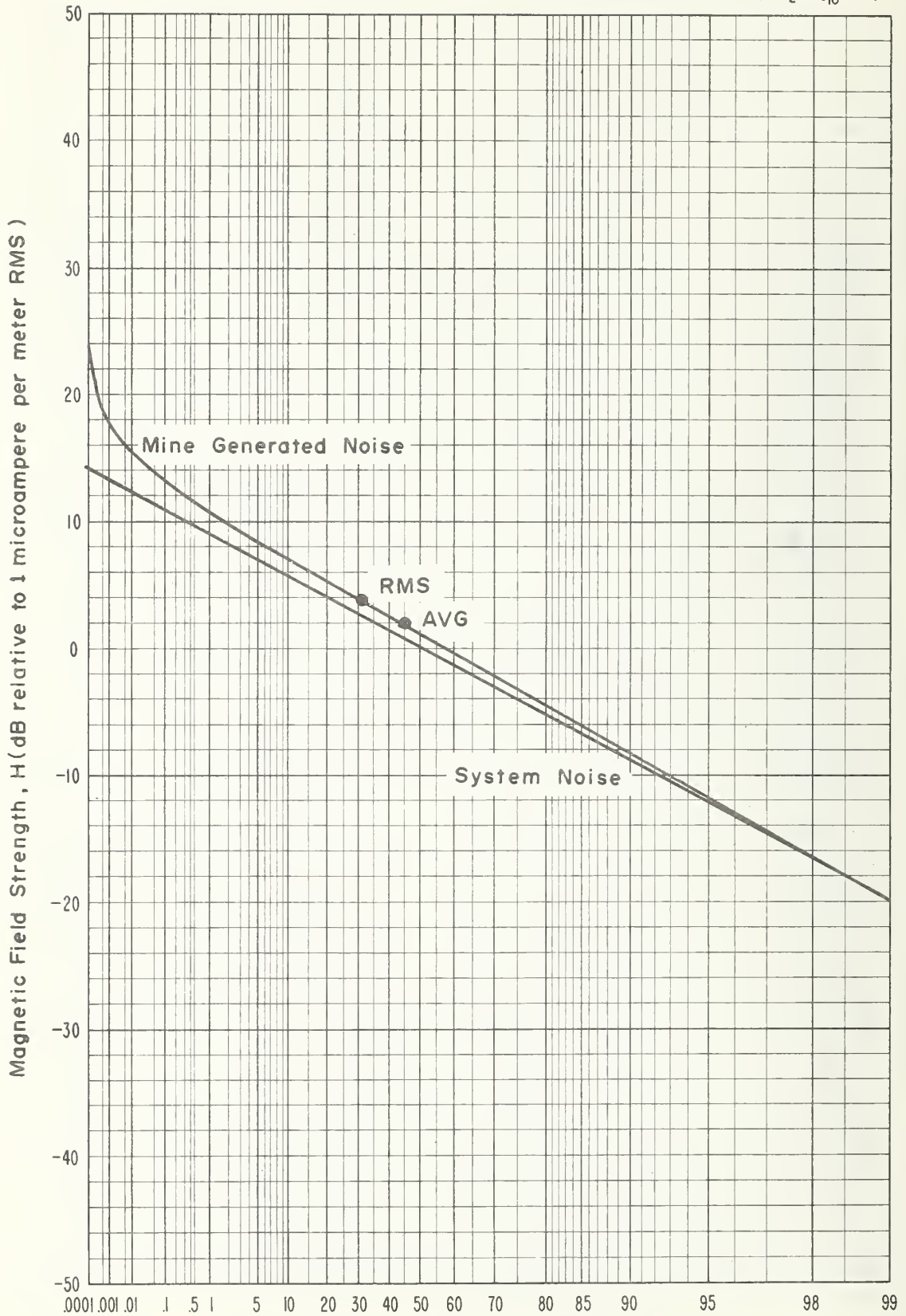


Figure 4-8 APD, 2 MHz, vertical component, 1.2 kHz predetection bandwidth, April 24, 1973, 11:05 a.m., development foreman office, Grace Mine.



Percent of Time Ordinate is Exceeded

Figure 4-9 APD, 6 MHz, vertical component, 1.2 kHz predetection bandwidth, April 24, 1973, 11:44 a.m., development foreman office, Grace Mine.

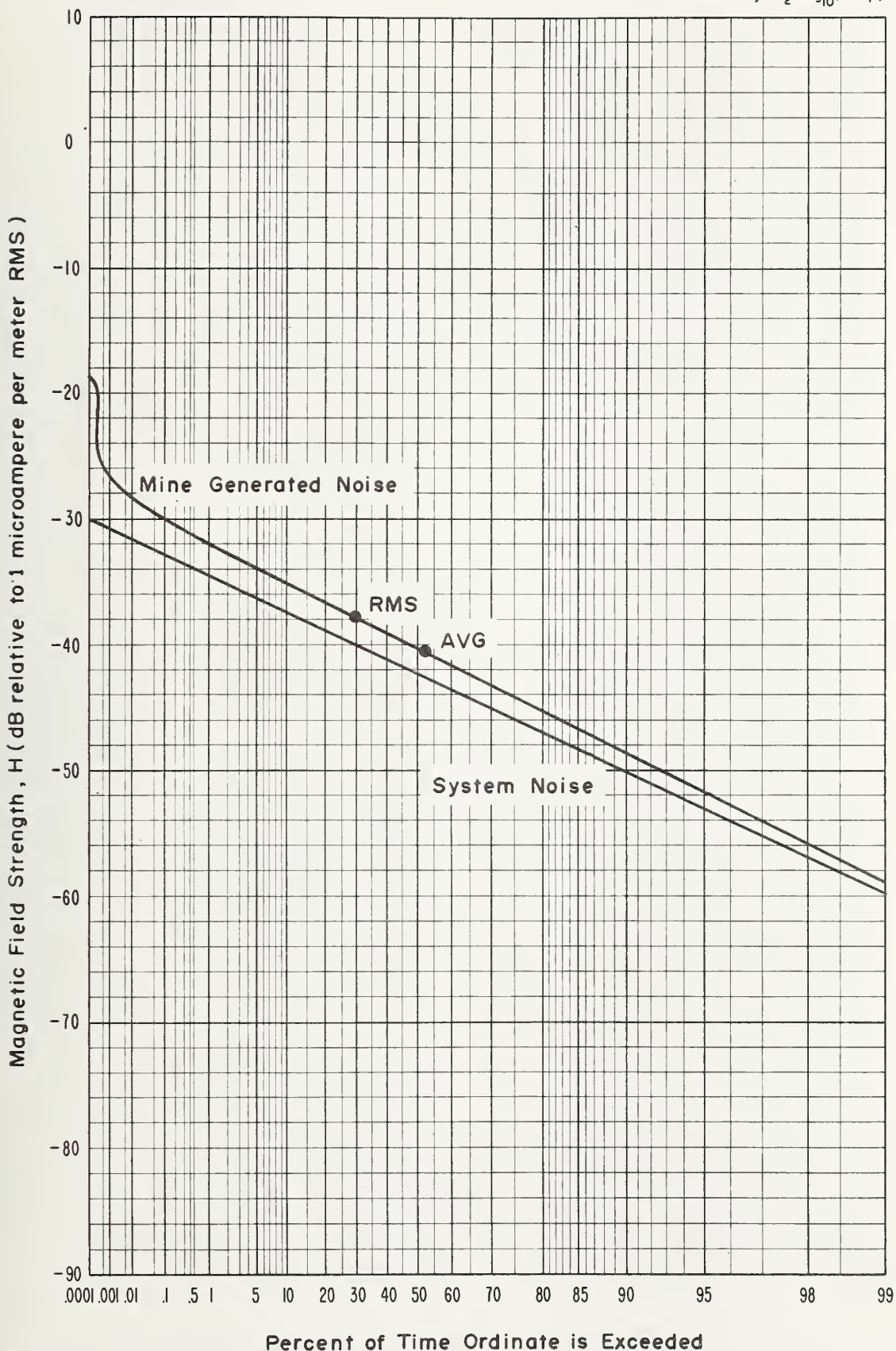


Figure 4-10 APD, 14 MHz, vertical component, 1.2 kHz predetection bandwidth, April 24, 1973, 12:10 p.m., development foreman office, Grace Mine.

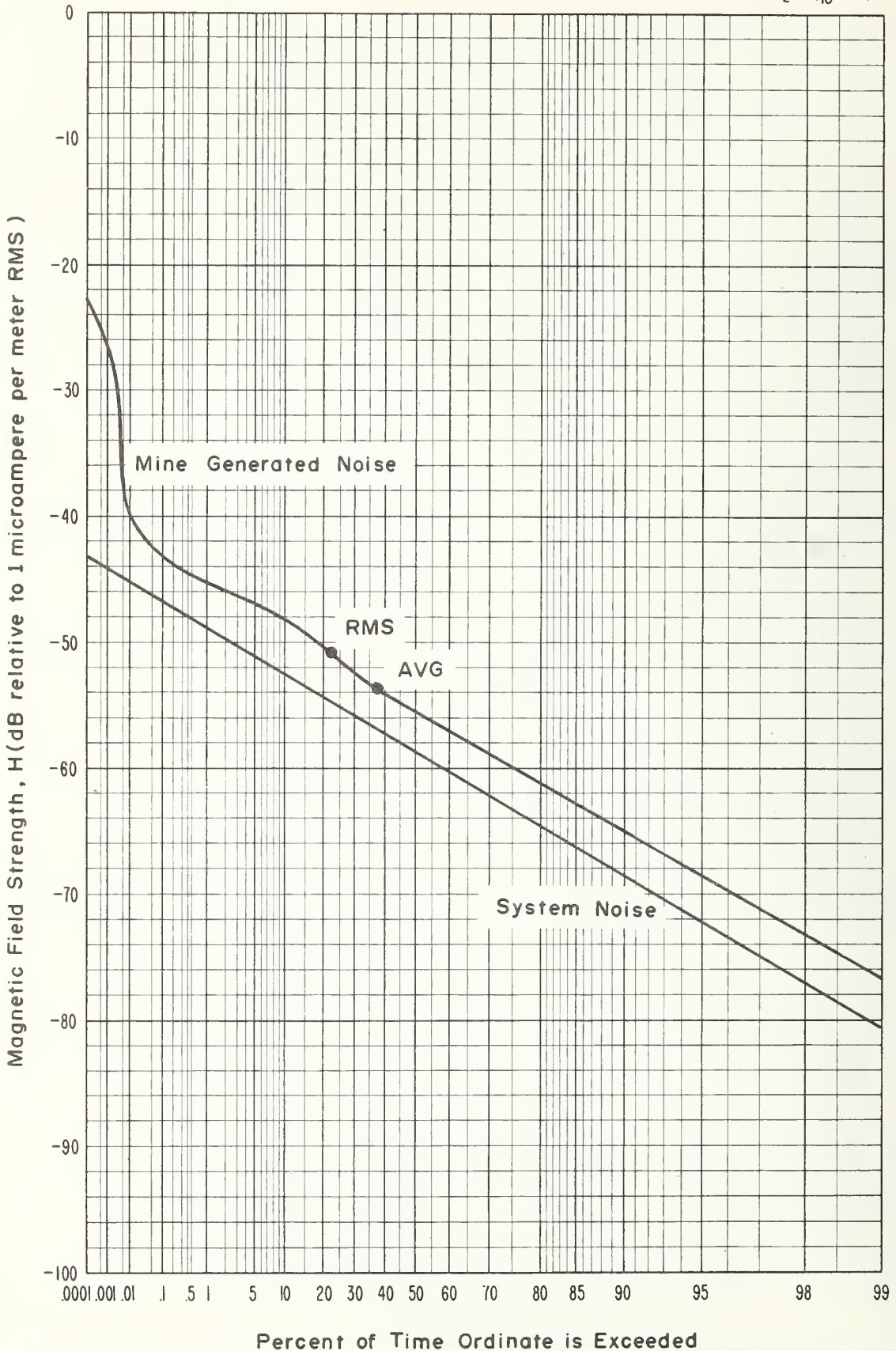


Figure 4-11 APD, 32 MHz, vertical component, 1.2 kHz predetection bandwidth, April 24, 1973, 12:40 p.m., development foreman office, Grace Mine.

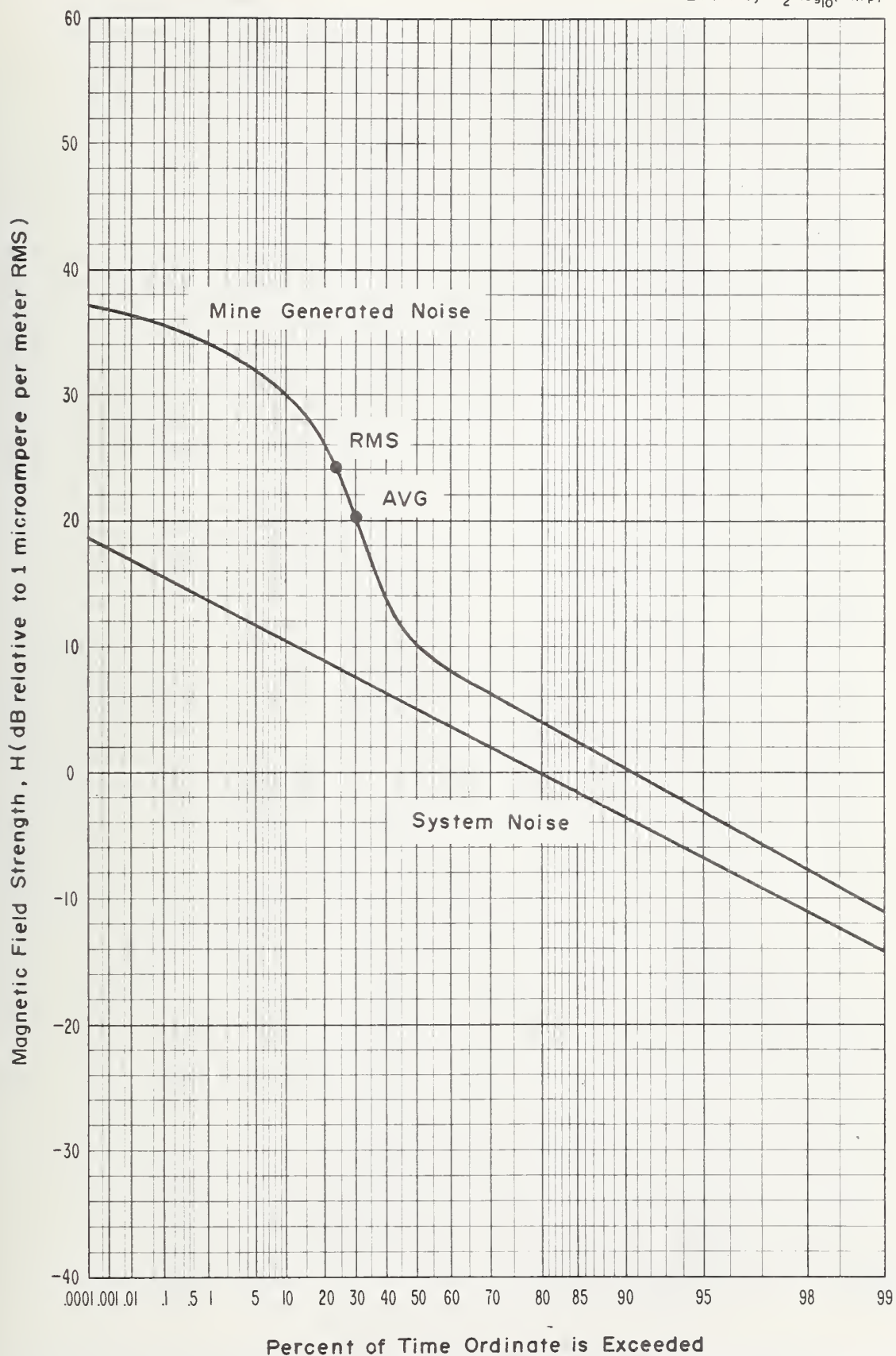


Figure 4-12 APD, 10 kHz, vertical component, 1.0 kHz predetection bandwidth, April 24, 1973, 3:00 p.m., crusher substation, Grace Mine.

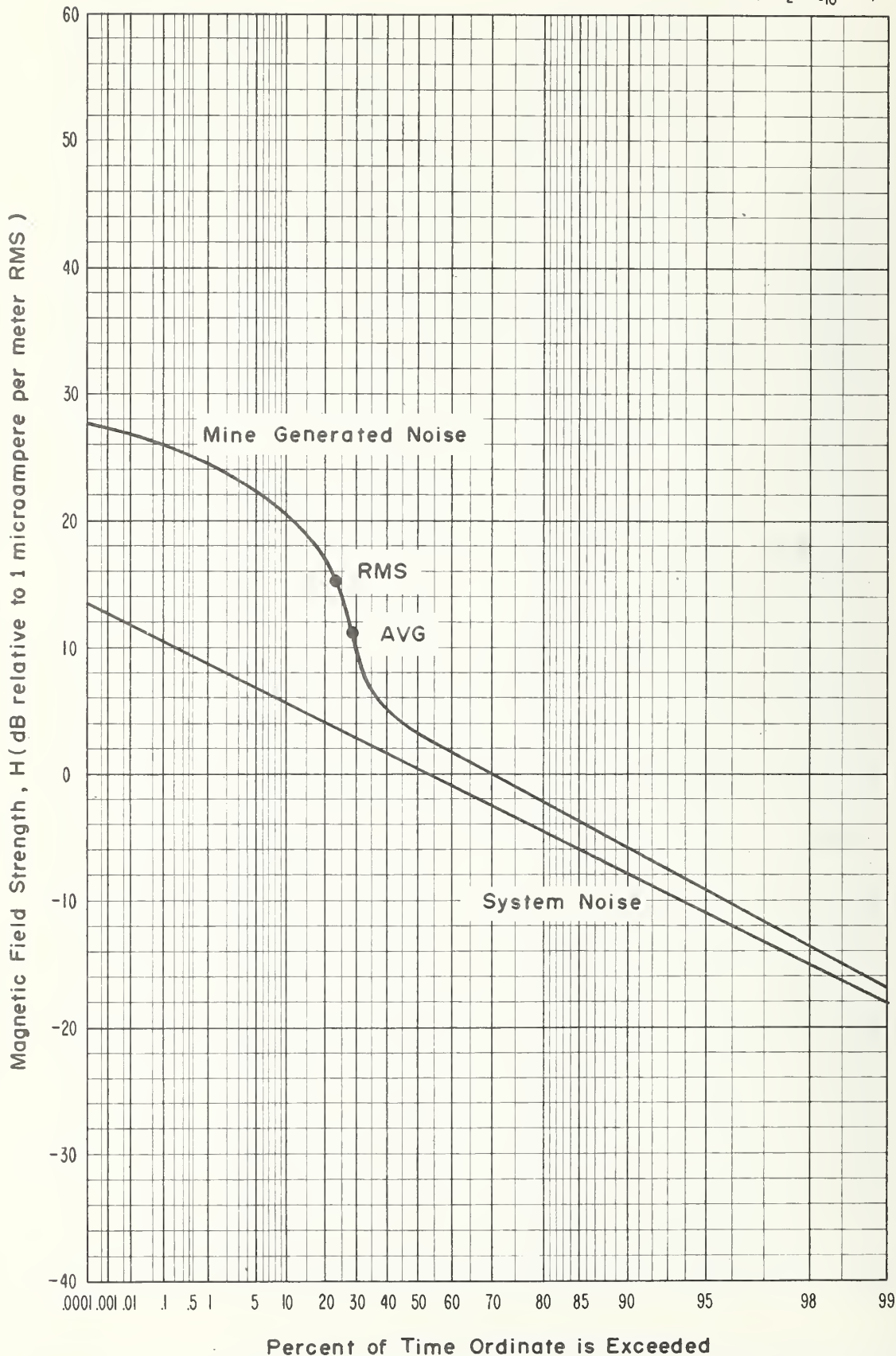


Figure 4-13 APD, 30 kHz, vertical component, 1.0 kHz predetection bandwidth, April 24, 1973, 3:30 p.m., crusher substation, Grace Mine.

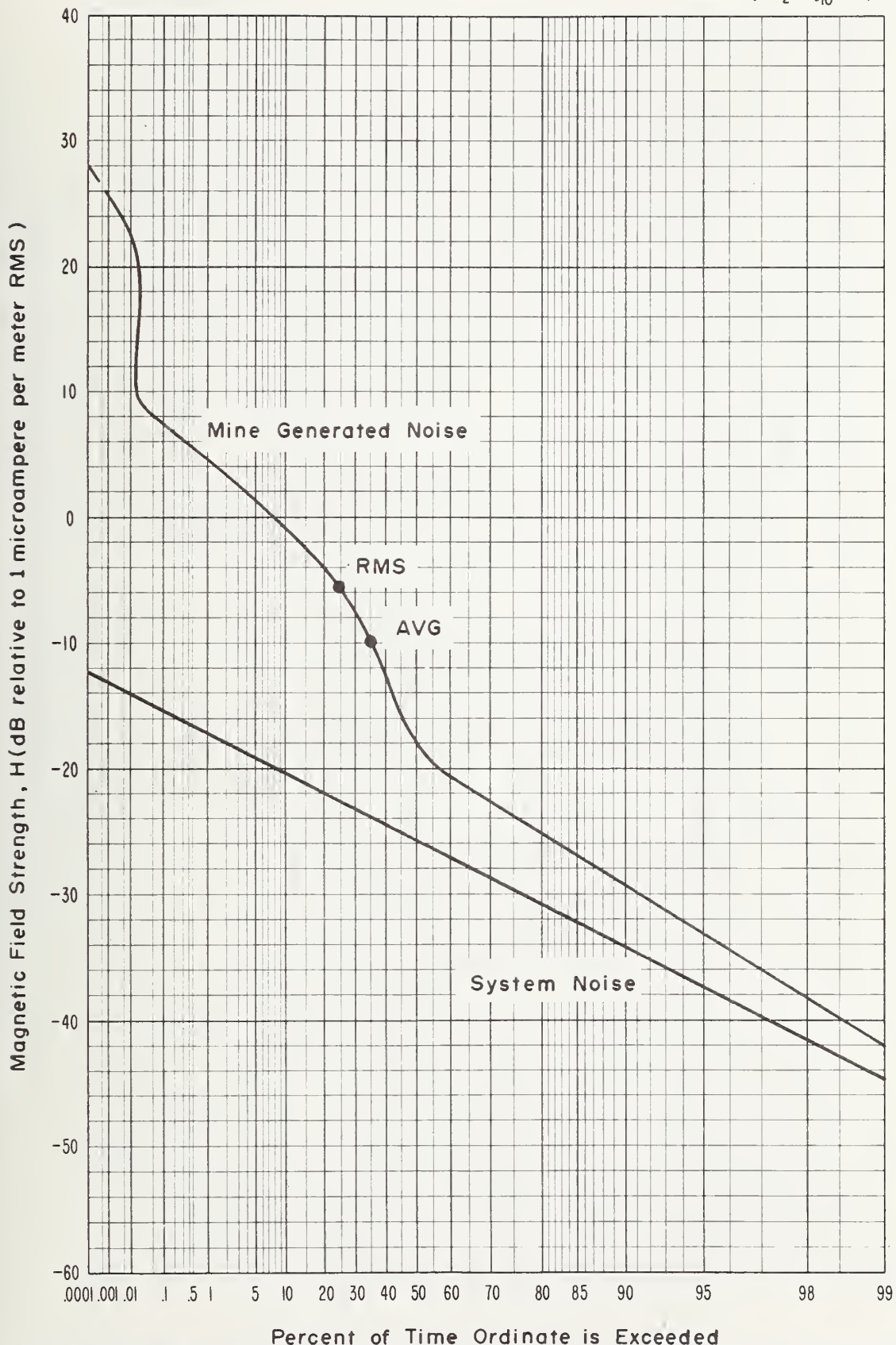


Figure 4-14 APD, 70 kHz, vertical component, 1.0 kHz predetection bandwidth, April 24, 1973, 4:05 p.m., crusher substation, Grace Mine.

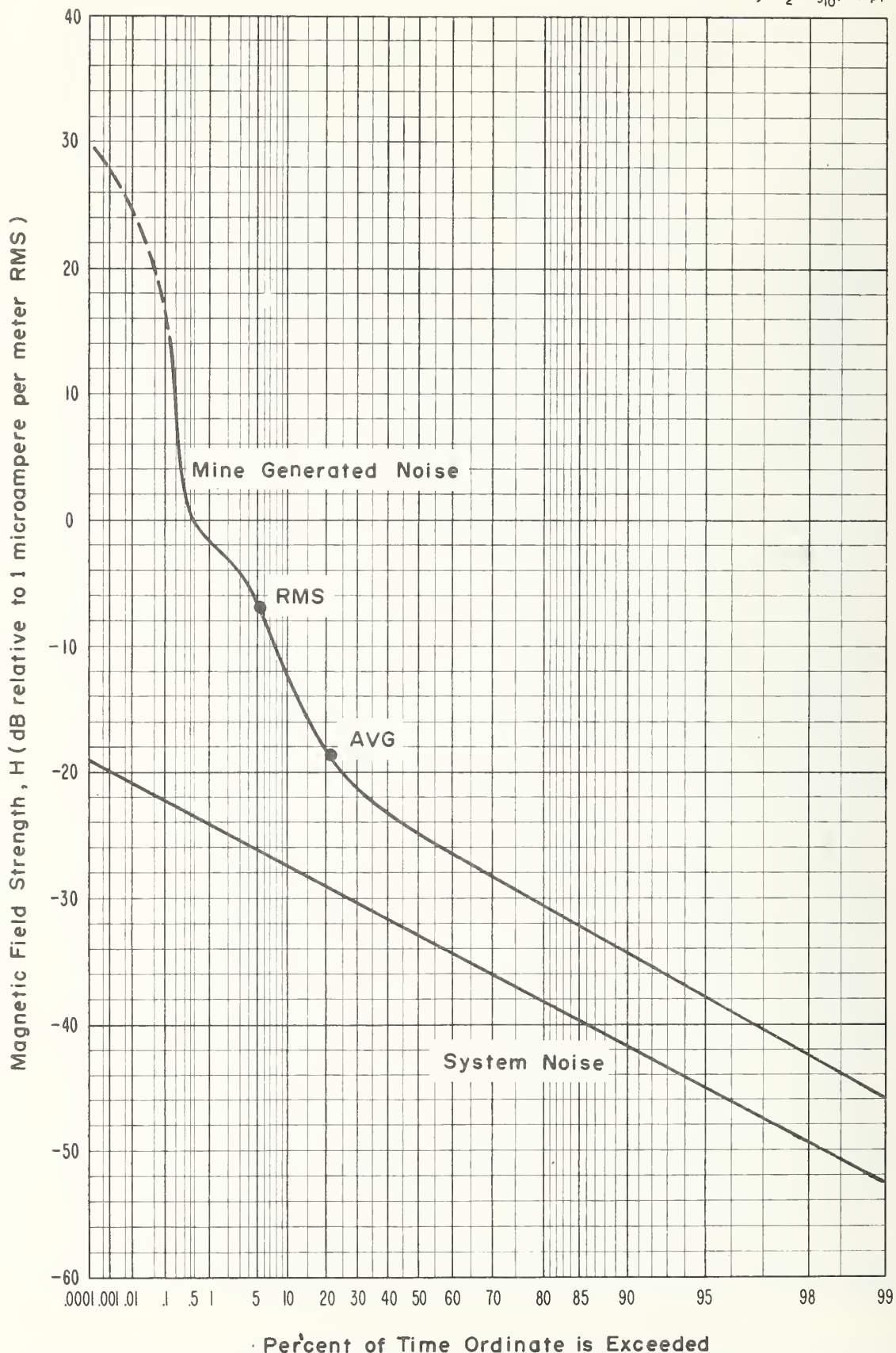


Figure 4-15 APD, 130 kHz, vertical component, 1.0 kHz predetection bandwidth, April 24, 1973, 4:35 p.m., crusher substation, Grace Mine.



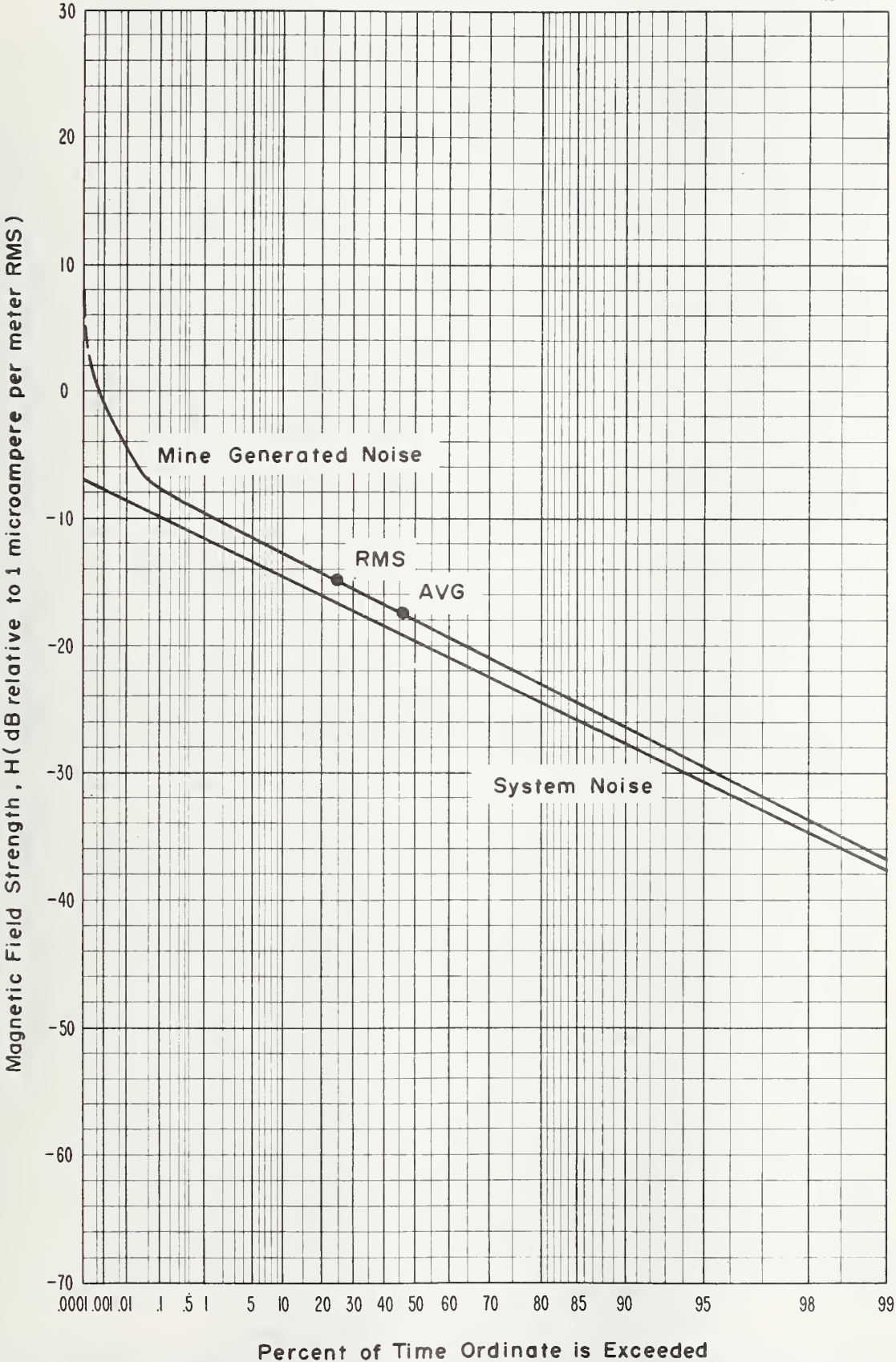


Figure 4-16 APD, 0.5 MHz, vertical component, 1.2 kHz predetection bandwidth, April 24, 1973, 3:00 p.m., crusher substation, Grace Mine.

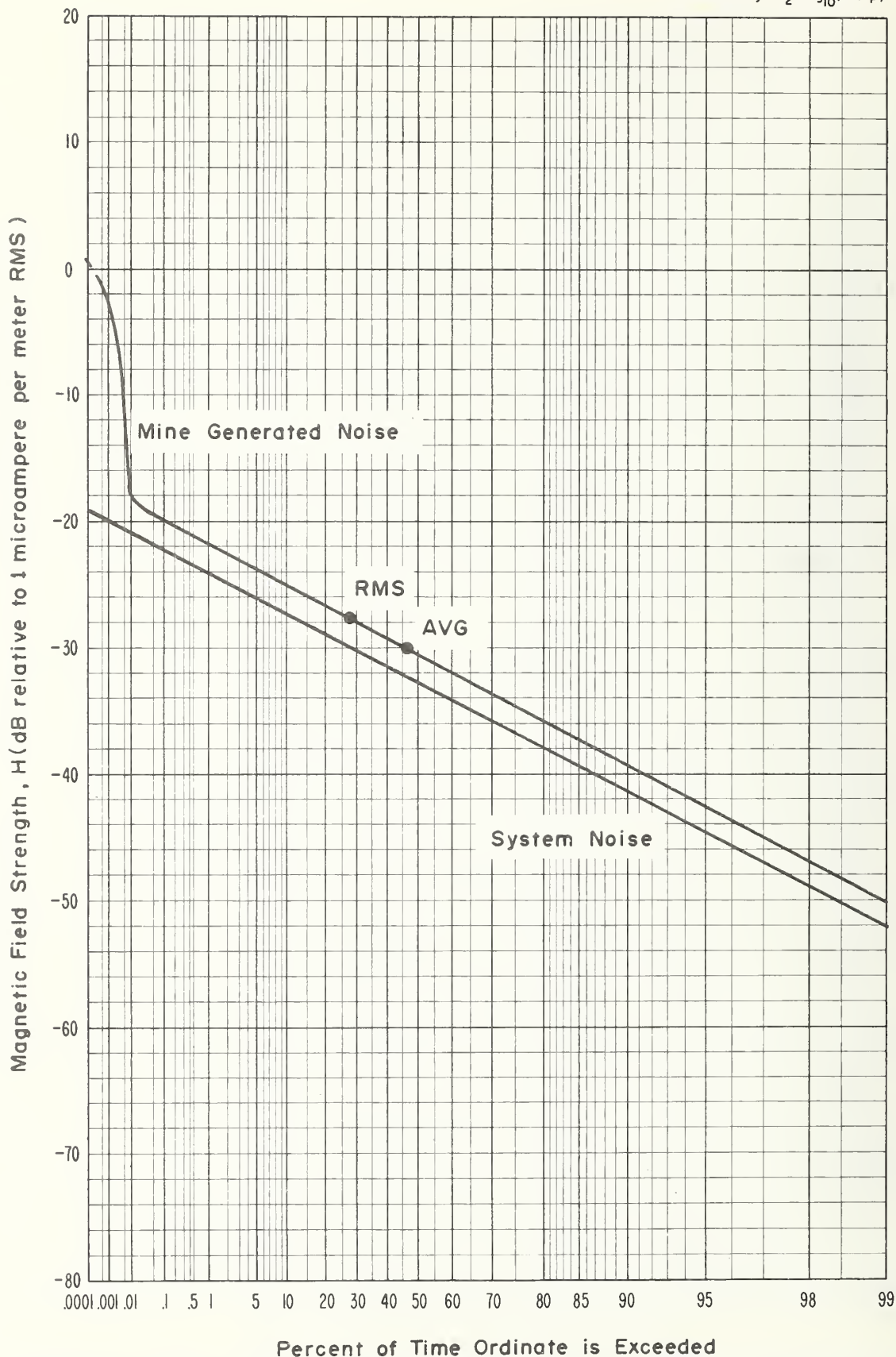


Figure 4-17 APD, 1 MHz, vertical component, 1.2 kHz predetection bandwidth, April 24, 1973, 3:30 p.m., crusher substation, Grace Mine.

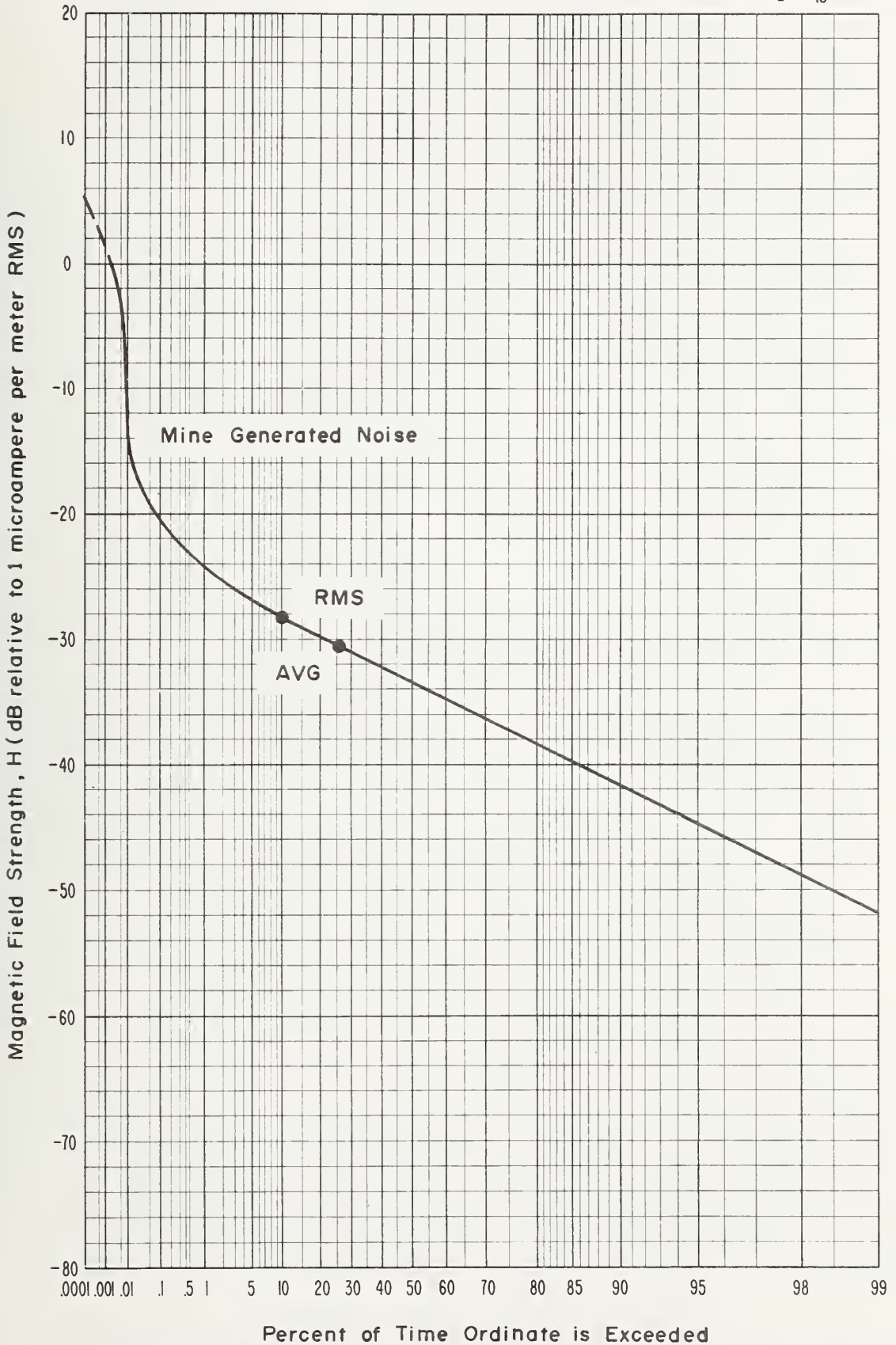


Figure 4-18 APD, 2 MHz, vertical component, 1.2 kHz predetection bandwidth, April 24, 1973, 4:05 p.m., crusher substation, Grace Mine.

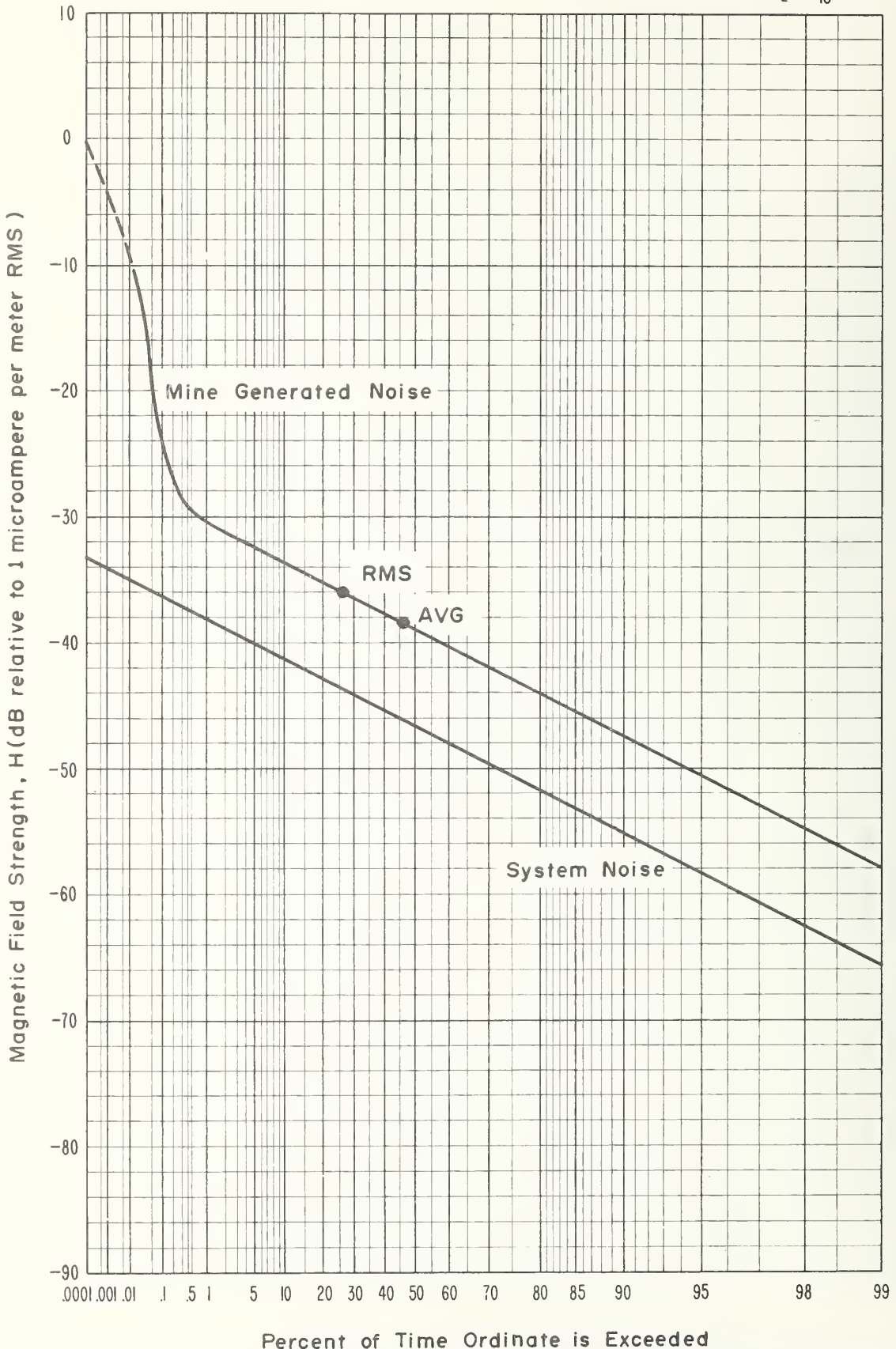


Figure 4-19 APD, 6 MHz, vertical component, 1.2 kHz predetection bandwidth, April 24, 1973, 4:35 p.m., crusher substation, Grace Mine.

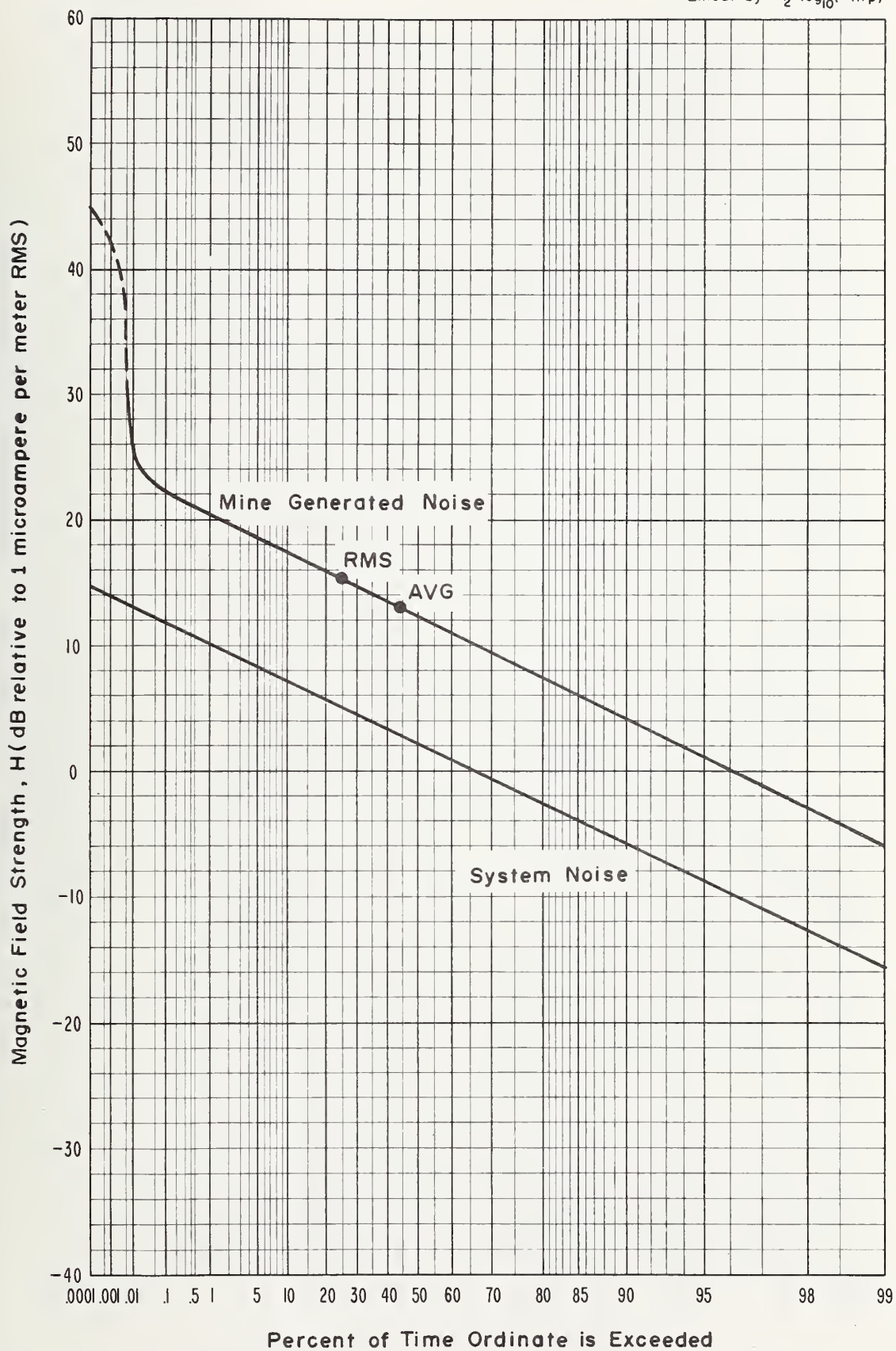


Figure 4-20 APD, 30 kHz, vertical component, 1.0 kHz predetection bandwidth, April 24, 1973, 11:07a.m., shop office, Grace Mine.

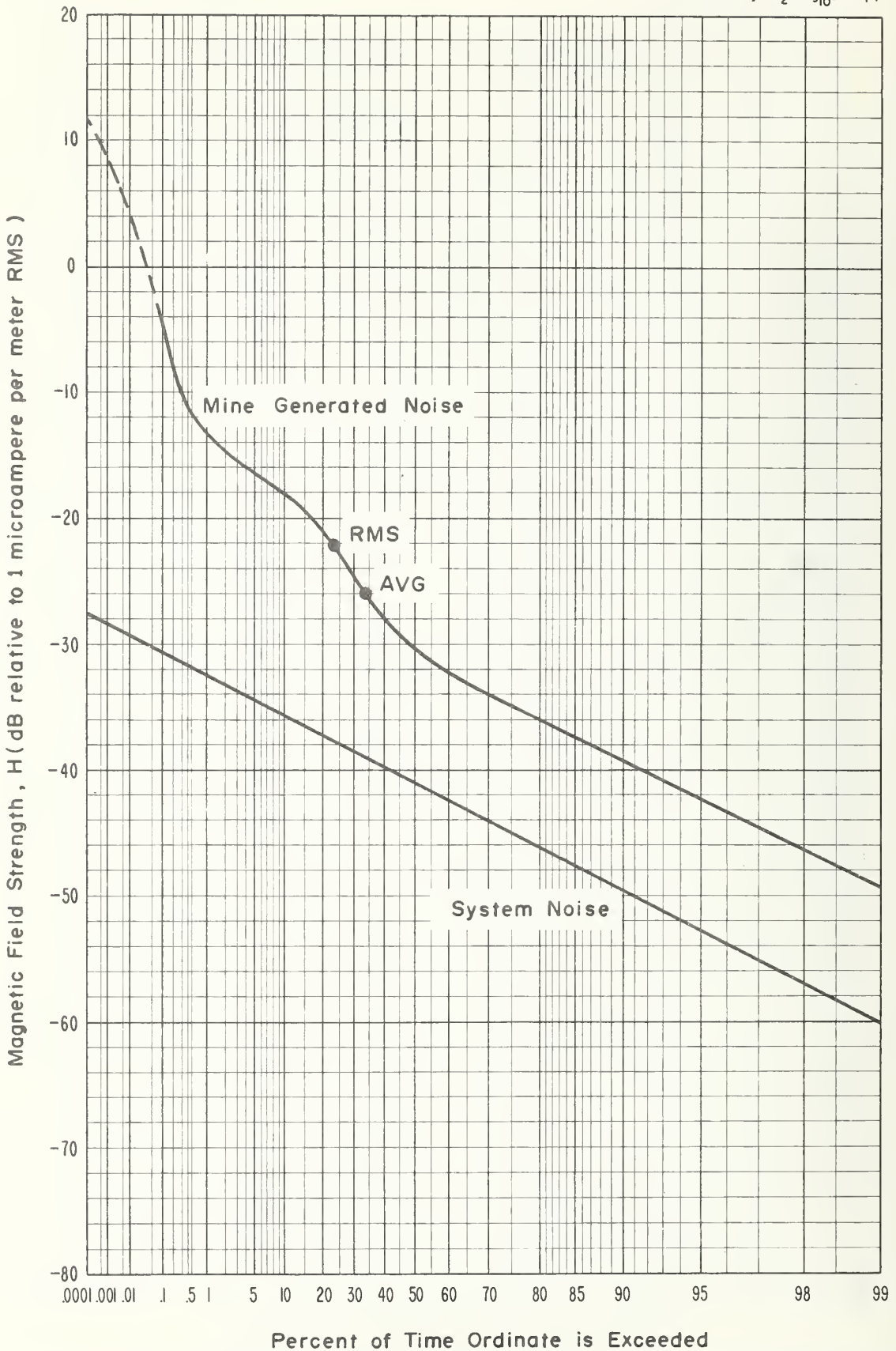


Figure 4-21 APD, 70 kHz, vertical component, 1.0 kHz predetection bandwidth, April 24, 1973, 1:00 p.m., shop office, Grace Mine.

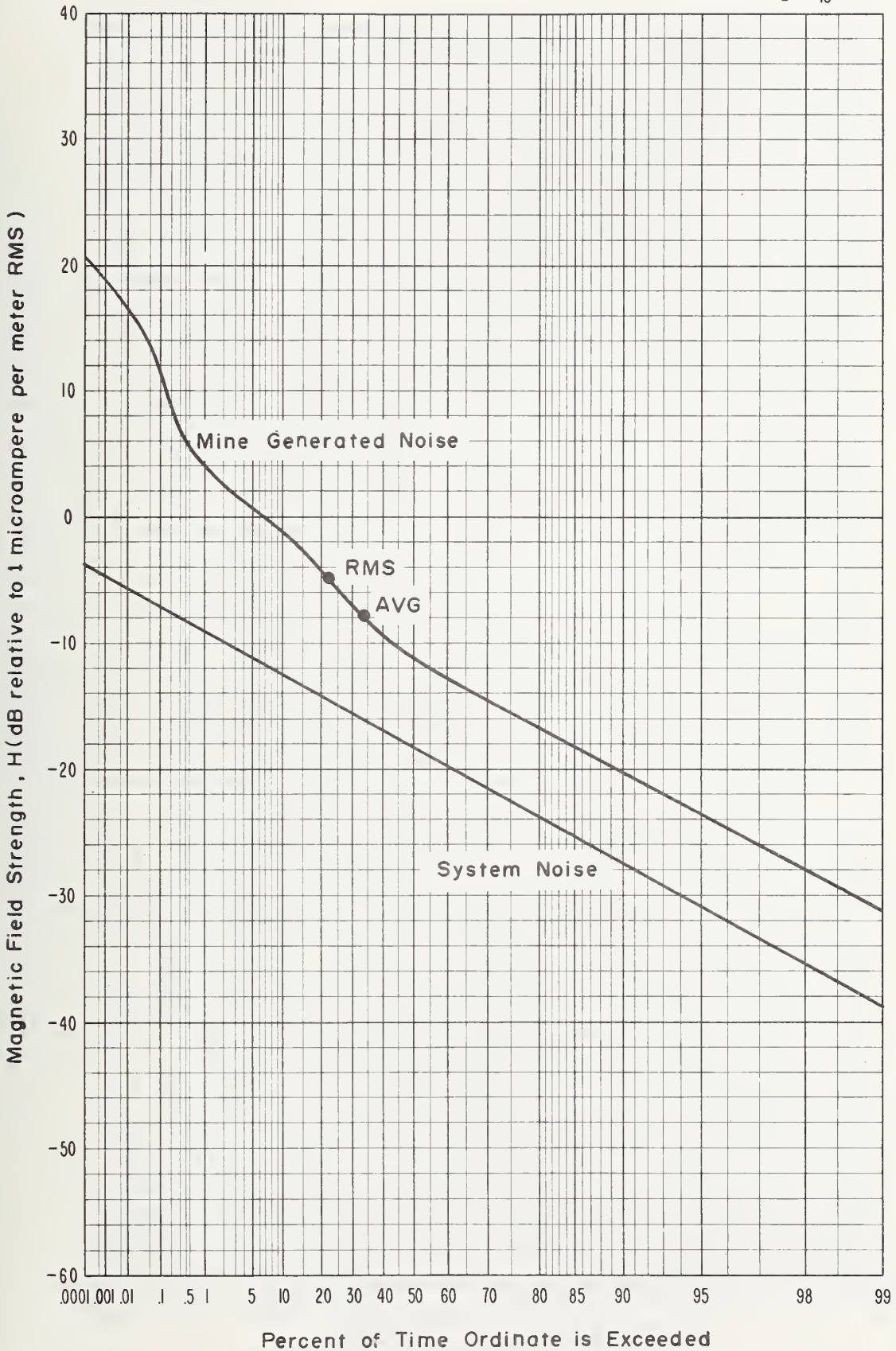


Figure 4-22 APD, 110 kHz, vertical component, 1.0 kHz predetection bandwidth, April 24, 1973, 5:15 p.m., shop office, Grace Mine.

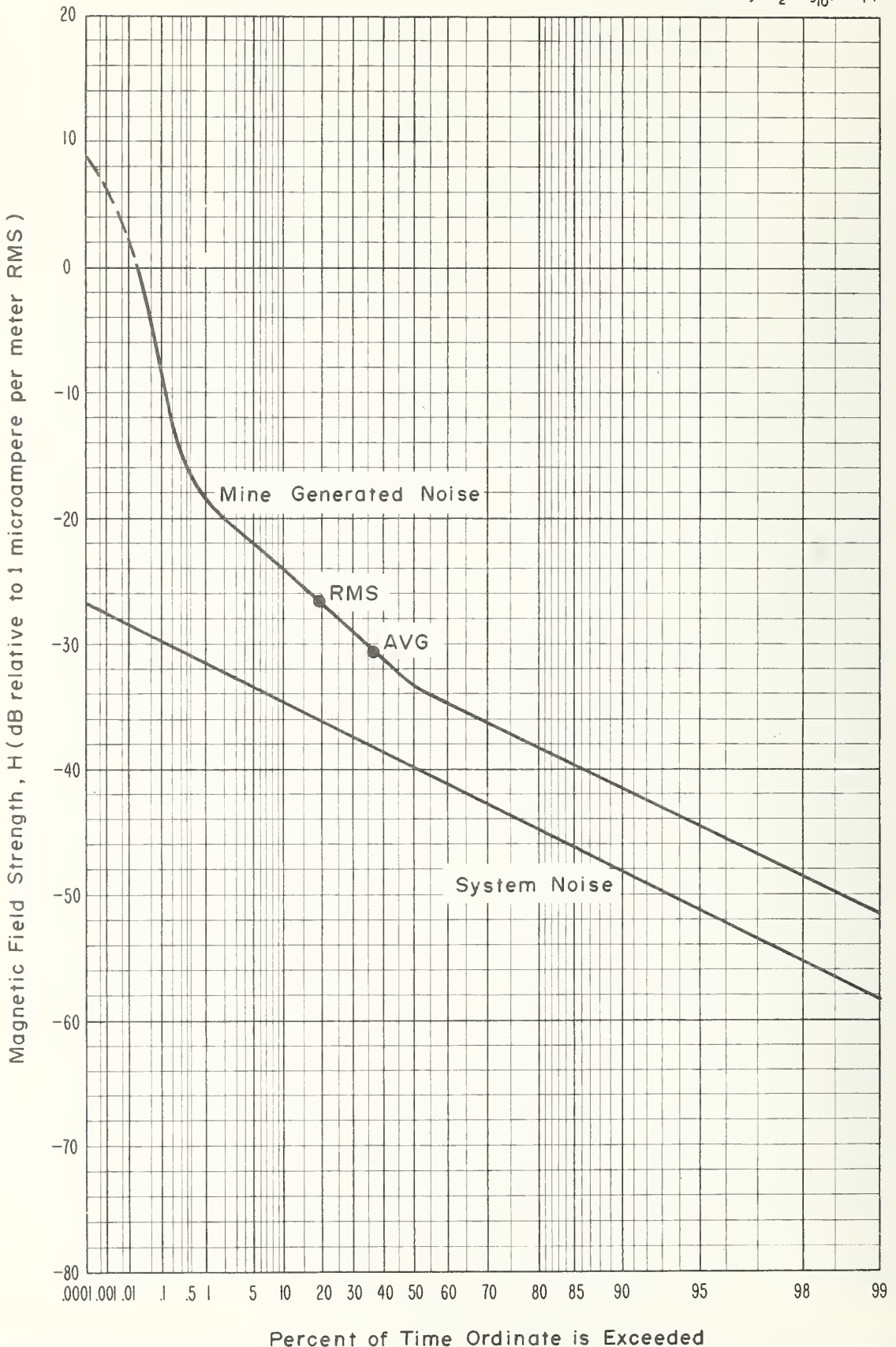


Figure 4-23 APD, 130 kHz, vertical component, 1.0 kHz predetection bandwidth, April 24, 1973, 2:15 p.m., shop office, Grace Mine.



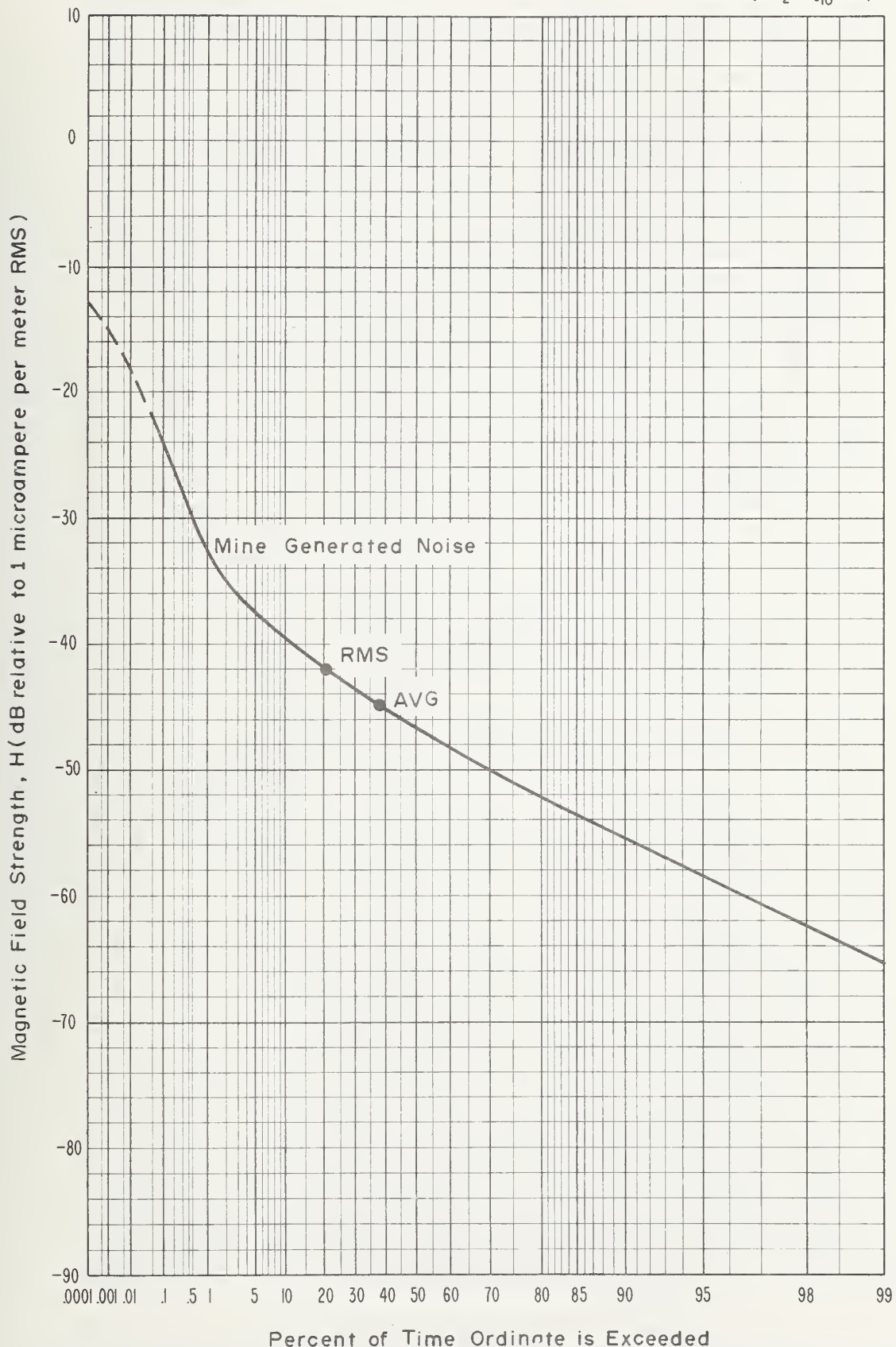


Figure 4-24 APD, 160 kHz, vertical component, 1.0 kHz predetection bandwidth, April 24, 1973, 4:45 p.m., shop office, Grace Mine.

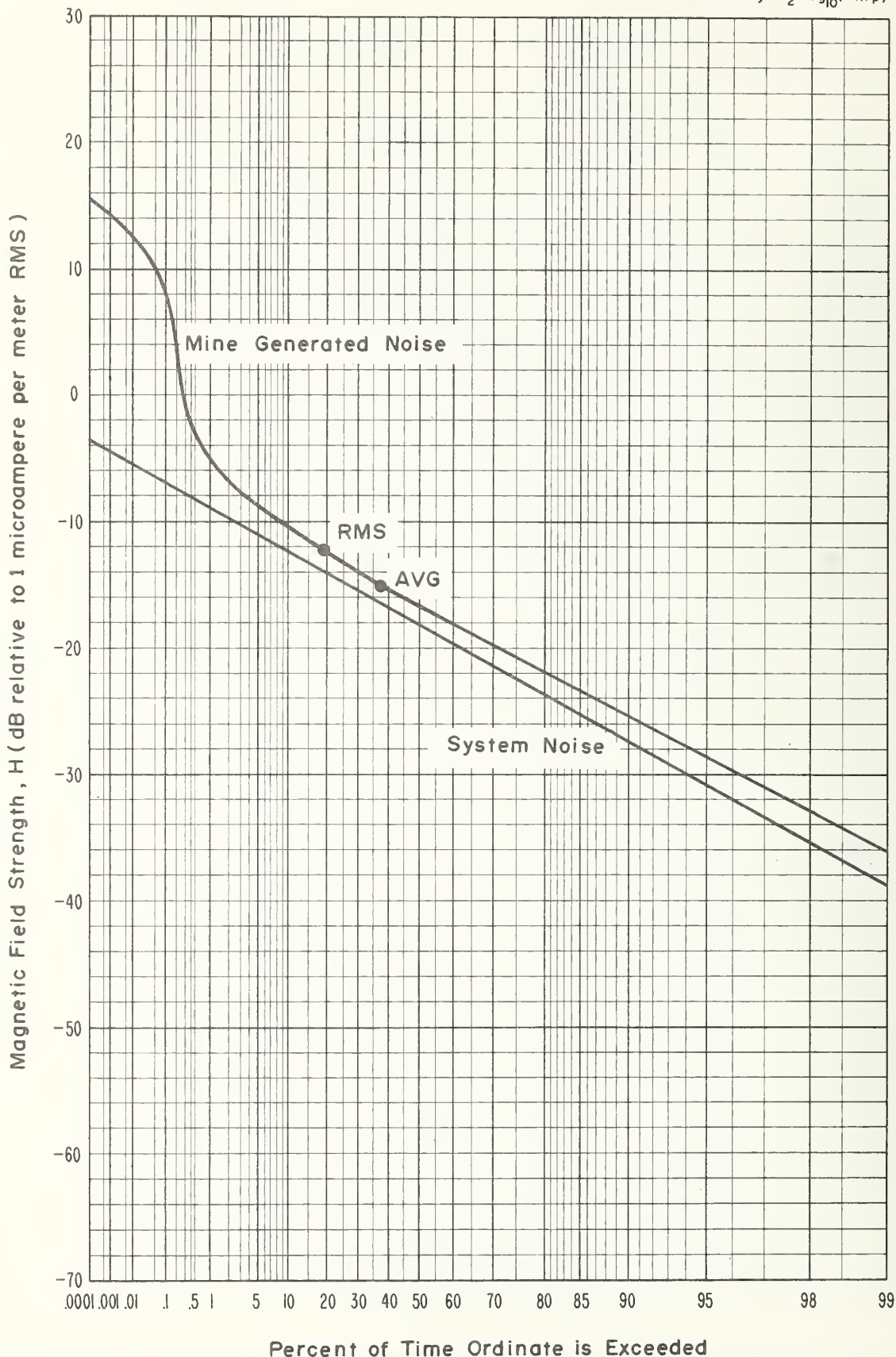


Figure 4-25 APD, 205 kHz, vertical component, 1.0 kHz predetection bandwidth, April 24, 1973, 5:33 p.m., shop office, Grace Mine.

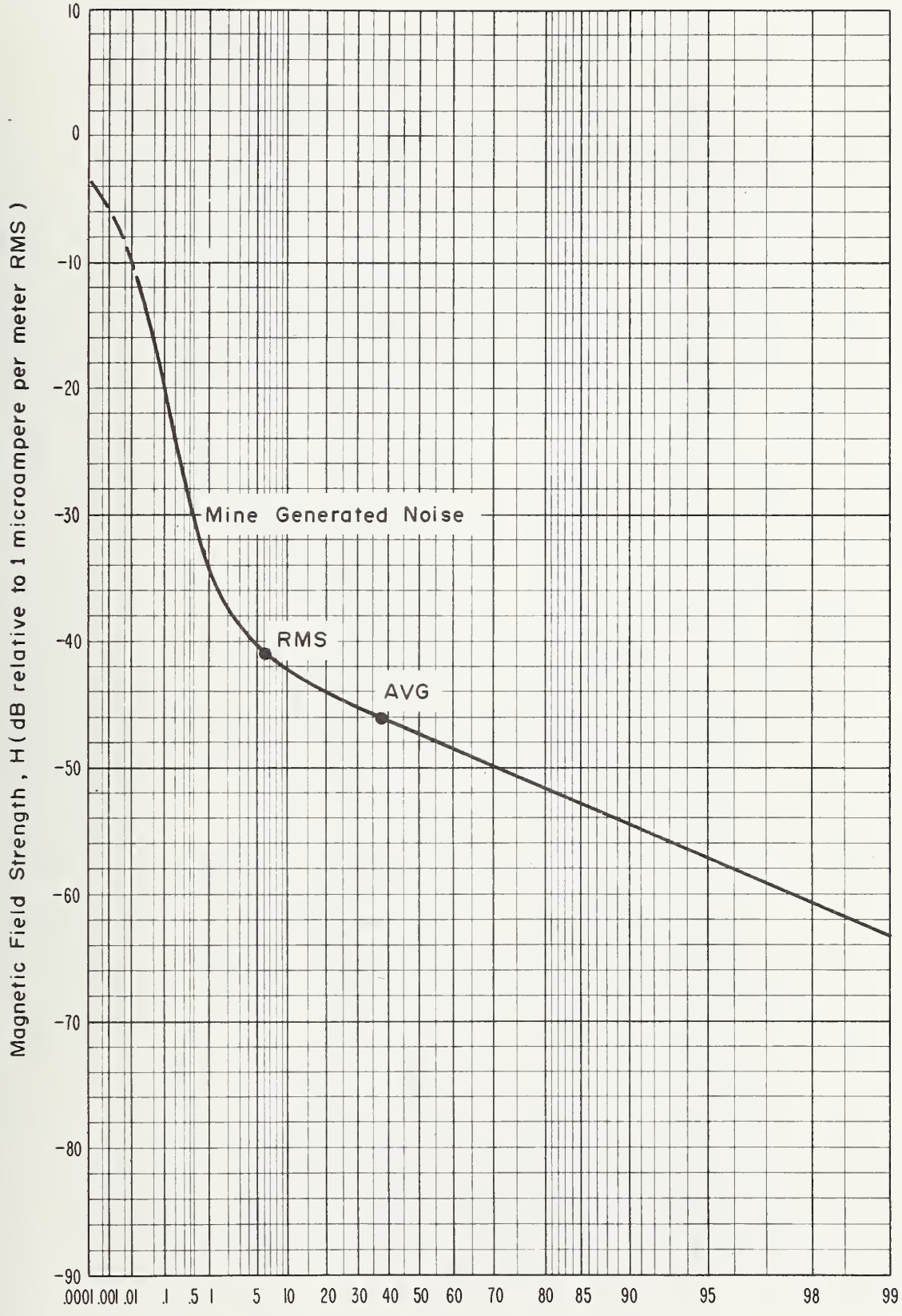


Figure 4-26 APD, 250 kHz, vertical component, 1.2 kHz predetection bandwidth, April 24, 1973, 10:27a.m., shop office, Grace Mine.

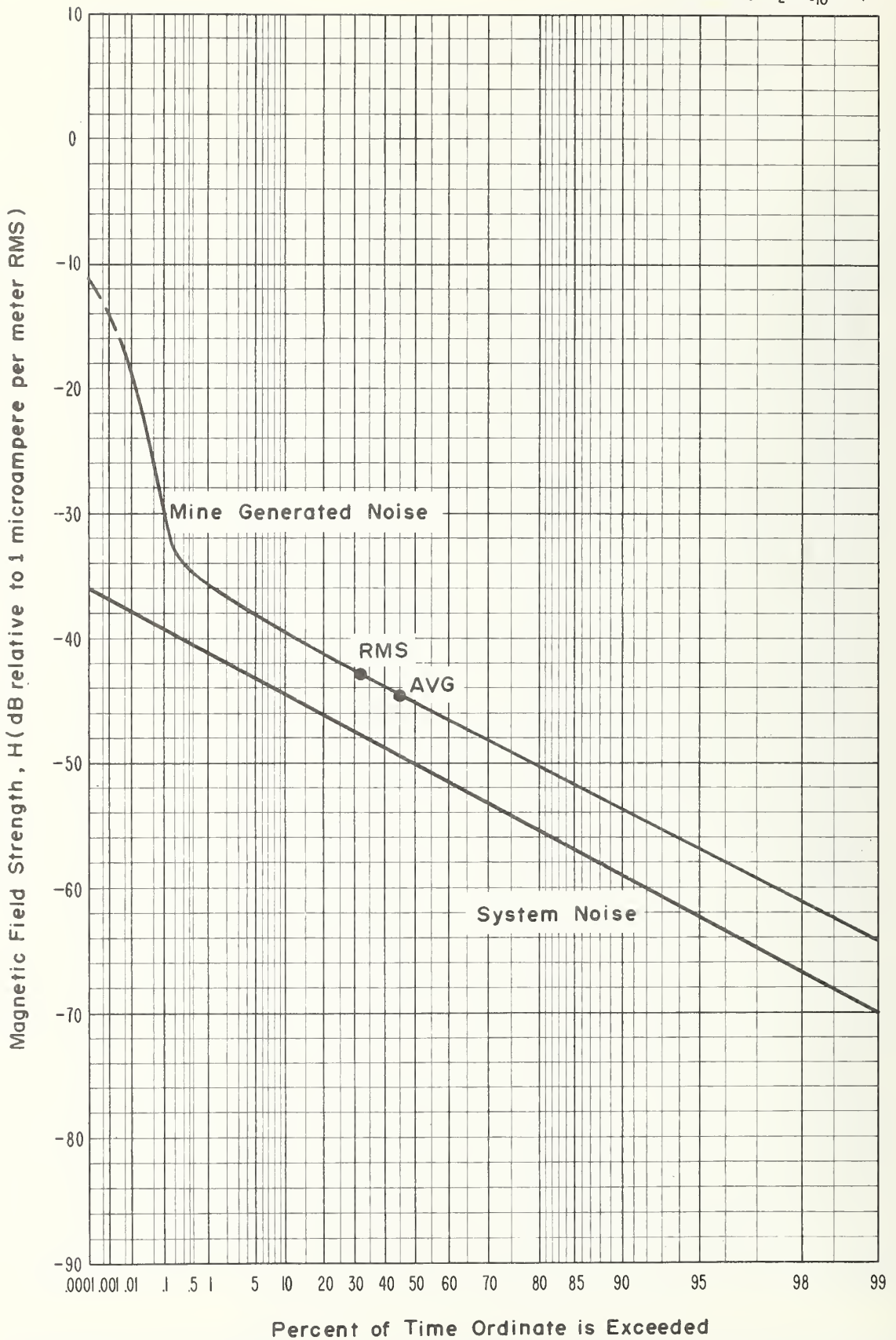


Figure 4-27 APD, 500 kHz, vertical component, 1.2 kHz predetection bandwidth, April 24, 1973, 11:07a.m., shop office, Grace Mine.

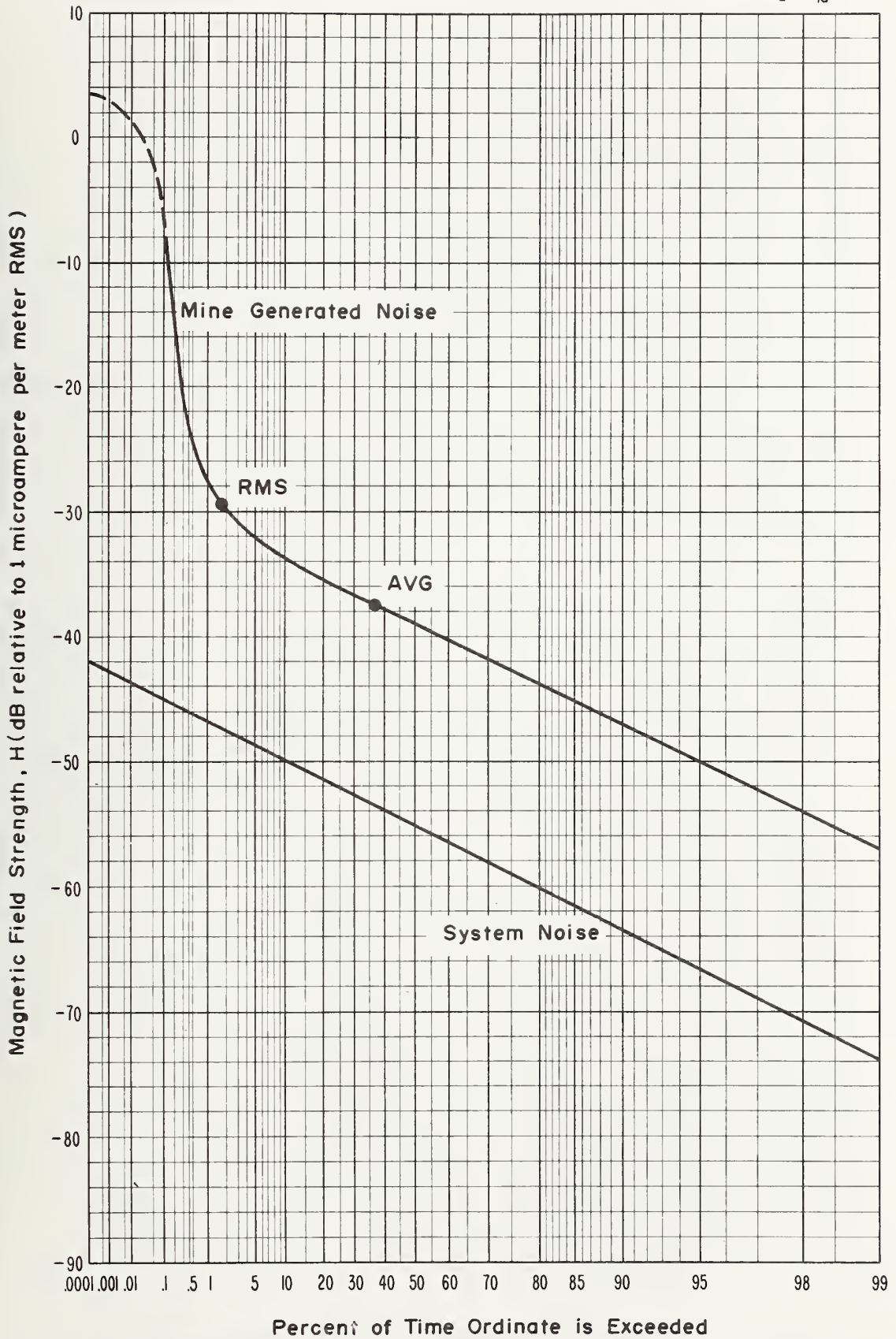


Figure 4-28 APD, 1 MHz, vertical component, 1.2 kHz predetection bandwidth, April 24, 1973, 1:00 p.m., shop office, Grace Mine.

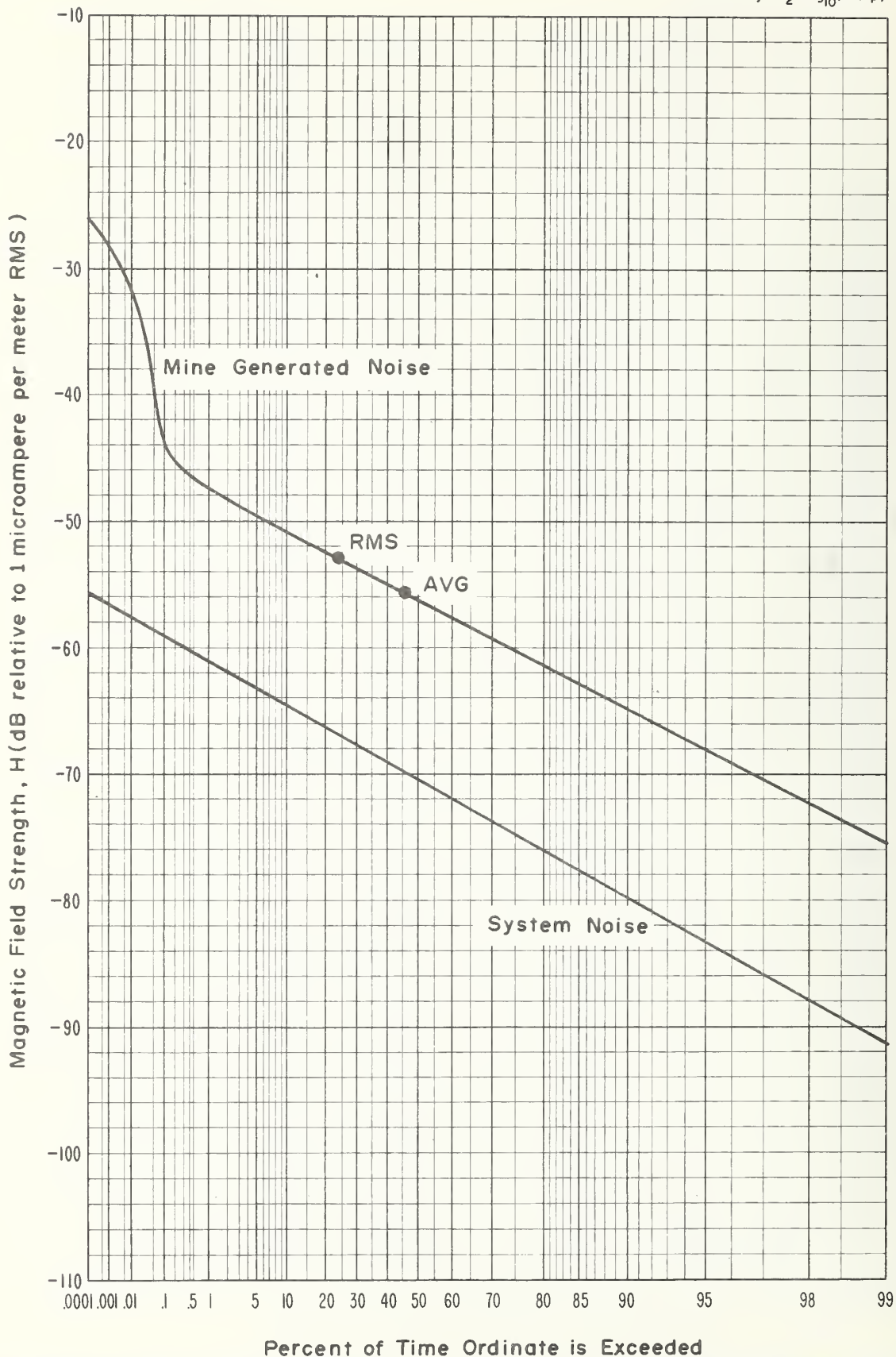


Figure 4-29 APD, 2 MHz, vertical component, 1.2 kHz predetection bandwidth, April 24, 1973, 2:15 p.m., shop office, Grace Mine.

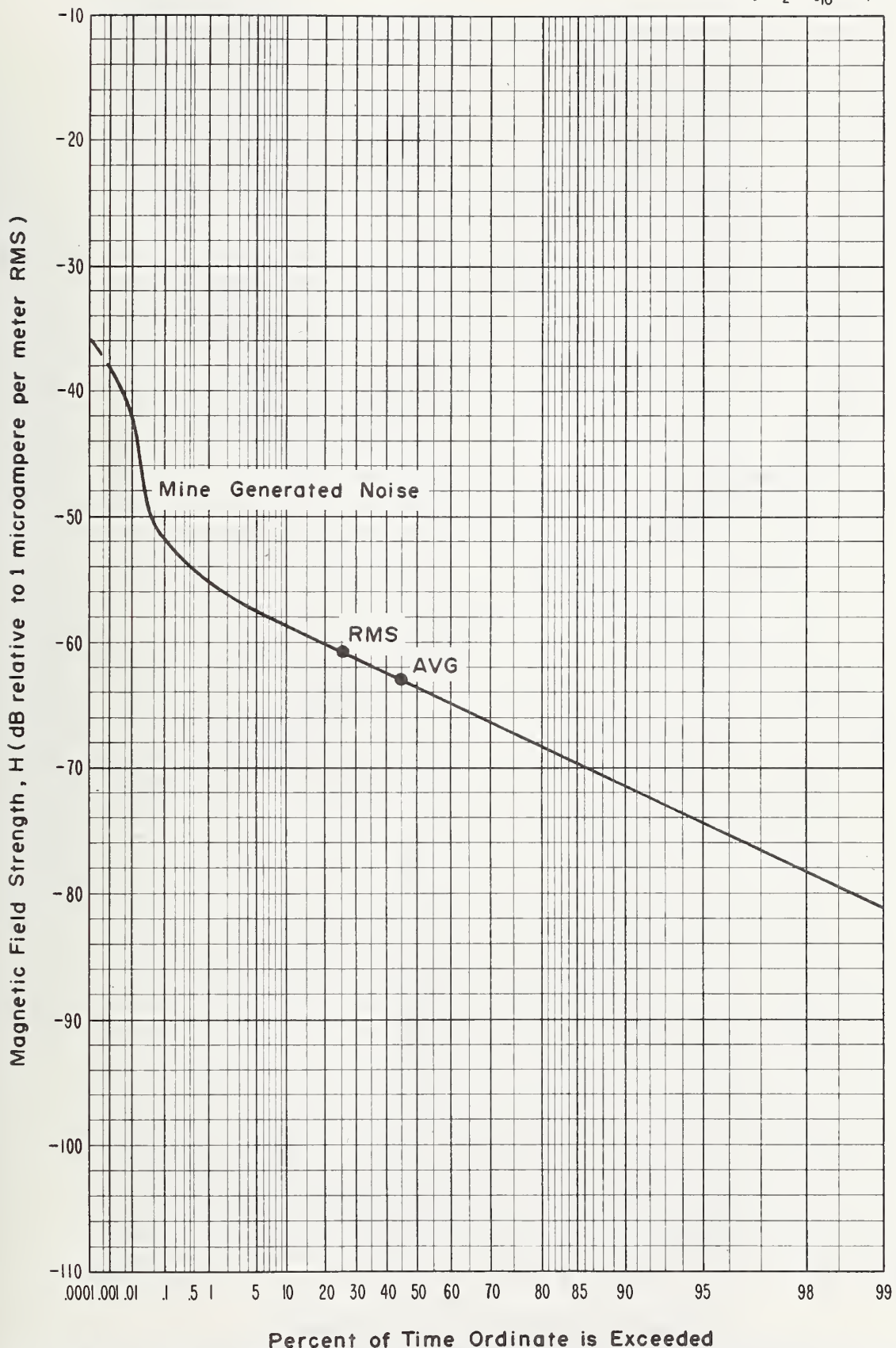


Figure 4-30 APD, 6 MHz, vertical component, 1.2 kHz predetection bandwidth, April 24, 1973, 4:45 p.m., shop office, Grace Mine.

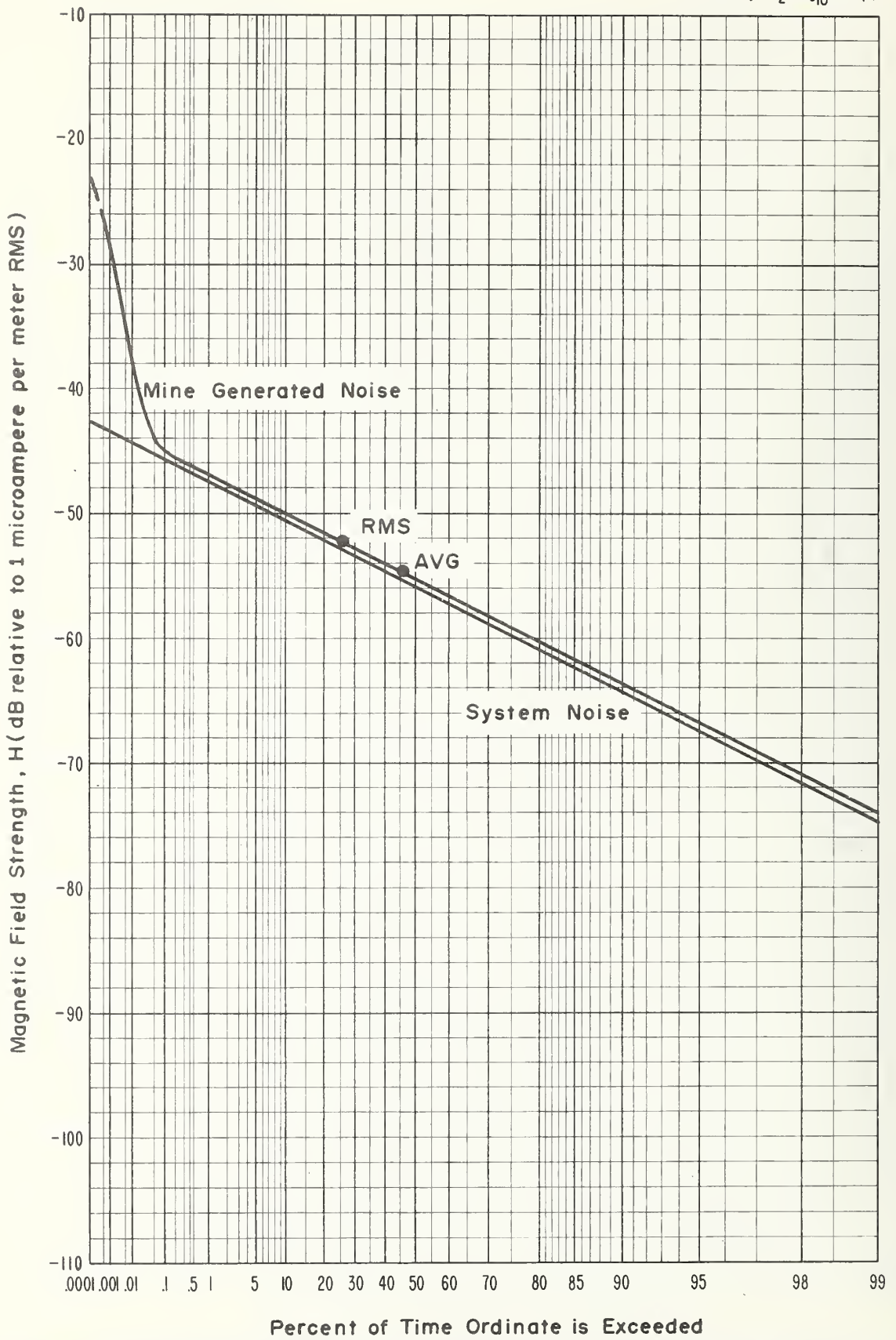


Figure 4-31 APD, 14 MHz, vertical component, 1.2 kHz predetection bandwidth, April 24, 1973, 5:15 p.m., shop office, Grace Mine.



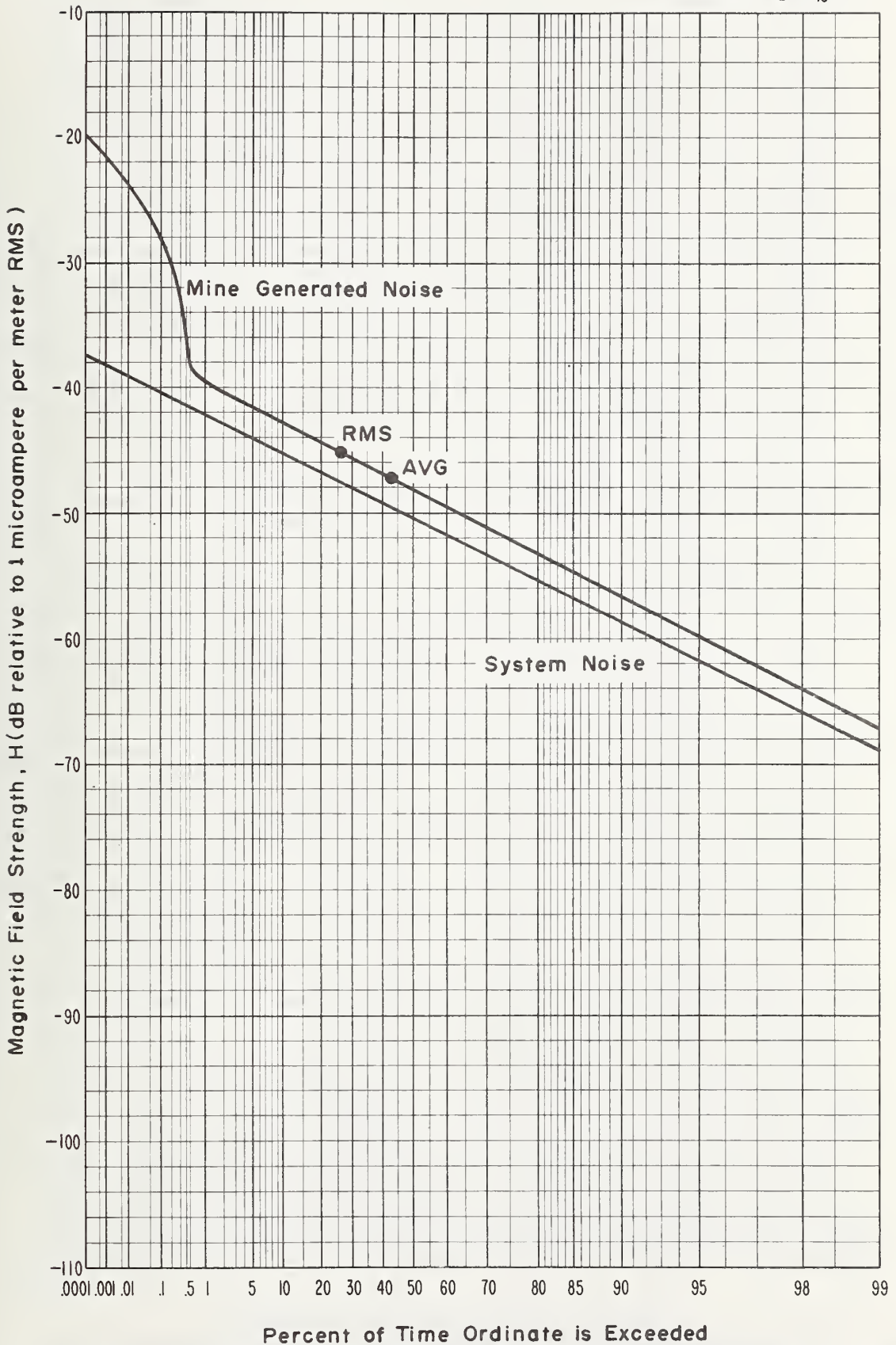
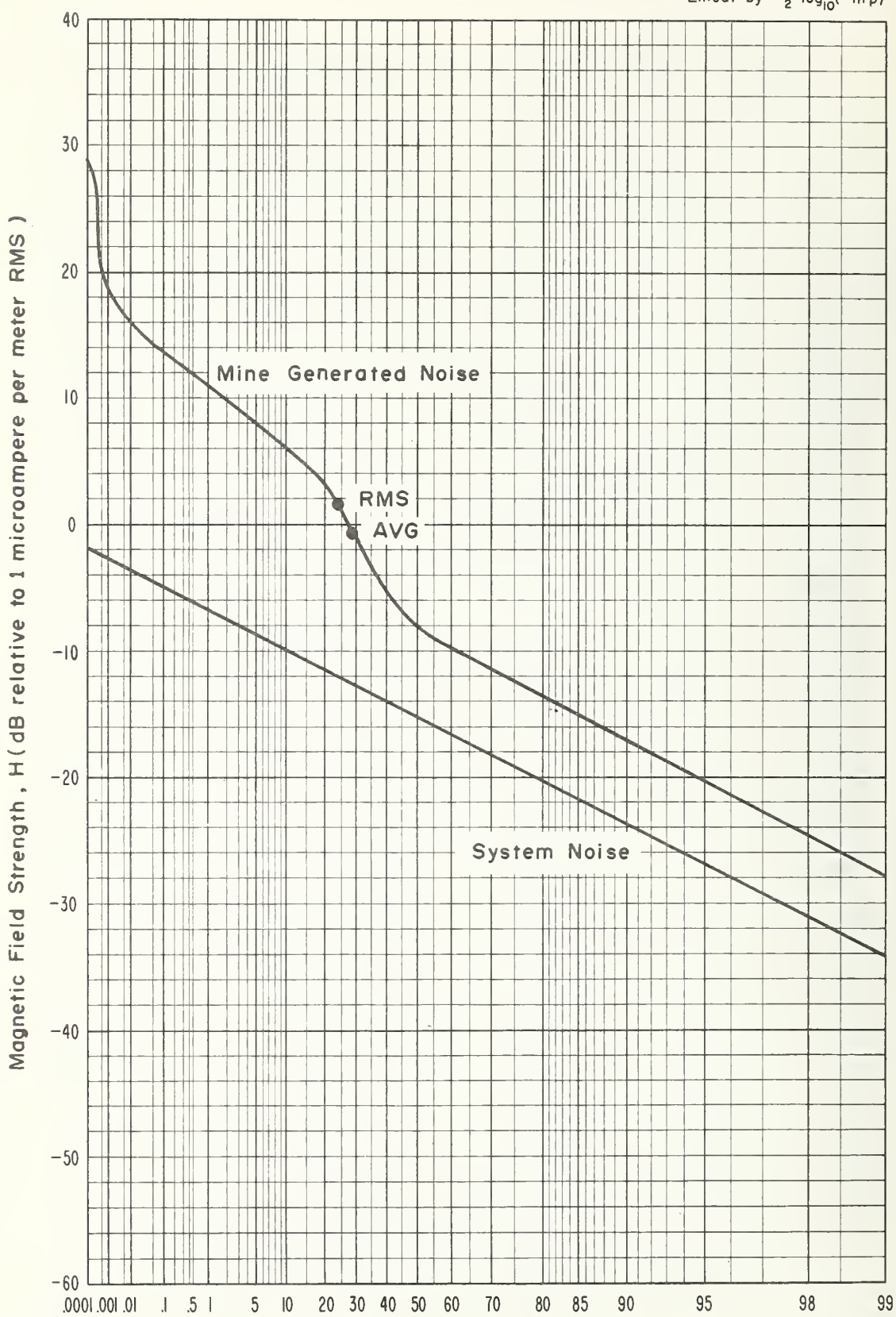


Figure 4-32 APD, 32 MHz, vertical component, 1.2 kHz predetection bandwidth, April 24, 1973, 5:33 p.m., shop office, Grace Mine.



**Percent of Time Ordinate is Exceeded**  
Figure 4-33 APD, 10 kHz, horizontal component E-W, 1.0 kHz predetection bandwidth, April 24, 1973, 3:35 p.m., shop office, Grace Mine.

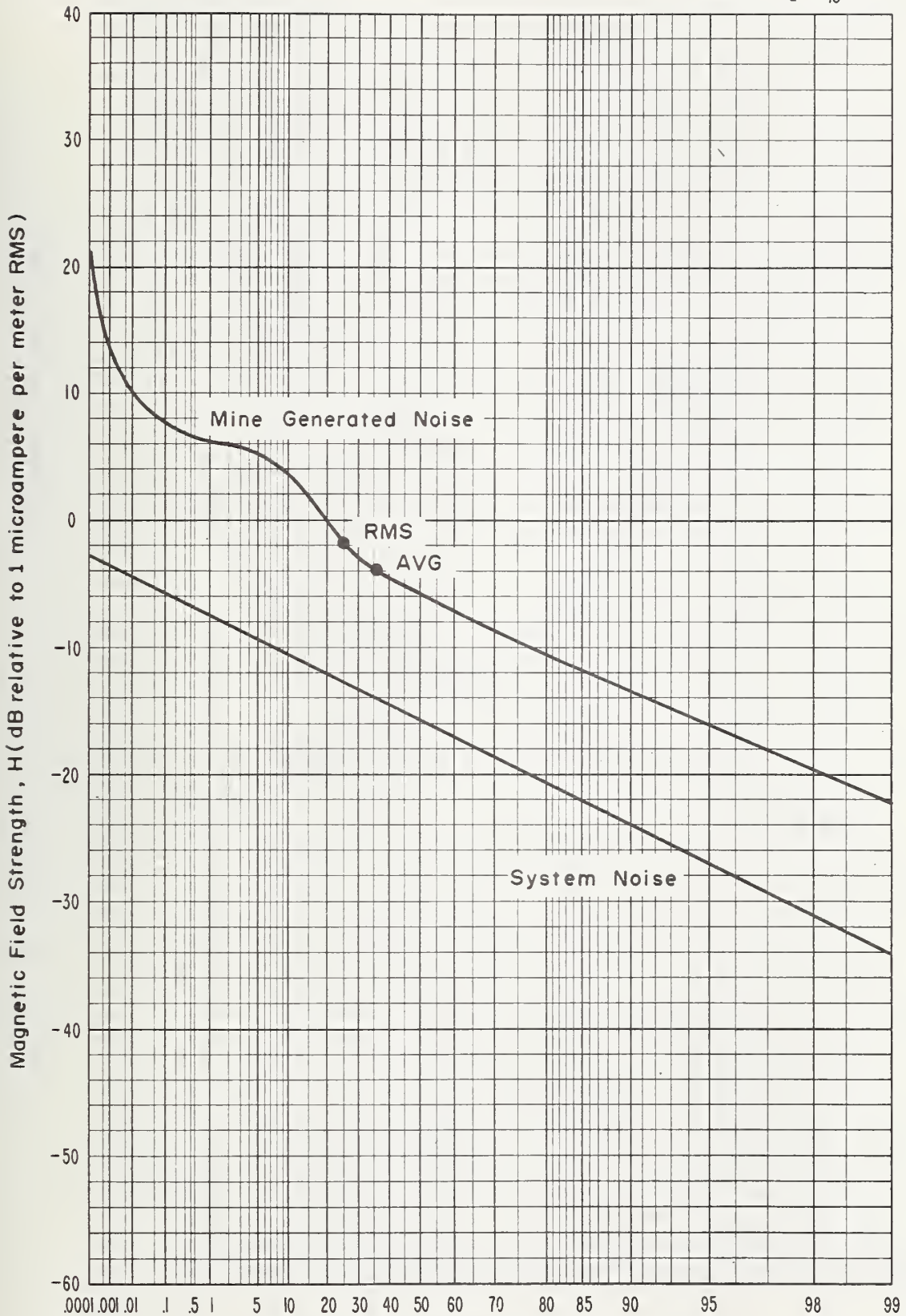
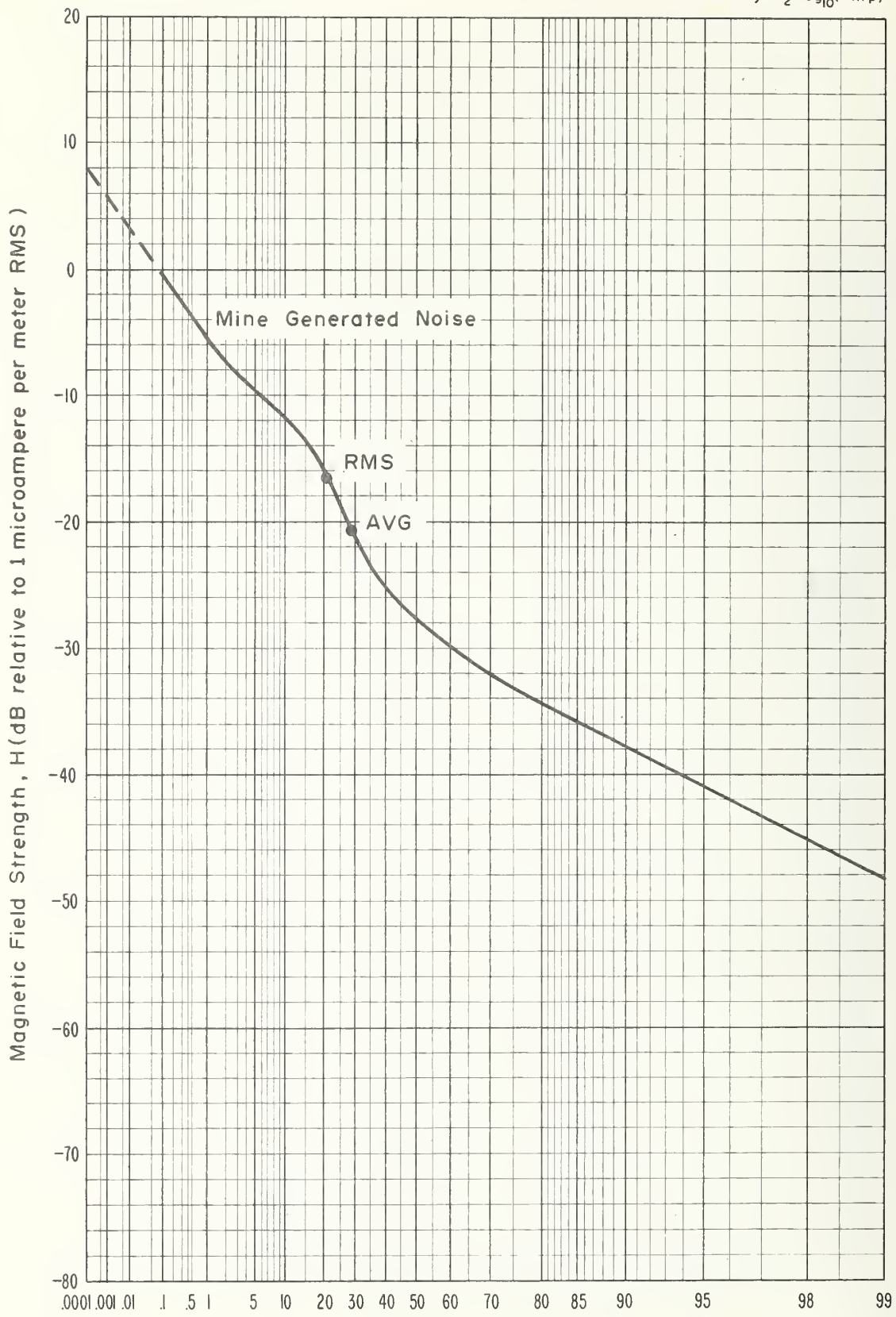


Figure 4-34 APD, 30 kHz, horizontal component E-W, 1.0 kHz predetection bandwidth, April 24, 1973, 12:18 p.m., shop office, Grace Mine.



Percent of Time Ordinate is Exceeded

Figure 4-35 APD, 70 kHz, horizontal component E-W, 1.0 kHz  
predetection bandwidth, April 24, 1973, 1:36 p.m.,  
shop office, Grace Mine.

USCOMM - ERL

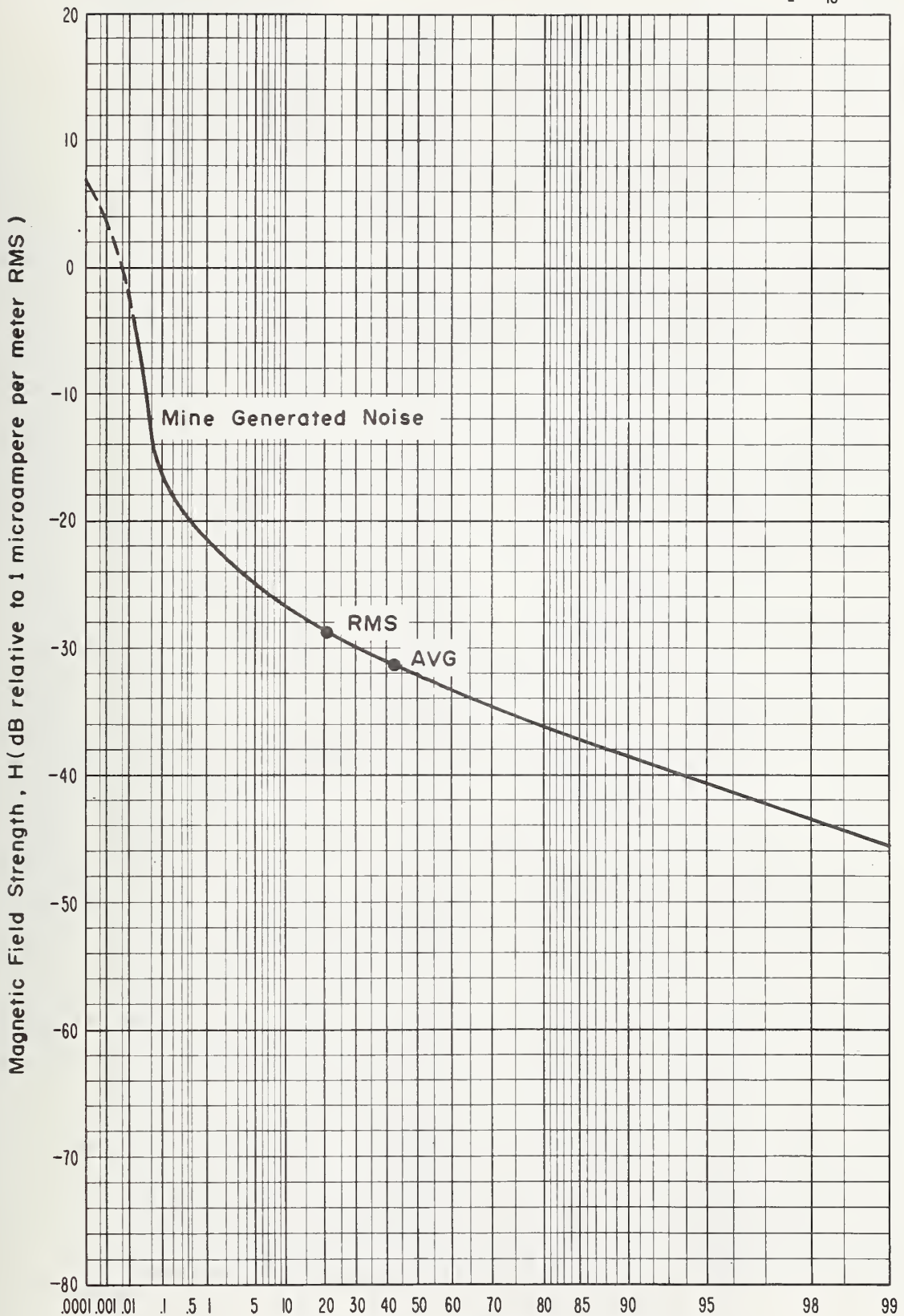
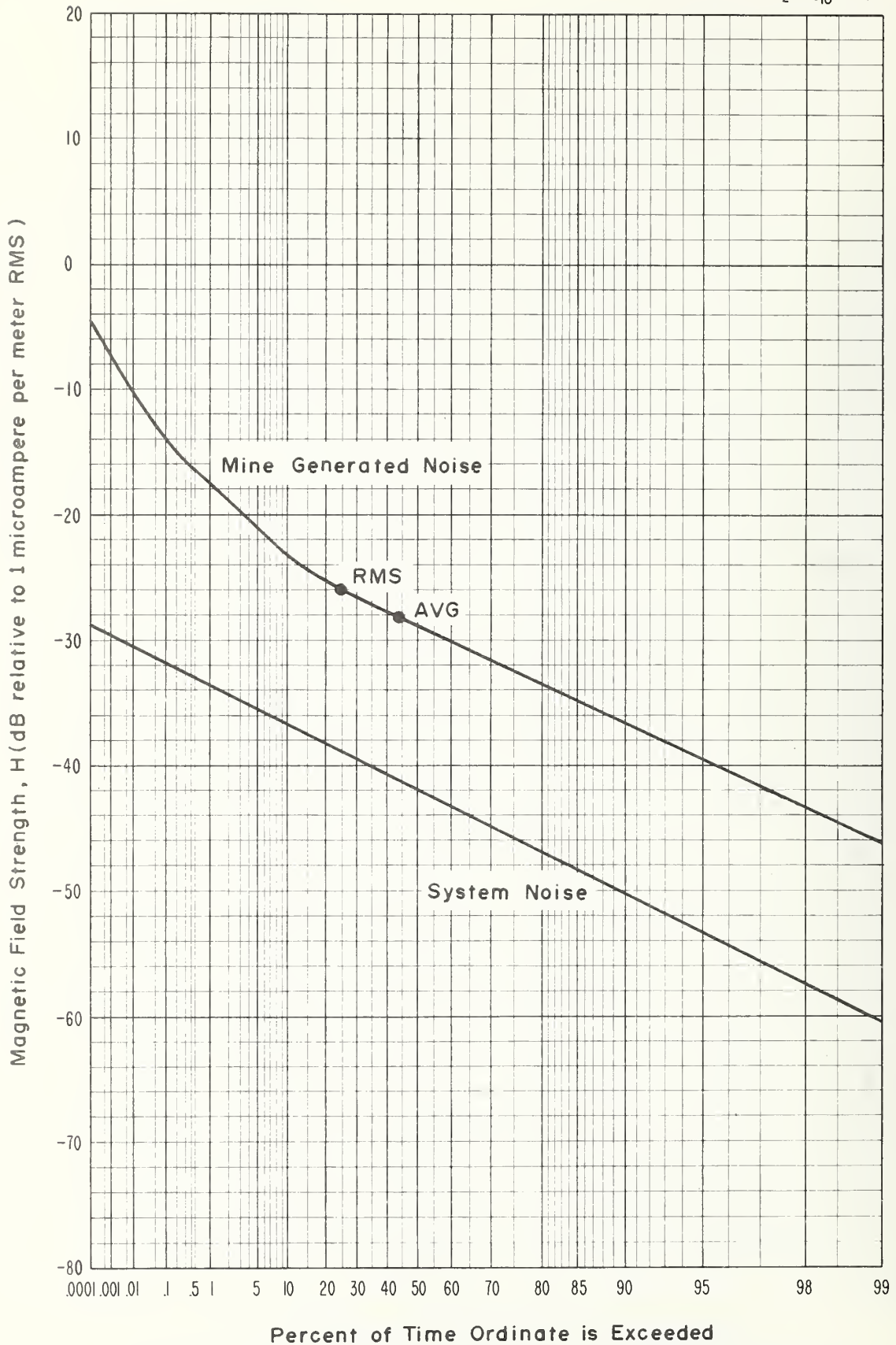
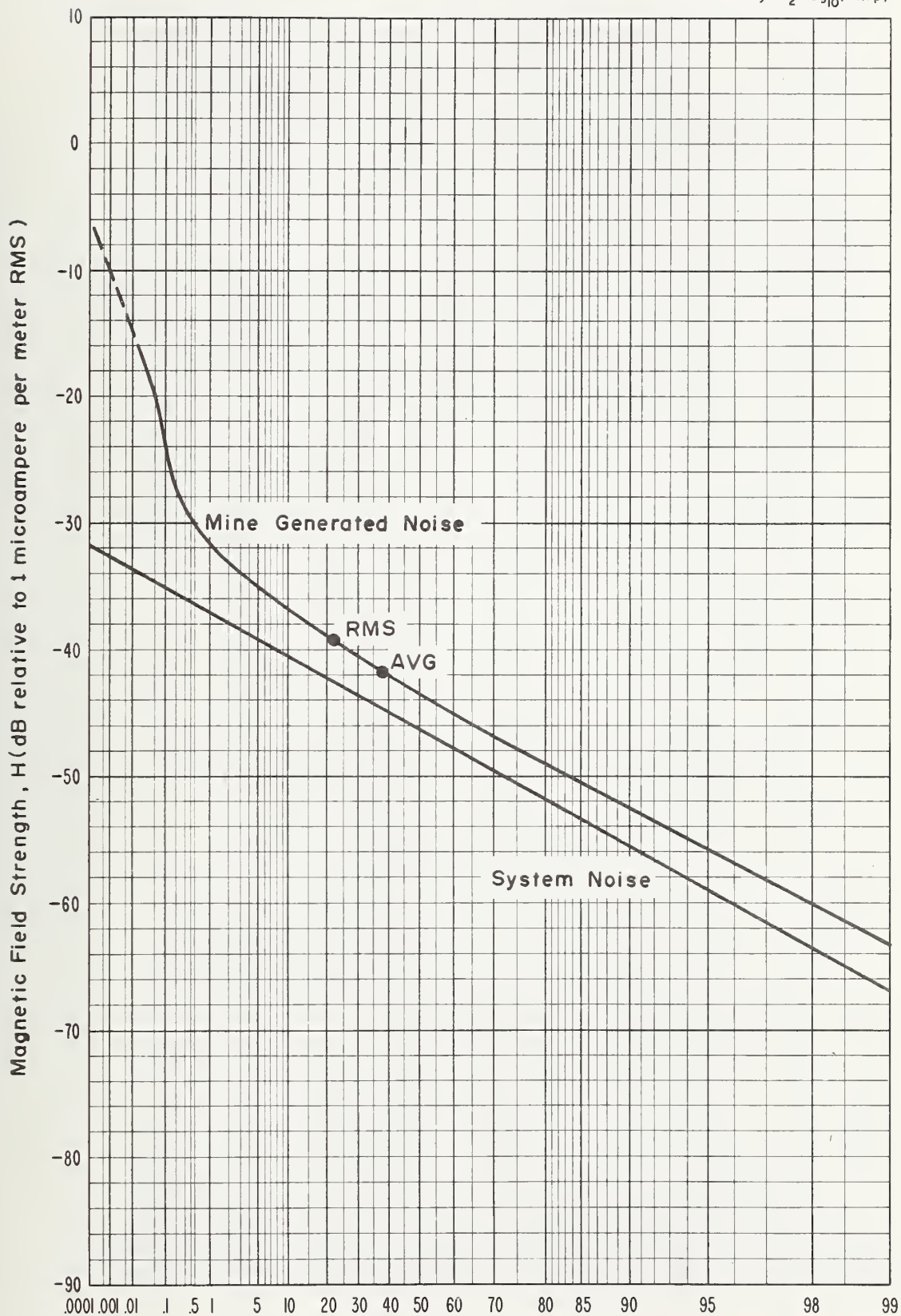


Figure 4-36 Percent of Time Ordinate is Exceeded  
 APD, 130 kHz, horizontal component E-W, 1.0 kHz  
 predetection bandwidth, April 24, 1973, 3:00 p.m.,  
 shop office, Grace Mine.



**Percent of Time Ordinate is Exceeded**  
 Figure 4-37 APD, 160 kHz, horizontal component E-W, 1.0 kHz  
 predetection bandwidth, April 24, 1973, 4:15 p.m.,  
 shop office, Grace Mine.



Percent of Time Ordinate is Exceeded  
 Figure 4-38 APD, 250 kHz, horizontal component E-W, 1.2 kHz  
 predetection bandwidth, April 24, 1973, 3:35 p.m.,  
 shop office, Grace Mine.

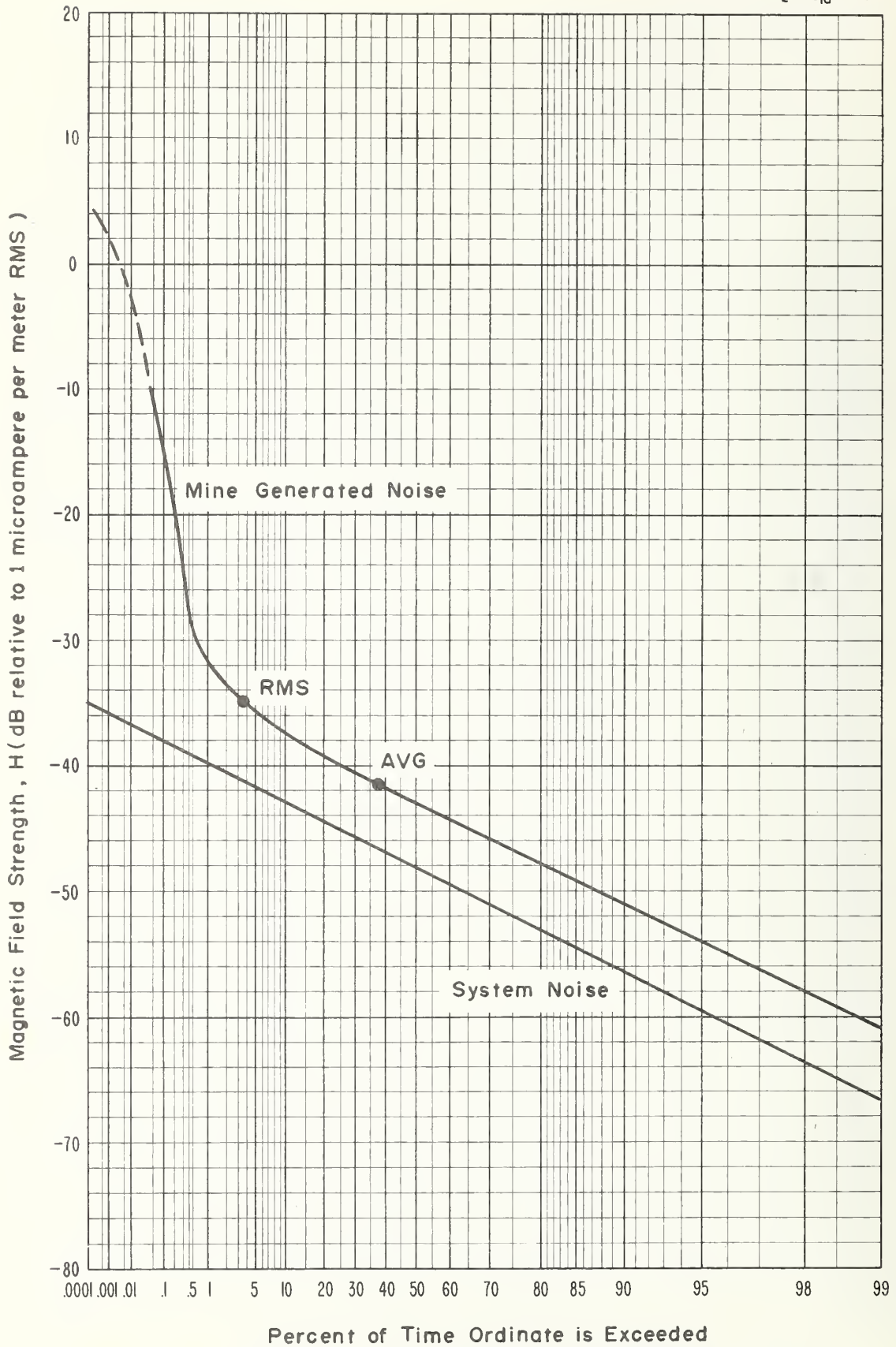
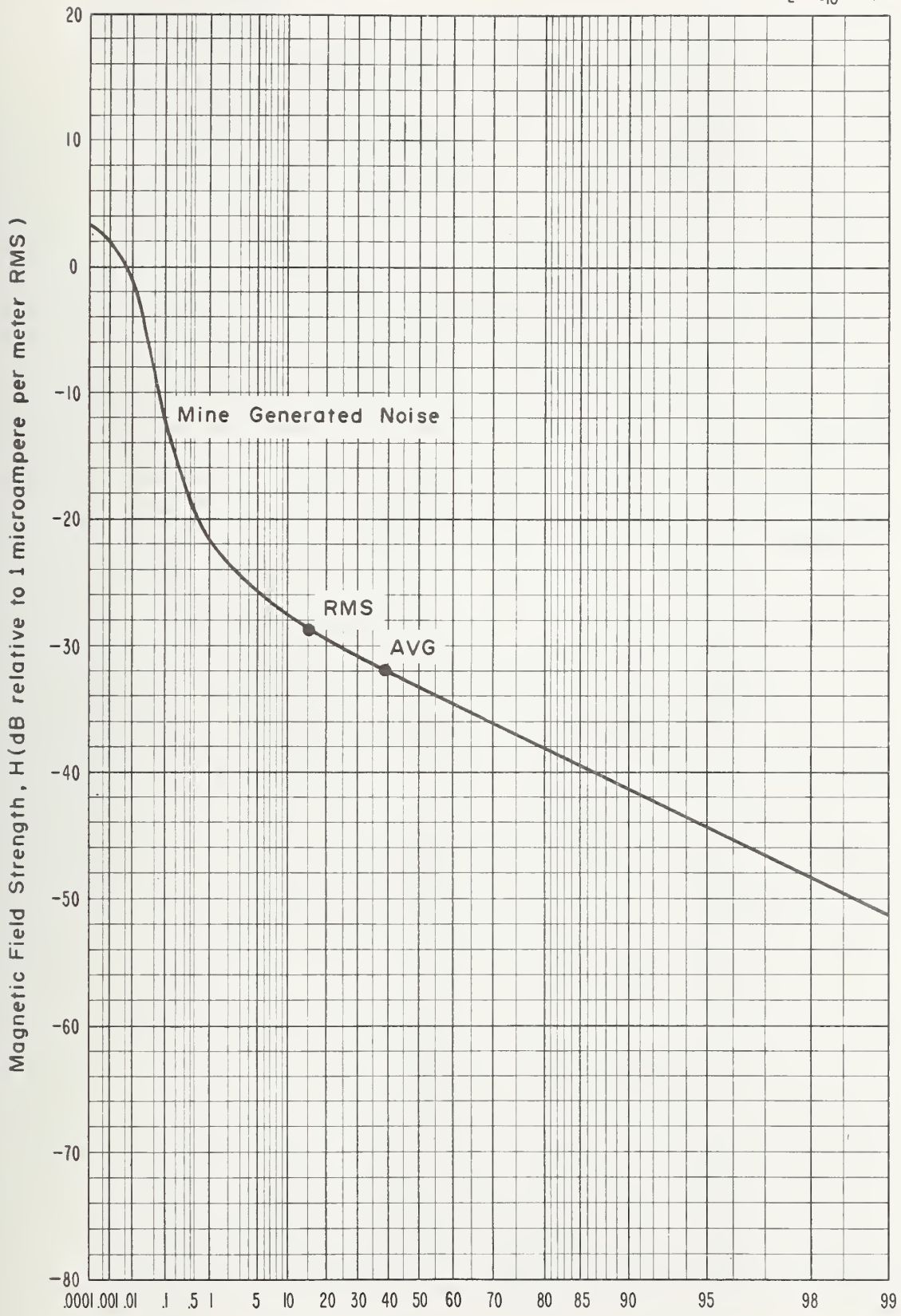


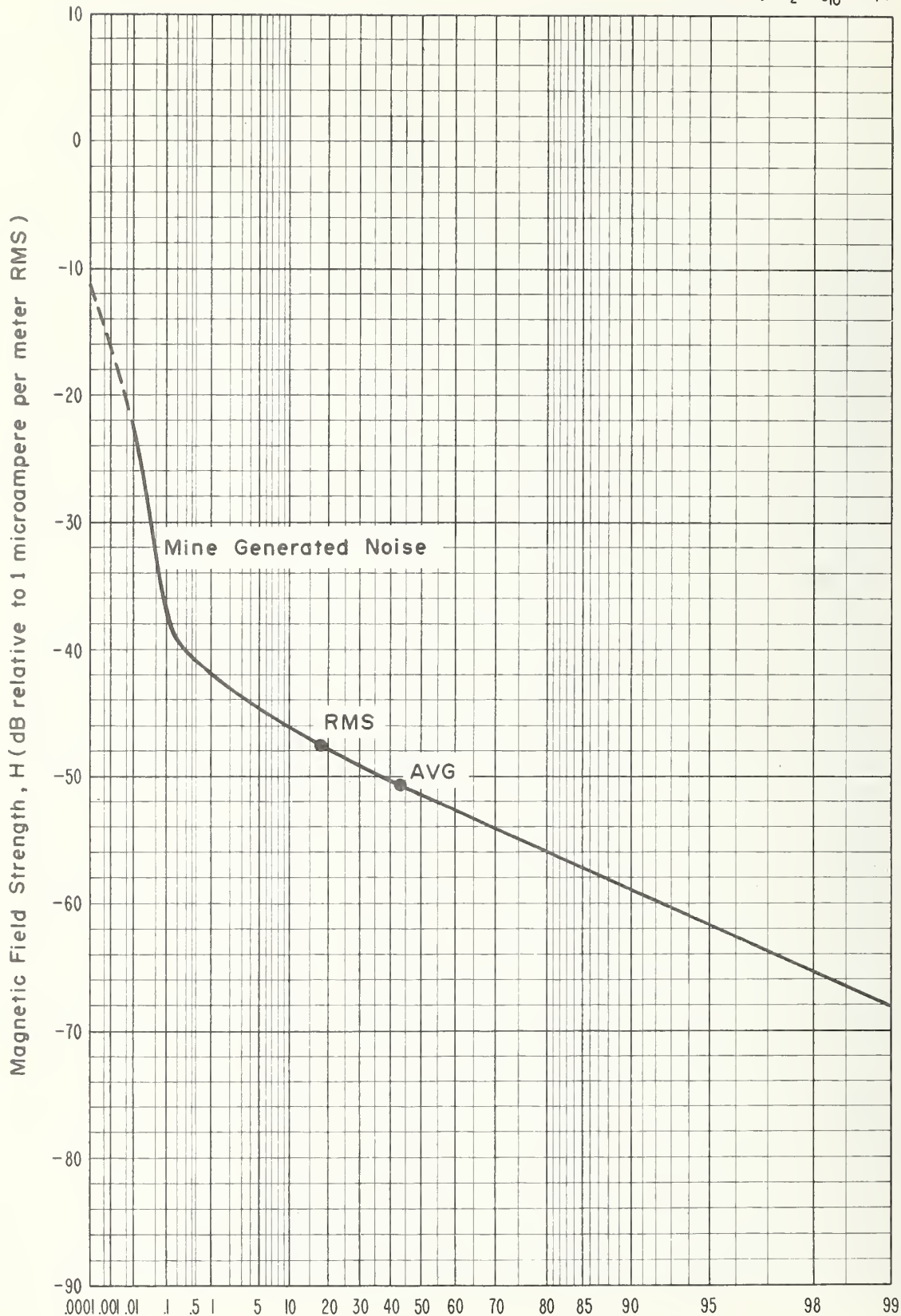
Figure 4-39 APD, 500 kHz, horizontal component E-W, 1.2 kHz predetection bandwidth, April 24, 1973, 12:18 p.m., shop office, Grace Mine.





**Percent of Time Ordinate is Exceeded**

Figure 4-40 APD, 1 MHz, horizontal component E-W, 1.2 kHz predetection bandwidth, April 24, 1973, 1:36 p.m., shop office, Grace Mine.



Percent of Time Ordinate is Exceeded  
 Figure 4-41 APD, 2 MHz, horizontal component E-W, 1.2 kHz  
 predetection bandwidth, April 24, 1973, 3:00 p.m.,  
 shop office, Grace Mine.

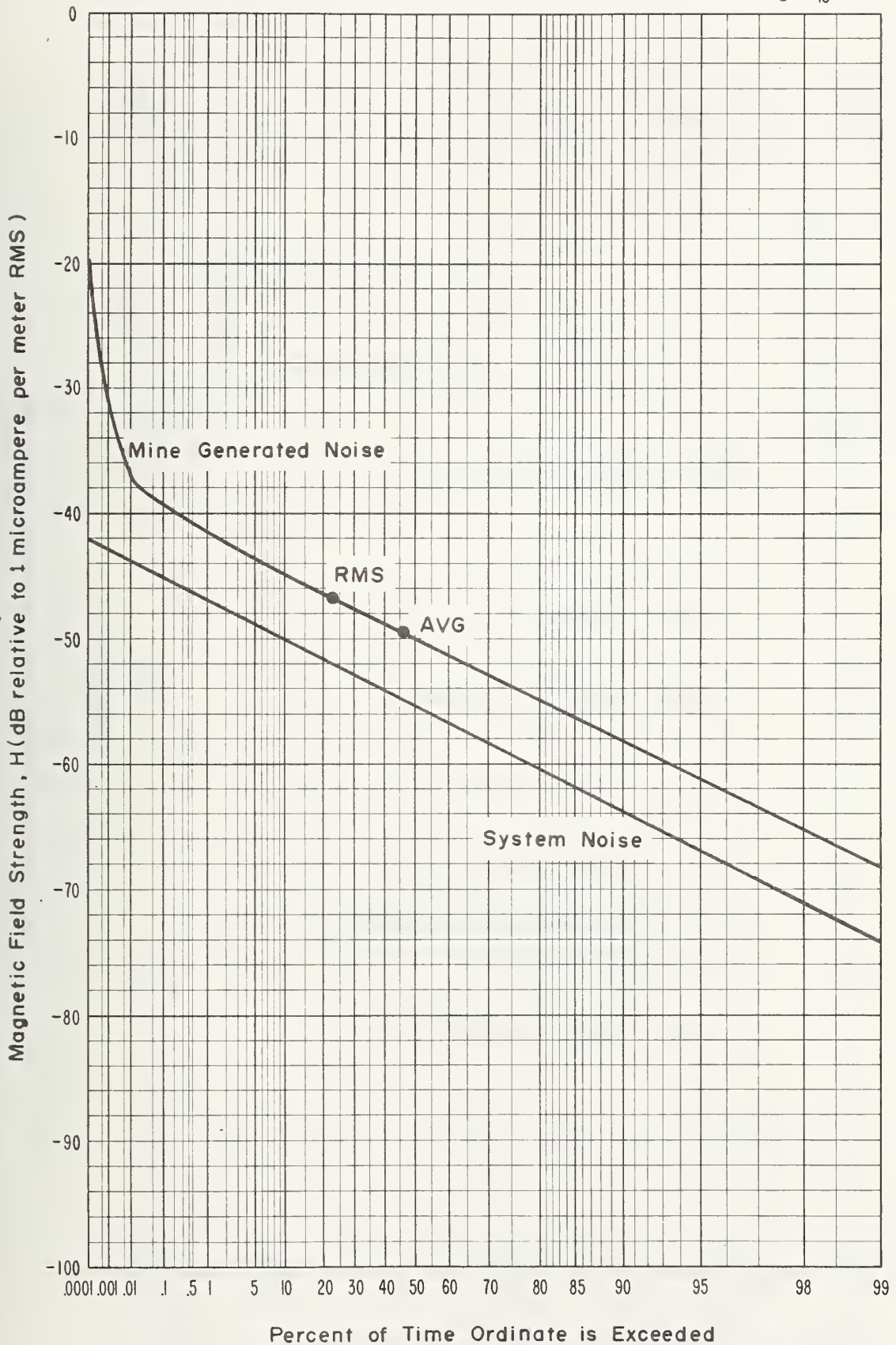


Figure 4-42 APD, 6 MHz, horizontal component E-W, 1.2 kHz predetection bandwidth, April 24, 1973, 4:15 p.m., shop office, Grace Mine.

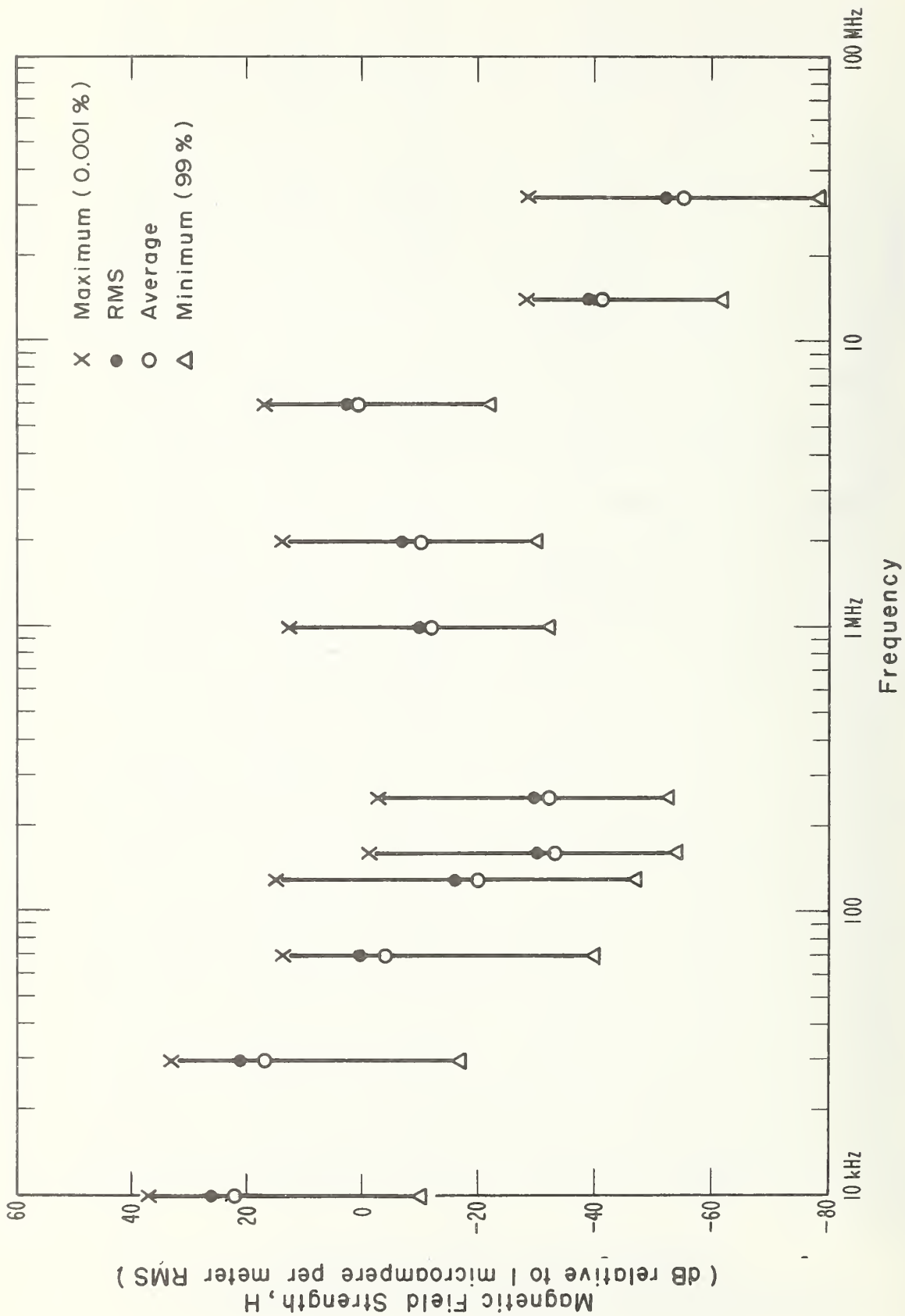


Figure 4-43 Field strength excursions between 0.001% and 99% of the time as a function of frequency, vertical component, 1.0 kHz predetection bandwidth, April 24, 1973, development foreman: office, Grace Mine.

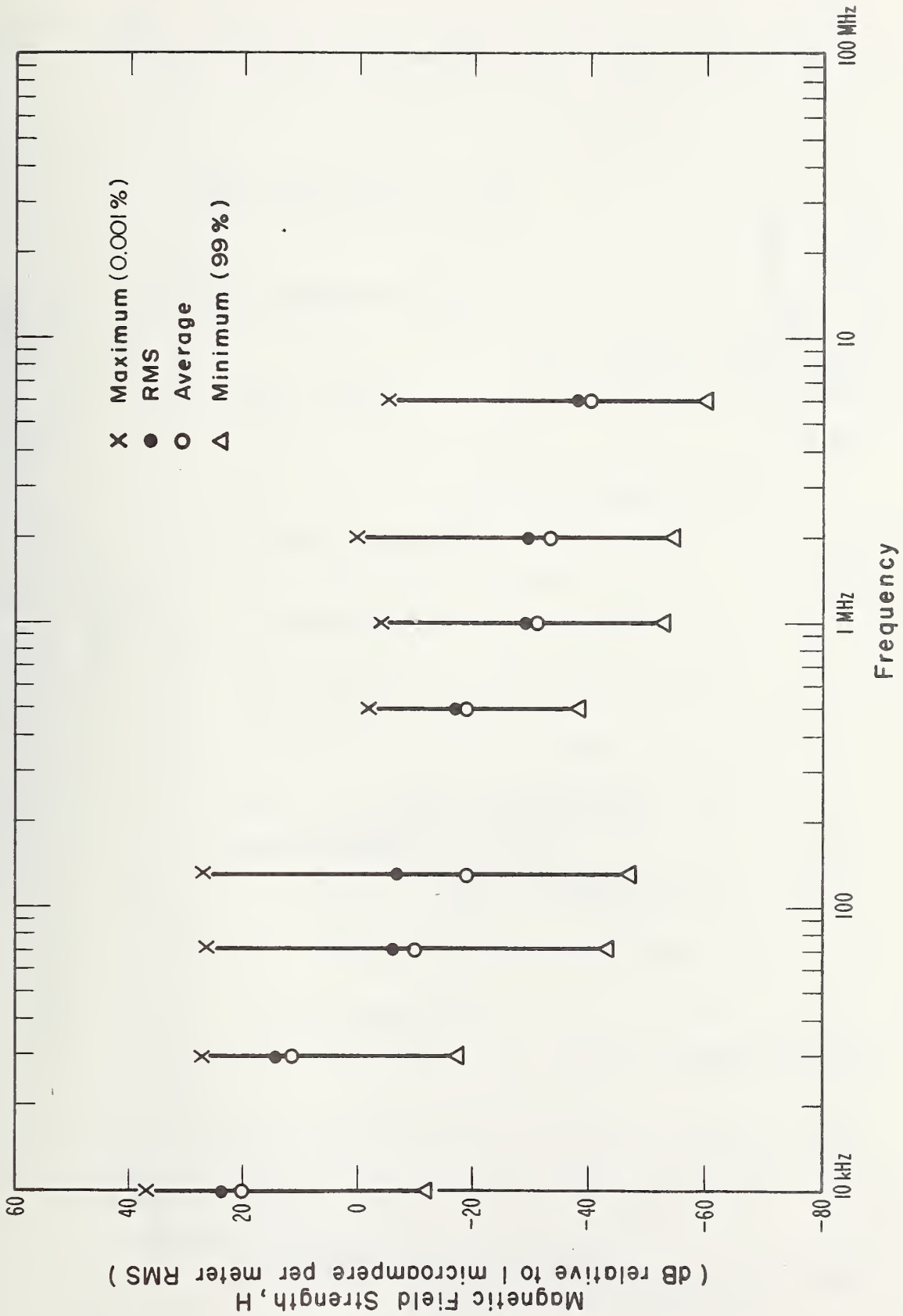


Figure 4-44 Field strength excursions between 0.001% and 99% of the time as a function of frequency, vertical component, 1.0 kHz predetection bandwidth, April 24, 1973, crusher substation, Grace Mine.

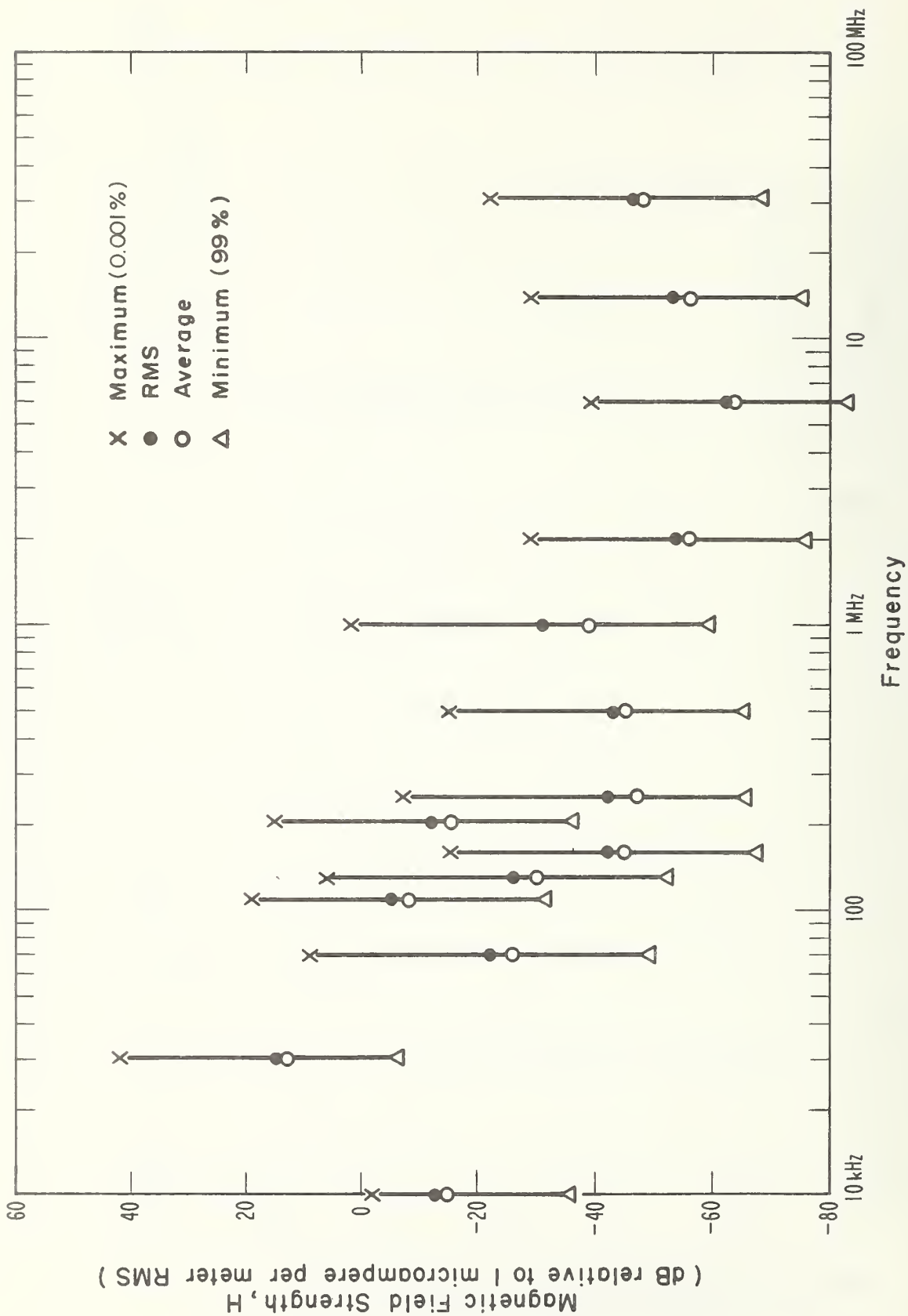


Figure 4-45 Field strength excursions between 0.001% and 99% of the time as a function of frequency, vertical component, 1.0 kHz predetection bandwidth, April 24, 1973, shop office, Grace Mine.

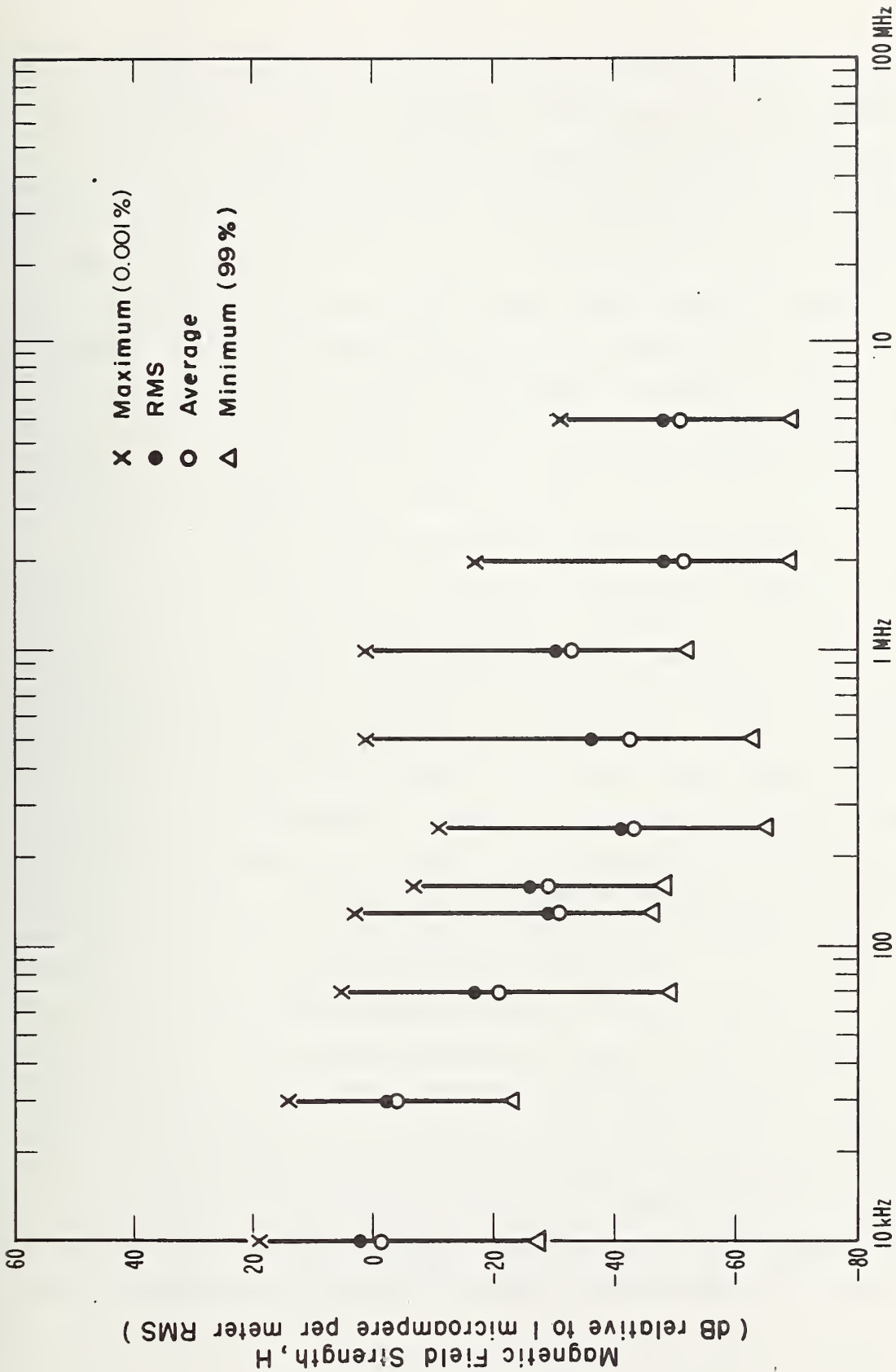


Figure 4-46 Field strength excursions between 0.001% and 99% of the time as a function of frequency, horizontal component, (E-W), 1 kHz predetection bandwidth, April 24, 1973, shop office, Grace Mine.

## 5. HOIST-PHONE MEASUREMENT RESULTS

There are two hoist-phone systems in use. The phone on the personnel skip in the shaft uses a transmission line (a single wire terminated in 25 ohms with earth return) installed specifically for the hoist phone. It operates at 100 kHz. At the surface, it is directly coupled. On the skip, a 16-turn, shielded loop of area 0.24 square meter, couples to the magnetic field from the transmission line. One edge of this loop is about 0.2 meters from the single wire of the transmission line. This system works very well.

During normal operation (ore hauling), there is no phone on the ore skip at the A shaft. One is added during maintenance shift (once a week). It operates at 65 kHz. A folding, wooden, rectangular core with 30 turns on each side forms a toroid that couples energy in and out of the hoist "rope" (2 1/4-inch (5.72 cm) diameter, stranded, steel cable). In this case, the hoist rope is one wire of the transmission line; earth is the return, but since the skip is guided with non-conducting rubber tires on metal guides, ground return is so poor that a bronze shoe is specially installed for better grounding during maintenance. Without the ground path through the metal shoe, communication is very poor and is not possible over a large portion of the 2200 foot path. Some hasty experiments performed in a shop at the mine indicated a 50 dB increase in signal with a resonant capacitive return path or 40 dB increase with a low-resistance return path. With the metal shoe making good connection while the skip is stopped, communication was reported to be good -- we did not have the chance to observe this first hand. For any conditions not providing a low-resistance ground, communication was not so good. Standing waves would certainly be probable. This indicates there may be difficulty in using single-wire (hoist



rope) transmission lines with ground return unless special attention is given to providing low-resistance ground returns. A side note is that these clamp-on, wooden frame toroids are tuned (fairly broadband) for a somewhat higher frequency than 65 kHz, and some slight improvement might be obtained with different tuning.

Measurements of magnetic-field noise and of attenuation of signal level were made on the hoist-phone system on the A shaft. A separate-wire, terminated transmission line was used; the noise and signal levels were relatively uniform, indicating no standing waves and little attenuation. The signal-to-noise ratio was over 70 dB.

Magnetic-field noise and magnetic-field signals were both measured every 200 feet while the hoist ran from 0 to 2200 foot depths. Measurements were made next to the carrier phone pick-up loop and next to the hoist rope. Antennas were positioned as shown in figure 5-1. The results for the transmission line are shown in figure 5-2 and the results for the hoist rope are shown in figure 5-3. Noise and signal are shown in dB relative one microampere per meter, while signal-to-noise (S/N) ratio is in dB; all the measured magnetic-field strengths are primarily a measure of the currents in each wire, as these currents are the nearest and hence dominant sources of magnetic field energy.

There are two key observations. One is that with a low-loss, terminated transmission line, there are no standing wave patterns, and levels vary only slightly within reasonable bounds indicating very low attenuation. The second is that the noise also is nearly uniform with depth. Some variations were noted near working levels, but not more than 10 to 15 dB, and with the very high signal-to-noise ratio that prevails, that size of variation would create no problem.

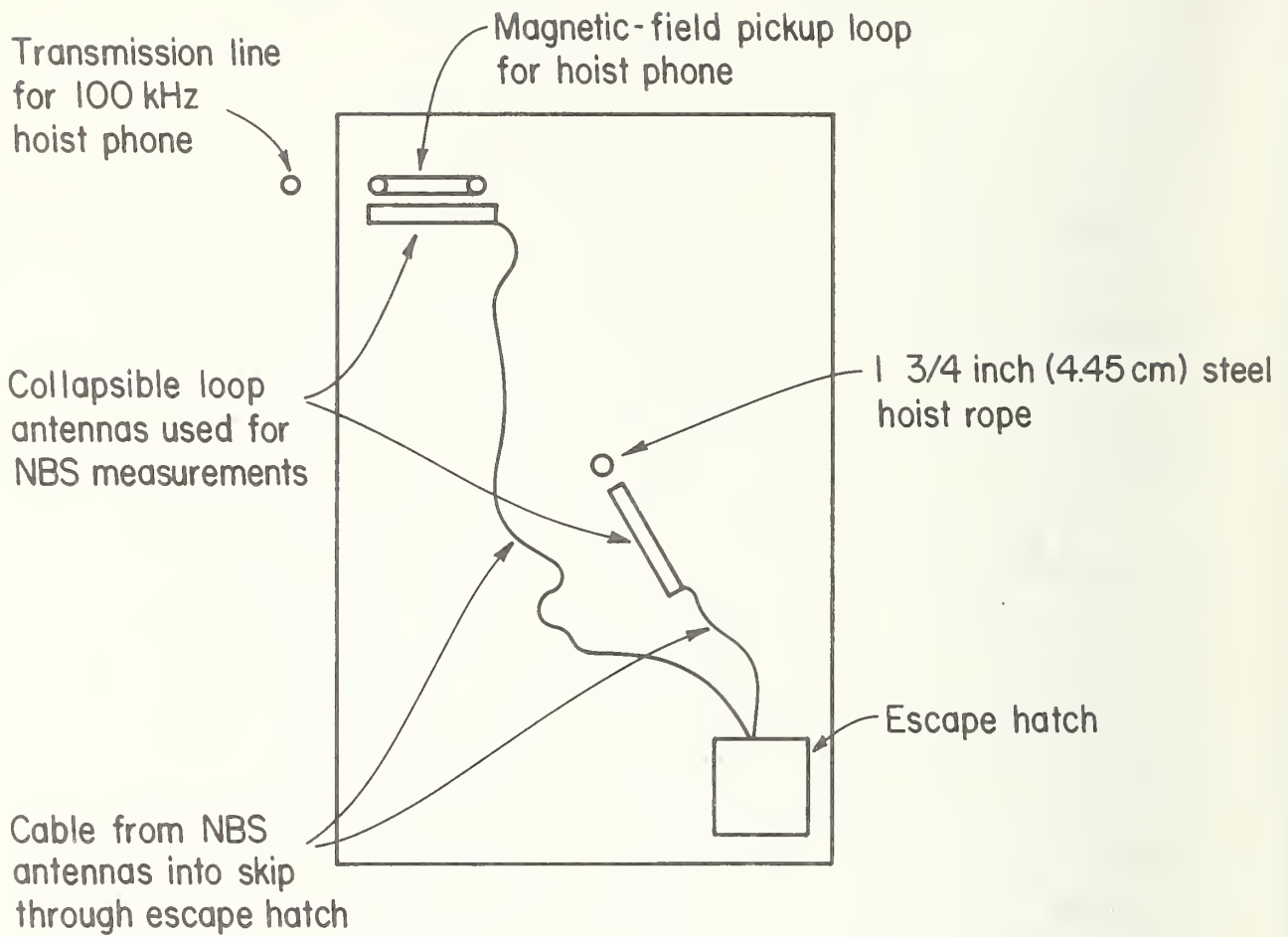


Figure 5-1 Top view of personnel hoist "A" skip.

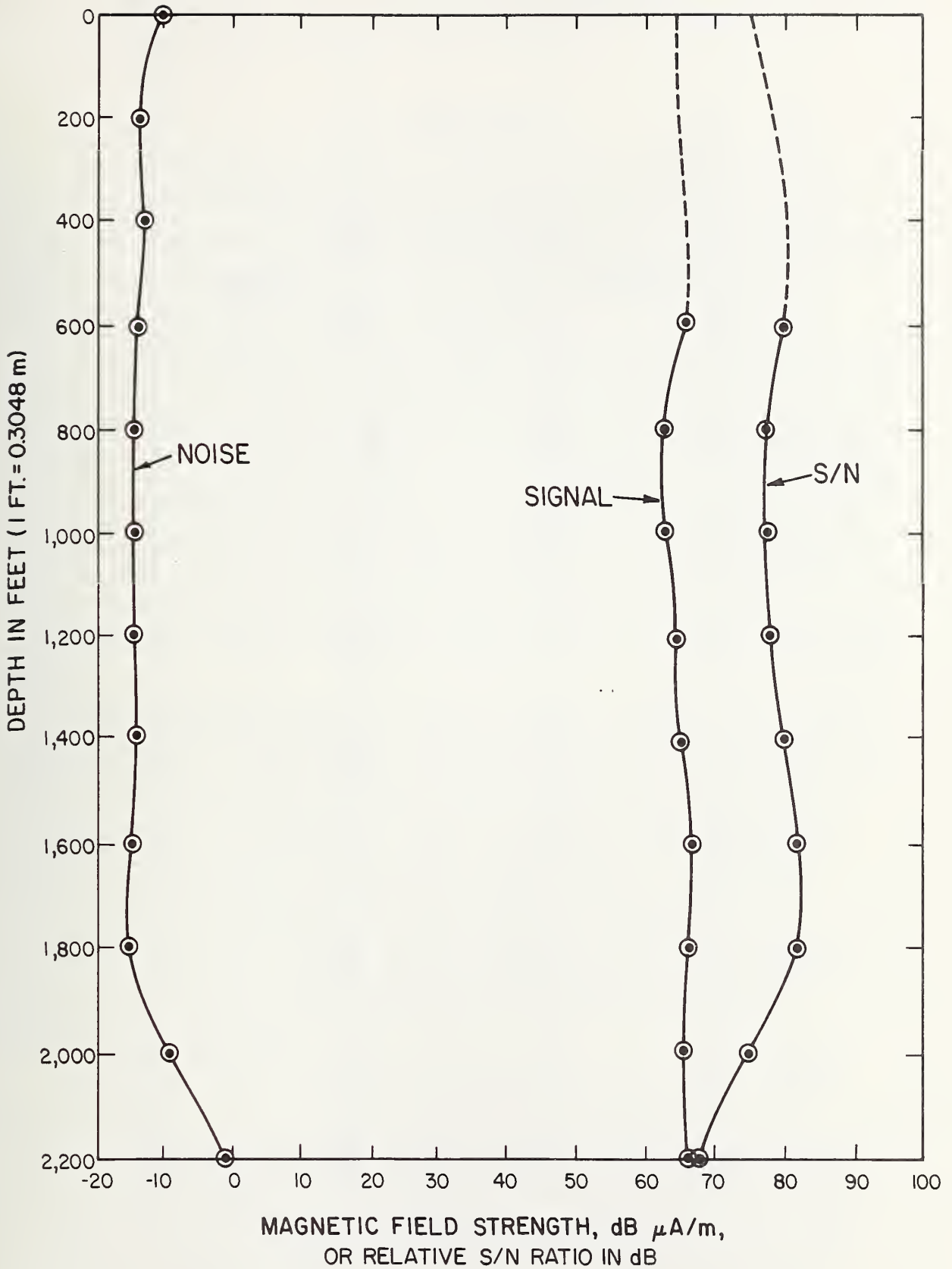


Figure 5-2 Magnetic field strength, dB $\mu\text{A/m}$ , or relative S/N ratio as measured along the transmission line for the personnel hoist located in "A" shaft.

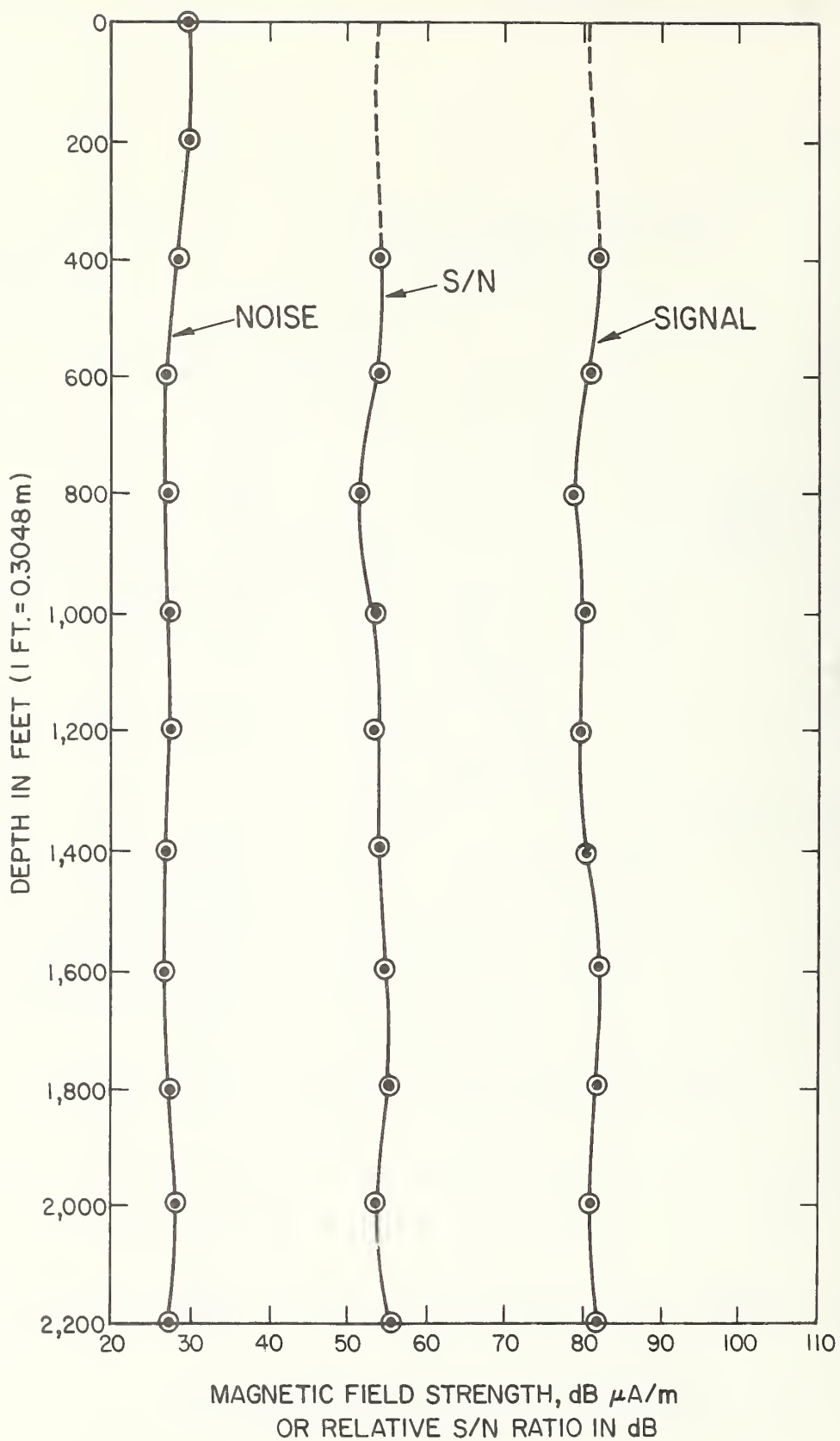


Figure 5-3 Magnetic field strength, dB $\mu\text{A}/\text{m}$ , or relative S/N ratio as measured along the hoist rope for the personnel hoist located in "A" shaft.

## 6. CONCLUSIONS

The spectral plots show a wide range of magnetic-field noise levels at different locations. In general, the noise levels decrease with frequency, although if there is a nearby dominant noise source, there are many variations that are characteristic only of that source.

The most important observation is that the magnetic-field noise levels in this mine are about 10 to 50 dB lower than in most coal mines. There are two exceptions. First, near the crusher-room substation, where heavy current is flowing, there are high power-line harmonics. Noise at higher frequencies is also relatively high. Second, the LHD's generate high fields anywhere in the mine they happen to be. Even near these "hot spot" areas, electromagnetic noise levels are significantly lower than near similar "hot spot" areas in coal mines.

Noise contour maps at 2 kHz, 10 kHz, 20 kHz and 60 kHz show a definite continuous source in or near the crusher room. Some type of fast-rise-time, full-wave, three-phase current pulse is present. Spectral lines produced by this source are separated by approximately 360 Hz. Since the separation is approximate, the source may be an arc.

There are electromagnetic impulses generated by chemical explosions. These create short-duration peaks higher (at frequencies above 5 kHz) than levels generated by other equipment in the mine.

The APD's also indicate relatively lower noise levels for horizontal and vertical fields at locations away from the crusher substation. However, noise variations with frequency are not monotonically decreasing as had been observed either in coal mines or for surface locations. The time variations are random; impulsive noise is present a lower percentage of time in Grace Mine than in coal mines, particularly at lower frequencies.

The hoist-phone measurements showed a high signal-to-noise ratio, practically no standing waves, and no measurable loss over the 670 meter (2200 feet) depth at the 100 kHz operating frequency, for the system with a separate, terminated cable that runs down the hoist shaft. The "ground" return path is mostly through metallic cables, pipes, etc., and therefore is not significantly affected by earth parameters. This is a common situation.

Although direct observations or measurements were not made on another hoist using only the hoist cable and either (1) no termination (open circuit condition), or (2) a brass shorting plate (short-circuit condition), reported operation was not satisfactory for case (1), open, and only moderately satisfactory for case (2), short.

## 7. RECOMMENDATIONS

The measured electromagnetic data in this report should be compared with similar data from coal mines. A different type of haulage locomotion (diesel rather than dc electrical) power is used in this mine; there are significant differences in the electromagnetic environment produced.

If a mobile (to LHD vehicle) communication system is to be designed, some shielding of electrical components on the LHD's may give high improvements relative to costs.

Where a separate personnel hoist is operated, e.g., the ore skip and the personnel skip are not the same, and hence where falling ore is not going to damage a special transmission line that can be run down the shaft, use of a separate transmission line appears very attractive. Where the ore and personnel skip are the same, practical considerations require the skip rope (cable) to be one path of a transmission line, while earth and/or metallic pipes and cables can provide the other path. In this case, standing waves will be a problem of unknown severity, since there is no reliable termination.

Elimination of the noise source in the crusher room would lower continuous in-mine background noise significantly.

Hardwire, dial telephones are used in this mine for point-to-point communication; this system works well for all locations where phones are available. In less static situations such as exist in working areas of coal mines, such a system might not always be practical.

## 8. ACKNOWLEDGMENTS

Those making significant contributions to this program are as follows: Laboratory development and field use of measurement equipment, Ed Neisen, Doug Schulze, and Tom Bremer; data processing, Ann Rumfelt, Nancy Tomoeda, Winston Scott, Frank Cowley, and David Stearns. Those making valuable but less time-consuming contributions are Gerry Reeve, Bob Matheson, Don Spaulding, John Chukoski, Lorne Matheson, Dave Lewis, and Sharon Foote.

Winston Scott provided much assistance in proofreading, while Sharon Foote and Janet Becker typed tirelessly through many versions. Jocelyn Spencer and Barbara Bolton provided drafting assistance.

Finally, none of this would have been possible without the excellent cooperation of Paul Vancura, Ray Shucavage, Fred Eben, Harold Kaley and others at Grace Mine of Bethlehem Steel Corporation.



## 9. REFERENCES

- [1] Bensema, W.D., Kanda, M., Adams, J.W., Electromagnetic Noise in Robena No. 4 Coal Mine, NBS Tech. Note 654, April 1974.
- [2] The Institute of Electrical and Electronic Engineers, Inc., IEEE Dictionary of Electrical and Electronic Terms, Std. 100, 1972.
- [3] Crichlow, W.Q., et al., Amplitude-Probability Distributions for Atmospheric Radio Noise, NBS Monograph 23, 1960b.
- [4] Thompson, W.I., III, Bibliography of Ground Vehicle Communications and Control, AKWIC index, Report No. DOT-TSC-UMTA-71-3, July 1971.
- [5] Taggart, H.E. and Workman, J.L., Calibration Principles and Procedures for Field Strength Meters (30 Hz to 1 GHz), NBS Tech. Note 370, March 1969.
- [6] Spaulding, A.D. and Disney, R.T., Man-Made Radio Noise -- Part 1: Estimates for Business, Residential, and Rural Areas, OT Report 74-38, June 1974.

## 10. APPENDIX

### Decoding of Spectrum Captions

Spectrum captions are generally organized into the following format:

First line: MP NDT NZS NDA NPO RC DF date, time, frame, serial, where

MP = Two's power of length of Fourier transform, example,  $2^{MP}$  where MP = 12

NDT = Detrending option, example, 0 (dc removed)

NZS = Restart spectral average after output, example, 0 (restarted)

NDA = Data segment advance increment, example, 2048

NPO = Number of spectra averaged between output calls, example, 20

RC = Integration time in seconds per spectra, example, 0.168

DF = Resolution bandwidth, spectral estimate spacing in hertz, example, 62.5

Date = Date of computer processing, example, 03/21/73

Time = Time of computer processing, example, 15:06:34

Frame = Frame set number, example, 10

Serial = Film frame serial number, example, 42.

Second line: DTA DA(1) DA(2) DA(3) NSA NRP NPP, where

DTA = Detrending filter parameter  $\alpha$ , example, 0.00195

DA(1) = Detrending filter average, K=1, example, 59.4

DA(2) = Detrending filter average, K=2, example, 0

DA(3) = Detrending filter average, K=3, example, 0

NSA = Number of periodograms averaged, example, 20

NRP = Number of data points processed since spectrum initialization, example, 43008

NPP = Number of data points processed since data initialization, example, 43008.

Third line: RUN, SESSION, MONTH, DAY, YEAR Gain corr., rec. =  
tot. constr. =, where  
Run and Session = the title of the portrayed frame identifying  
the digitizing session and run number,  
example, 21 83  
Month, Day, Year = date data were recorded in the mine,  
example, 8 25 73  
Gain corr. rec. = receiver gain correction, example, -6  
tot. const. = constant gain correction of entire system,  
example, -46.4

Fourth line: C =, RG =, DG =, FG =, AG =, where  
C = correction curve used with data, example, 25  
RG = receiver gain and accompanying correction in dB added to  
the data, example, 200 (-6 dB)  
DG = digitizer gain, example, 0  
FG = filter gain in dB, often rounded to nearest single digit,  
example, 0  
AG = absolute gain correction added to data, example, 52

Fifth line: Top of Scale, Standard Error, Spectral Peak, where  
Top of Scale = largest scale marking for computer drawn  
graph, example, 1.000+004 ( $1.0 \times 10^4$ )  
Standard Error = standard error of curve, example, 0.3162  
Spectral Peak = largest spectral peak observed, example,  
4.108+003 ( $4.108 \times 10^3$ )

U.S. DEPT. OF COMM. BIBLIOGRAPHIC DATA SHEET	1. PUBLICATION OR REPORT NO. NBSIR 74-388	2. Gov't Accession No.	3. Recipient's Accession No.
4. TITLE AND SUBTITLE  ELECTROMAGNETIC NOISE IN GRACE MINE		5. Publication Date June 1974 6. Performing Organization Code	
7. AUTHOR(S) John W. Adams, William D. Bensema, and Motohisa Kanda		8. Performing Organ. Report No.	
9. PERFORMING ORGANIZATION NAME AND ADDRESS  NATIONAL BUREAU OF STANDARDS DEPARTMENT OF COMMERCE Washington, D.C. 20234		10. Project/Task/Work Unit No. 2768412 11. Contract/Grant No.	
12. Sponsoring Organization Name and Complete Address (Street, City, State, ZIP) U. S. Bureau of Mines Pittsburgh Mining and Safety Research Center 4800 Forbes Avenue Pittsburgh, Pennsylvania 15213		13. Type of Report & Period Covered 14. Sponsoring Agency Code	
15. SUPPLEMENTARY NOTES			
16. ABSTRACT (A 200-word or less factual summary of most significant information. If document includes a significant bibliography or literature survey, mention it here.)  Two different techniques were used to make measurements of the absolute value of electromagnetic noise in an operating hardrock mine, Grace Mine, located near Morgantown, Pennsylvania. Diesel-powered haulage equipment is used in this mine, and the electromagnetic noise environment it creates was measured to see how it differs from the environment created by electric-powered haulage equipment. One technique measures noise over the entire electromagnetic spectrum of interest for brief time periods. It is recorded using broadband analog magnetic tape and the noise data is later transformed to give spectral plots. The other technique records noise amplitudes at several discrete frequencies for a sufficient amount of time to provide amplitude probability distributions.  The specific measured results are given in a number of spectral plots and amplitude probability distribution plots.			
17. KEY WORDS (six to twelve entries; alphabetical order; capitalize only the first letter of the first key word unless a proper name; separated by semicolons) Amplitude probability distribution; coal mine noise; digital data; electromagnetic interference; electromagnetic noise; electromagnetic pulse (chemical); emergency communications; Fast Fourier Transform; Gaussian distribution; impulsive noise; magnetic field strength; measurement instrumentation; spectral density; time-dependent spectral density.			
18. AVAILABILITY <input checked="" type="checkbox"/> Unlimited  <input type="checkbox"/> For Official Distribution. Do Not Release to NTIS  <input type="checkbox"/> Order From Sup. of Doc., U.S. Government Printing Office Washington, D.C. 20402, SD Cat. No. C13  <input type="checkbox"/> Order From National Technical Information Service (NTIS) Springfield, Virginia 22151		19. SECURITY CLASS (THIS REPORT)  UNCLASSIFIED	21. NO. OF PAGES
		20. SECURITY CLASS (THIS PAGE)  UNCLASSIFIED	22. Price